Development of a wet fine screen model integrating the effect of operating and design variables on screening performance

A thesis submitted for the degree of Master of Science in Chemical Engineering

Prepared by: Seipati Mabote

Supervised by: Prof Aubrey Mainza, Mr Paul Bepswa

Department of Chemical Engineering
University of Cape Town

February 2016

Declaration

“I know the meaning of plagiarism and declare that all the work in the document, save for that which is properly acknowledged, is my own"

Signature: Signed by candidate

Acknowledgements

I would like to thank my supervisor Prof. Aubrey Mainza for his assistance throughout my MSc project. Without his guidance and constant encouragement this project would have hardly been completed. I would also like to thank my co-supervisors for helping me in different aspects of the project.

Sincere thanks to the sponsors Amira P9, for funding the project. I would also like to thank the UCT CMR group for assisting with the laboratory work and technical advice.

I am deeply grateful to the Mintek Mineral Processing Division for allowing me to use their facilities for the testwork. Special thanks to Thandaza Maseko, for helping out during the course of the testwork.

Thanks to my friends for encouraging me to keep pushing until the end. To Saliya and Bokang, thank you so much for offering me a place to stay during the last days of my thesis write-up.

Last but not least, to my mom, dad and sister thank you for your encouragement. I greatly appreciate the love and support that you gave me during this time.

Abstract

Mineral processing is the process that involves liberation and beneficiation of valuable constituents of an ore. Several physical beneficiation processes exist and one such process is classification. Screens are classification devices sometimes used in the classification stage of closed grinding circuits to separate mill product into different size classes. Poor classification of particles results in reduced throughput, high power consumption and over-grinding. Most of the research on screening has been done in scalping applications or classification at relatively large cut sizes. There is limited work done on screening at feed sizes of minus 150 µm and there are no robust models for wet fine screening application for use in circuit simulation studies.

The effect of feed flow rate, solids concentration and aperture size on wet fine screening performance was evaluated in this study. The range of values of the factors investigated were the feed rate (9, 13, 19, 25, 30 and 35 t/h), screen aperture size (45, 75, 106 and 150 µm) and solids content (30, 40, 50 and 60%). A pilot Derrick screen plant at Mintek in Johannesburg was used for the experiments on a UG2 and chromite ore blend. Screen undersize and oversize samples were collected for particle size distribution analysis and mass balance calculations. The samples collected were filtered, de-lumped and split down to masses ranging between 200 and 300 grams for wet screening using the Malvern MasterSizer particle analyser. The results were used to analyse the effect of the investigated factors on the wet fine screening performance. These results were used to develop a wet fine screening model.

Results indicate that increased feed flow rate and solids concentration lead to finer cut sizes, reduced sharpness of separation and higher water recoveries to the oversize. An increase in aperture size increased the sharpness of separation and decreased the water recoveries to the oversize. The solids concentration appeared to have a higher effect on cut size than the feed flow rate. The highest cut size and sharpness of separation and lowest water recovery to oversize were attained at the lowest feed rate. The lowest solids concentration produced the best performance with regards to all partition curve properties. The cut size approached the aperture size at the lowest throughput and solids concentration for all aperture sizes. All the efficiency curves exhibited fish hooks at fine particle sizes with the fish hooks becoming more pronounced at higher feed flow rates and solids concentration and smaller aperture sizes.

A wet fine screen model that includes multi component ores as well as changes in operating conditions was developed using the 2-parameter Whiten screen model as a basis. The dimensional analysis approach was applied in developing the sub-models that relate the operating and design parameters to the Whiten model parameters. The dimensional analysis approach was further applied to develop the model that describes the fish hook

effect for subsequent incorporation into the overall modified fine screen model. Generally, the modified model is capable of predicting the performance of the wet fine screen reasonably well with minor errors and accommodates for the data that exhibits the fish hook. The model also reduces the fitting process required in the original Whiten model.

Table of Contents

List of Figures

List of Tables

List of Symbols

E_{oi}	Recovery of size i particles to the oversize
M_o	Mass flow rate of the oversize
μ_{sl}	Feed slurry viscosity
A_o	Open Area
C	Water split to the undersize
d_{50}	Cut size
d_{50c}	Corrected cut size
E_{oc}	Corrected efficiency to the oversize
f	Weight fraction of the feed
f_o	Fraction open area
M_f	Mass flow rate of the feed
M_u	Mass flow rate of the undersize
u	weight fraction of the undersize
R_f	Water split to the oversize
o	Weight fraction of the oversize
α	Sharpness of separation
β	Whiten fish hook parameter
β*	Whiten fish hook parameter
π	Dimensionless groups
ρ_p	Pulp density
σ	Whiten screen model parameters
n	Number of times a particle gets presented to the screen surface
p'	Probability of passage for n presentations to the screen surface
p	Probability of passage for a single presentation to the screen surface
L	Screen length
W	Screen width
T	Rate of travel of bed
A	Angle of inclination
x_a	Aperture diameter
x_w	Wire diameter
x_{ae}	Effective aperture diameter
x_i	Geometric mean size
T	Velocity of the bed

D	Bed thickness

CHAPTER 1. INTRODUCTION

The intention of this thesis is to develop a model for wet fine screens based on experimental investigations performed to assess the effect of feed flow rate, solids concentration and aperture size on the overall screen performance.

Communition is the primary stage in the mineral processing industry whose main goal is to reduce the size of the ore whilst liberating valuable minerals. With comminution identified as the most energy and capital cost intensive process (Wills & Napier-Munn, 2006), it has been acknowledged that associating it with classification results in a more efficient and less expensive operation. Over the years, classification has been incorporated in grinding circuits to separate mineral mixtures into different size classes by using either the screens or hydrocyclones as classifying devices. The main function of classifiers in closed grinding circuits is to remove fine material from the circuit and recirculate coarse particles to the mill for regrinding (Mainza, 2004).

The separation mechanism employed is different for each classifier. Screens classify feed particulate into two or more different size classes using particle size as the main variable due to which separation occurs (Drzymala, 2007). This is achieved by means of a physical barrier with apertures of a certain size. Particles smaller than the aperture size (fine particles) will pass through the barrier and the coarser particles will remain on the surface. Screens are one of the oldest and most widely used physical size separation devices with applications in sizing, scalping, grading, media recovery, dewatering and desliming (Wills & Napier-Munn, 2006). They can be used both in wet and dry screening applications. Choice of application is governed by the size of the feed material and the targeted efficiencies. Dry screening is generally used for coarse feed material, i.e. for containing particle sizes greater than 5 mm. Particles below 5mm are characterised as fine particles and are generally separated using wet screening process down to 45 μm (Gupta & Yan, 2006; Wills & Napier-Munn 2006; Svarovsky, 2000).

Wet fine screening is normally accomplished with high frequency, low amplitude, vibrating screens with either elliptical or straight-line motion (Valine & Wennen, 2002). The vibration induced increases the rate of stratification of undersize particles and ultimately the rate of passage of fine particles through the screen surface. It also assists in conveying oversize particles across the screen length (Napie-Munn, et al., 2005). The screening process is affected by different variables including the particle size, aperture size, feed solids concentration, feed flow rate and others (Lawrence & Beddow, 1968; Standish et al., 1986; Soldinger, 2000; Tsakalakis 2001; Trumic & Magdalinovic, 2011).

While screens have been used in mineral processing in over sixty years, they were widely used only in scalping applications or classification at relatively large cut sizes. They were considered impractical in fine grinding circuits due to factors such as high screen panel wear rates, low capacities and excessive panel blinding (Albuquerque et al., 2008). As a result, hydrocyclones became the most commonly used devices for classifying fine slurries due to their ability to process high tonnages when compared to screens. Improvements in wet screening technology have addressed concerns that contributed to the screen inefficiencies. With these improvements, fine screening has shown substantial advantages of screens over traditional hydrocyclone operation in terms of reduced circulating loads and more stringent product control, albeit at limited throughput in comparison. There is renewed interest in the use of screens in fine classification duty as a possible replacement for hydrocyclones in closed milling circuits or as key devices in hybrid classification circuits. The economic advantages of the screen enhancements are the increased production rate and reduced energy consumption due to lower recirculation loads (Valine & Wennen, 2002). Furthermore, the introduction of wear resistant polyurethane panels has decreased both the panel wear and blinding rates.

Despite the developments in screening technology, the publications on fundamental screening research in the past two decades are very few (Hilden, 2006). Most of the research done (Lawrence & Beddow, 1968; Standish et al., 1986; Soldinger, 2000; Tsakalakis, 2001; Trumic & Magdalinovic, 2011) focused on dry screening of relatively coarse particles (>150 µm). There is limited information on screening at sizes below 150 µm and no robust models exist for use in circuit simulation studies. Most screen models do not accurately describe the wet screening operation since they were developed for dry screening. Furthermore most of these models require experimental data to allow for determination of the screen performance and cannot be used for predictions outside the experimental conditions from which they were developed. It is therefore essential to develop a model that is applicable to wet fine screening and incorporates changes in operating and design conditions to enable prediction of the screen performance while minimising the need to perform a lot of experiments.

This study assessed the effect of feed flow rate, feed solids concentration and aperture size on the screening performance using a mixture of the Upper Group 2 (UG2) and Chromite ores. The main aims were to generate a database that will be used to provide insights on the screen performance in wet fine applications and to develop correlations and subsequently provide data towards developing a robust model that predicts the performance of a wet fine screen. The envisaged model will be useful in predicting the screen performance thereby facilitating the simulation of comminution circuits incorporating wet fine screening.

1.1 Hypotheses

The hypotheses for this study are as follows:

For the same feed size distribution:

- An increase in feed flow rate deteriorates the screen performance because of the increased load and rate of transport of particles across the screen length. The finer particles on top layers of the particle bed do not get to be presented to the surface.

- Decreasing the aperture size decreases the screen performance. Decreasing the screen aperture size while maintaining the screen strength will reduce the capacity and efficiency of the screen due to a decrease in open area.

- Increasing the solids concentration will result in a decrease in screen efficiencies. At higher concentrations, the amount of water that transports the fine particles to the screen undersize is reduced and the particle bed presented to the screen surface is thicker and closely packed. The interactions between particles restrict movement of undersize particles through the particle bed which decreases the number of presentations of particles to the screen surface.

- A model can be developed based on the partition curve properties to predict the performance of wet fine screens because apart from the capacity the influence of key operating and design variables are manifest in changes to the partition curve.

1.2 Research Objectives

The main objectives of this work were to:

- Perform experiments to investigate the effect of feed rate and feed solids concentration on the screening performance for screens operating at less than 150 µm aperture.

- Develop a mathematical model to predict the performance of wet fine screens for changing feed conditions and aperture sizes.

1.3 Key Questions

The following key questions were formulated:

1. How does increasing feed flow rate and feed solids concentration affect the performance of wet fine screens assessed by the partition curve properties?
2. How does increasing aperture size affect the performance of wet fine screens?

3. Can a partition curve based model developed from experimental data be used to describe the performance of wet fine screens?

1.4 Thesis Structure

This section describes the structure of the thesis; highlighting the key subjects that are discussed in each chapter.

Chapter 2: Literature Review

This chapter discusses the research done on fundamental screening with regards to how different operating and design conditions affect the screen performance both in wet and dry screening applications. A critical review of the existing industrial screening models is given, highlighting the different approaches taken by each author and discussing the limitations of each model. The principal aim is to identify the gaps in literature and justify why a new model is needed.

Chapter 3: Experimental Methodology

A detailed description of the experimental methodology used for the screening test work is presented in this chapter. It includes description of the experimental test matrix used and the justification for choosing the particular test conditions. The in depth explanation of the sample preparation procedure as well as the test rig set up is given.

Chapter 4: Results and discussion

In this chapter, the experimental results obtained from the screening test work are given. The similarities and differences observed in the results obtained at different conditions are highlighted. A detailed discussion of results, with reference to the literature, is also provided.

Chapter 5: Model development and fitting

The screening efficiency is often reported as a dimensionless number. Chapter 5 describes the dimensionless approach adopted in developing a screen model using a well-known model as the basis. A discussion of the advantages and limitations of the modified model is given alluding to other models found in literature.

Chapter 6: Conclusions and Recommendations

The final chapter summarises the key findings and conclusions drawn in this study and makes recommendations for future work.

CHAPTER 2. LITERATURE REVIEW

This chapter presents an overview of the industrial screening process, different types of screens available and their various applications in the mineral processing industry. While there are a lot of types of screening machines available, the discussion will focus mostly on the vibrating sizing screen. A review of the research done on the effect of operating conditions on the vibrating screen performance is presented. With more attention on the effect of feed flow rate, feed solids concentration and aperture size. The models available for the screening process and the methods used to develop the screen models are discussed. In addition, the gaps in literature are identified to show the necessity for a different approach in wet fine screen modelling.

2.1 Industrial Screening

Screening is a process used to separate solid particulate feed into different size classes. It is one of the oldest and most widely used physical size separation methods for separation of sizes between 40 µm and 300 mm (Wills & Napier-Munn, 2006). The screening process is classified into dry screening and wet screening. Dry screening refers to screening in the absence of water and wet screening utilises water to transport the fine particles through the screen surface. While dry screening is generally used for coarser material (> 5mm), it can also be used to separate particle sizes down to 75 µm (Drzymala, 2007). However, sizes smaller than 75 µm tend to stick on to coarser particles and require wet screening to improve the efficiency of separation (Drzymala, 2007).

There is a wide range of screening devices available in industry and different types are chosen for different applications. Factors such as the ore feed size, screening objective, the desired capacity and efficiency of screening determine the type of screen to use for a particular application (Fuerstenau & Han, 2003; Napier-Munn et al., 2005). Table 2.1., adopted from Fuerstenau and Han (2003), shows the classes of screens as well as their uses. Of these screens, vibrating screens have gained the most success in the mineral processing industry and have made other older screen types (e.g. shaking and reciprocating screens) obsolete (Wills & Napier-Munn, 2006). The discussions in this section are mainly focused on the research done using the vibrating screen. This is the type of screen that was used in this study.

Table 2.1: Classes of screens and their typical uses (Matthews, 1985)

Screen Class	Uses
Grizzly, stationary	Scalping of coarse rock preceding crushers, bins, belts.
Grizzly, moving	Scalping of coarse rock preceding crushers, bins, belts.
Vibrating screen, inclined	Crushing circuits, scalping, high capacity.
Shaking screen, oscillating	0.5 in. + 60 mesh, light, free flowing.
High-speed screen	For fine and ultrafine screening.
Revolving screen	Scrub, wash, rough size; placer mining; capacity and efficiency low.
Sieve bend Dutch State Mines (DSM)	Wet scalping and dewatering from 10 mesh and finer

2.2 Vibrating Screens

2.2.1 Vibration motions

Vibrating screens can be manufactured comprising of one or more screening decks. Thus more than one product with different size classes can be obtained from a single screen. The separation is enhanced by introducing a vibration to the screen according to the desired motion. The types of vibration motions that are commonly used in the mineral processing industry are the circular, straight line and elliptical motions (Figure 2.1). These motions can be used on both the inclined decks and horizontal decks.

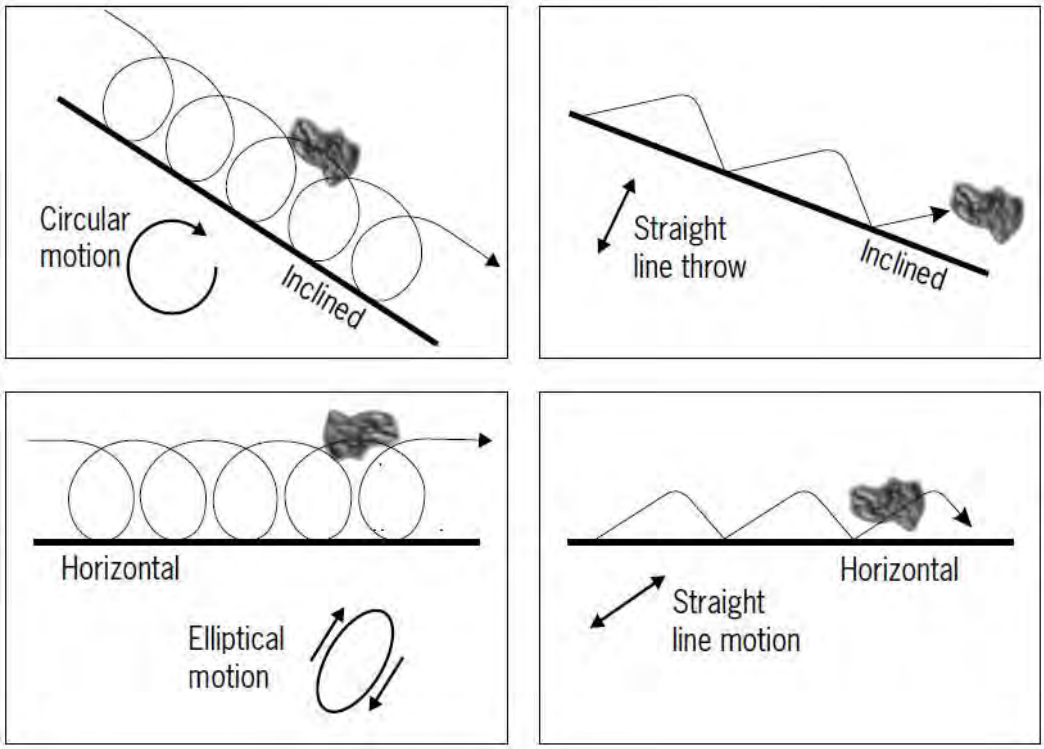

Figure 2.1: Summary of the screen motions (Metso, 2007)

Circular motion is commonly used in inclined vibrating sizing screens. The deck is inclined at angles ranging from 15^0 and 28^0 allowing gravity to assist the flow of material across the screen length (Wills & Napier-Munn, 2006). Low-angle or the linear vibration motion screens are either perfectly horizontal or are inclined at very low angles ($<10^0$) (Gupta & Yan, 2006). These type of screens are commonly designated a "4-bearing", two shafts vibrator which produce either the linear or elliptical vibration motion. The low angle motion screens do not rely on gravity to achieve separation; as a result, they are subject to larger structural forces and higher accuracies of particle sizing (Napier-Munn et al., 2005). However, they have lower capacities in comparison to the inclined screens (Krause, 2005). These types of screens are largely used in fine screening applications where the efficiency is important.

Linear motion can also be installed in a multi-slope screen, for example, the banana screens. The banana screens have varying slopes. Near the feed end the slope is steeper ($20\text{-}30^0$) and gets smaller ($10\text{-}\ 15^0$) towards the discharge end (Beerkircher, 1997). This kind of design cause rapid removal of fine material at the feed end due to the fast flowing feed material. Towards the discharge end, the particle bed is thinner and allows for separation of particles that are slightly smaller/bigger than the screen aperture. The banana screens are used in applications where the feed material has a significant amount of fine particles and they have been reported to have larger capacities compared to conventional vibrating screens (Meinel, 1998). Pictures showing the inclined, linear and banana screens are shown in Figure 2.2.

a)

b)

c)

Figure 2.2: Pictures of different types of vibrating screens: a) Inclined Screen; b) Linear Screen; c) Banana Screen (Wills & Napier-Munn, 2006; Derrick Corporation, 2009)

2.2.2 Screening Media

The choice of the screening surface is important in determining efficiencies and capacities of a screen in a particular application. Types of screening surfaces are categorised according to different sizes, aperture shapes and types of material (Fuerstenau & Han, 2003).

2.2.3 Surface material

The most commonly used screen surface materials are (Napier-Munn et al., 2005):

- woven wire
- perforated plates
- wedge wire
- grizzly bars
- rubber
- polyurethane

Woven wires are the cheapest screening surfaces accounting for about 75 % of sales (Fuerstenau & Han, 2003). However, the polyurethane screen surfaces have become popular in wet screening applications. This is because the polyurethane surfaces known to be wear resistant and reportedly have 10 times the wear life over traditional wire cloth (Wills & Napier-Munn, 2006). They are available with openings as fine as 45 microns and have slotted openings designed with a tapered relief angle to minimize blinding. Figure 2.3 shows pictures of the polyurethane panels. These are the type of panels that were used in this study.

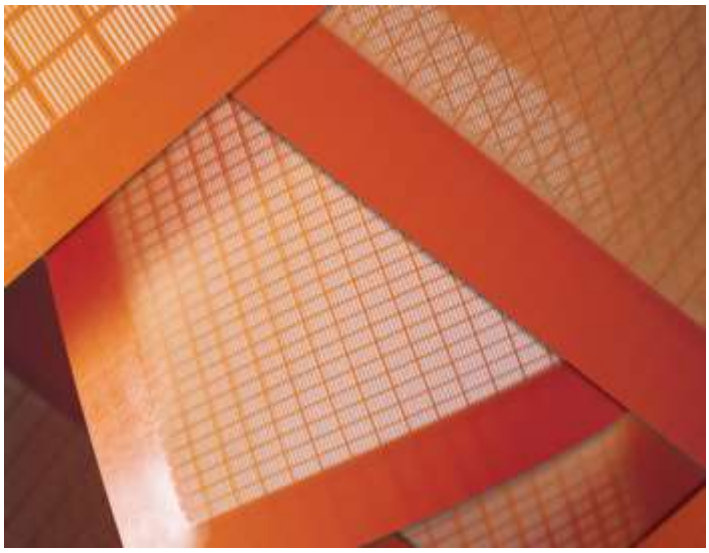

Figure 2.3: A picture showing polyurethane screen panels (Barkhuysen, 2009)

2.2.4 Aperture shapes

As discussed in the previous sections, the degree of separation of a screen is also influenced by the shape of the apertures. The most commonly used aperture shapes include the square, rectangular and round shaped apertures. These are shown in Figure 2.4.

The square mesh apertures are often used for coarse applications. They are mostly used for feeds that contain flabby particles and they provide the most accurate sizing, good wear life and sufficient open area (Napier-Munn et al., 2005). On an incline, the square mesh surfaces provide a small open area compared to the rectangular mesh surfaces (Hilden, 2006).

The rectangular mesh surfaces are used in applications where maximum open area is required. For example, in dry screening these type of surfaces have shown improved separation of material with high moisture content and high clay content (Fuerstenau & Han, 2003). The rectangular shaped apertures were used in this work. The round mesh surfaces are also available in the screening industry and are commonly used in heavy duty applications(Fuerstenau & Han, 2003). Their disadvantage is that they are more susceptible to blinding, which decreases the accuracy of separation.

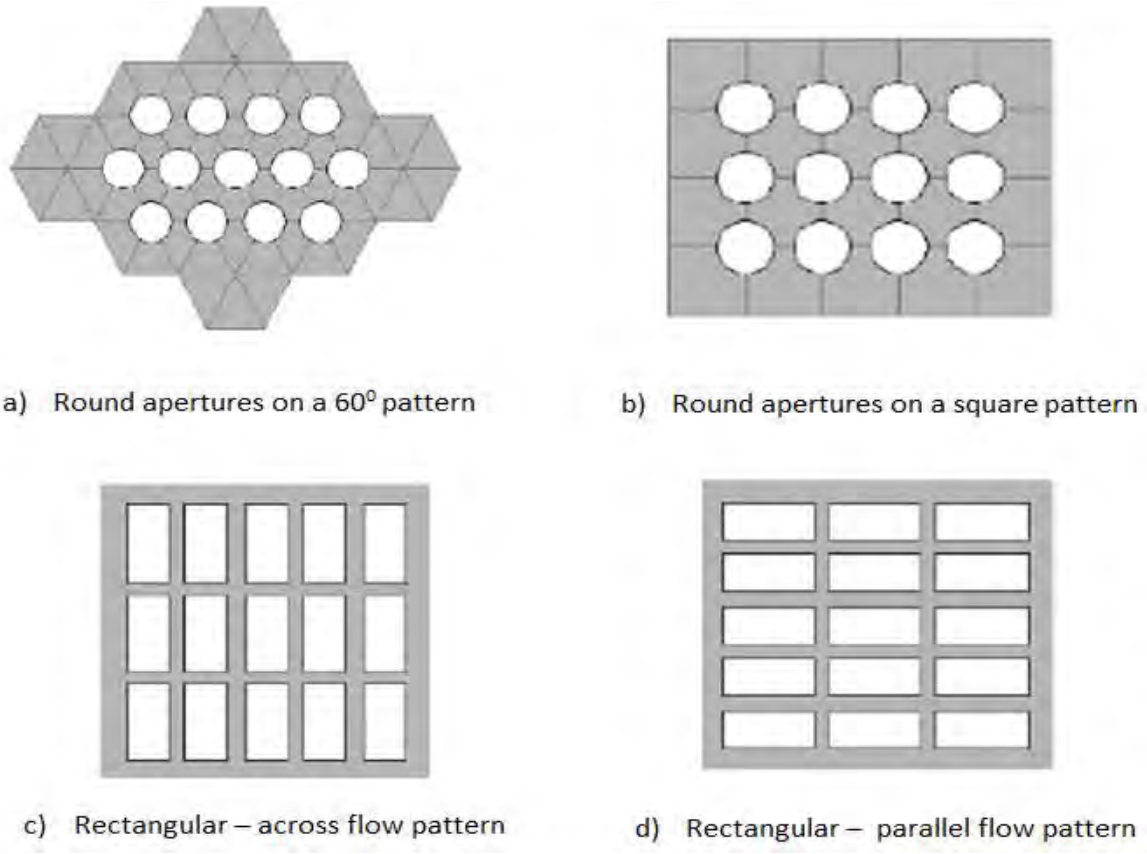

Figure 2.4: Perforation patterns on screen surfaces (Gupta & Yan, 2006)

2.3 The screening separation process

A screen is a separation device used for separating solid-solid material (Wills & Napier-Munn, 2006). In its simplest form, it is comprised of one feed end, one screen panel and two discharge ends. The slurry or solid material is presented to the screen through the feed end and conveyed across the screen length by vibration. As the particles move across the screen, they are separated according to their different particle sizes and are discharged into either the oversize or the undersize discharge products (Gupta & Yan, 2006). A schematic that illustrates the screening process is shown in Figure 2.5.

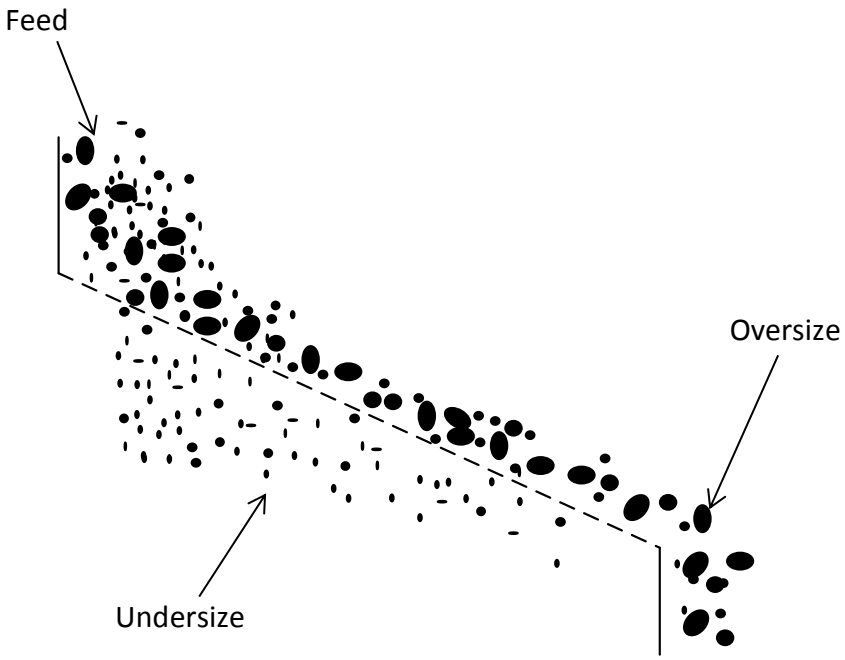

Figure 2.5: Schematic of the screening separation process (Gupta & Yan, 2006)

The separation of particles occurs as particles move along the screen surface/panel. A screen panel is a physical barrier having apertures usually with uniform dimensions (Wills & Napier-Munn, 2006). When the particles are presented onto the screen surface, they will either pass through the apertures or be retained on the screen surface according to whether they are smaller or larger than the size of the screen aperture. Particles that are larger than the aperture are referred to as the oversize particles and those smaller than the aperture are the undersize particles. The oversize particles move along the screen length and are discharged into the oversize collecting chamber while the undersize particles pass through the screen surface and are collected in the undersize stream.

Soldinger (1999) describes the screening process as a combination of three processes, namely the rate of transport of material across the screen length, stratification of fine particles through the particle bed and rate of passage of particles through the screen apertures. The rates at which these processes occur across the screen length vary.

Subasinghe et al. (1989) suggested a three-region behaviour across the screen as shown in Figure 2.6. The curves in Figure 2.6 show the rate of passage of particles and the fraction of material retained on the screen surface with screen length.

At the feed end of the screen (Region I) most of the undersize particles move from upper layers of bed towards the surface of the screen. This is where the rate of stratification of smaller particles beneath the larger ones occurs. Stratification occurs very quickly hence the narrrow region. Region II is where replacement of material from upper layers of the bed equals the flow rate of material passing through the screen aperture. In Region III both the rates of stratification and passage of undersize particles through the apertures decrease (Subasinghe et al., 1989).

The interactions between particles on the screen surface determine whether the screening process is separated or crowded. *Separated screening* refers to screening conducted at very low flow rates such that the particle-particle interactions are negligible (Ferrara and Preti, 1975). In such conditions, the fine particles are presented to the screen surface more frequently and have higher probability to pass through. *Crowded screening* occurs when the interaction between particles is significant (Ferrara and Preti, 1975). This essentially happens at higher flow rates whereby a thicker particle layer is presented on the screen. The interactions between particles restrict movement of undersize particles through the particle bed which decreases the number of presentations of particles to the screen surface.

The particles of sizes closer to the aperture (0.75 to 1.5 times the aperture size) are known as the “near size particles”. These particles are the most difficult to screen because they get stuck in the screen apertures resulting in what is known as screen *pegging*. *Blinding* happens when fine particles agglomerate and form a particle build up that blocks material from passing through the screen aperture. These two phenomena significantly affect the screen performance. When the feed contains dump material, particles tend to agglomarate and blind the screen apertures (Wills & Napier-Munn, 2006). Higher screening rates are achieved when the feed material is completely dry or wet. In wet screening, the material is presented to the screen in the form of a slurry. The fluid in the feed is important because it transports the fine particles to the screen undersize at a higher rate.

Screening can therefore be explained as a combination of the processes explained above. The rate at which these processes occur determines the overall performance of the screen. In this study wet screening was used to test the performance of the vibrating sizing screen.

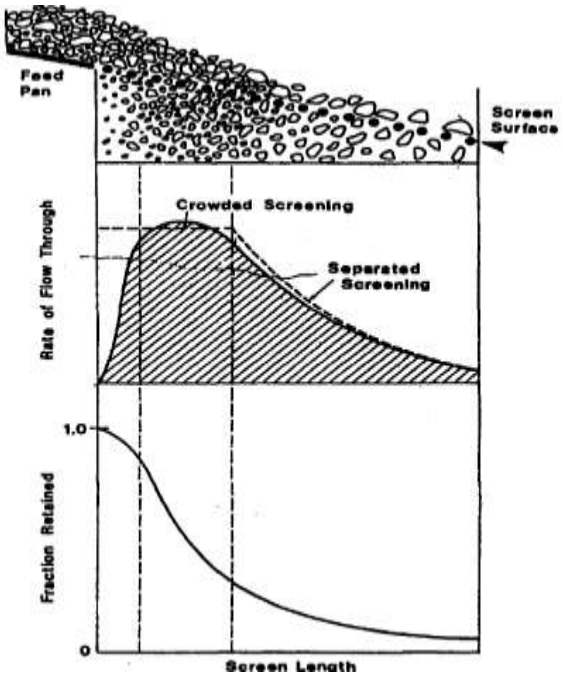

Figure 2.6: Major regions occurring on a screen (Subasinghe, Schaap, & Kelly, 1989)

2.4 Screening efficiency

A universally accepted definition of screening efficiency has not been established and various methods/definitions that describe screening efficiency have been adopted (Wills & Napier-Munn, 2006). The efficiency curve, also known as partition curve, is a kind of classification curve that represents the performance of classifiers and is used to describe the screen performance. It expresses the fraction of a particular size class in the feed that reports to the screen undersize or oversize. The efficiency curve is obtained from performing a mass balance around a separator and calculating the fraction of a particular size class in feed that reports to the oversize (E_{oi}) using an Equation 1 (Napier-Munn et al., 2005). The efficiency to the undersize can be calculated by subtracting E_{oi} from one.

$$\mathrm{E_{oi}} = \left(\frac{\mathrm{o_i} M_o}{\mathrm{f_i} \mathrm{M}_f}\right) \qquad 1$$

Where E_{oi} = actual recovery of size i to the oversize

M_o = total mass flow rate of solids in the oversize stream

o_i = weight fraction of material of size i in the oversize stream

M_f = total solids mass flow rate of the feed stream

f_i = weight fraction of material of size i in the feed stream

A typical efficiency curve shown in Figure 2.7 is generated by plotting the recovery of particles of size i to the oversize against the geometric mean size. In Figure 2.7 the curves are drawn for ideal and actual classification. Ideal classification occurs when there is a perfect separation of particles. Under these conditions, the separation point (cut size) occurs at the size equal to the aperture size. The cut size value gets smaller with larger deviations from ideality as shown by the actual curve in Figure 2.7.

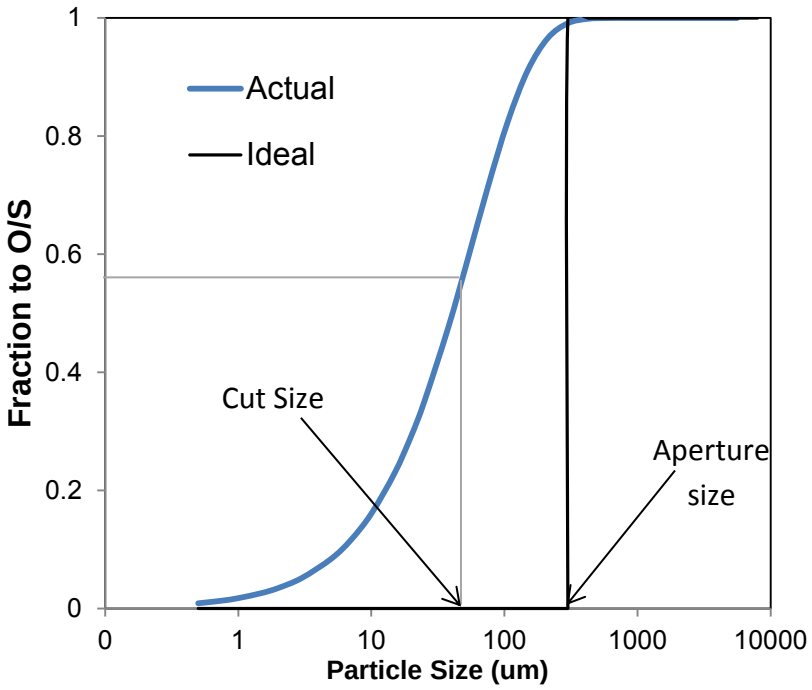

Figure 2.7: The ideal and actual efficiency curves (Wills & Napier-Munn, 2006)

Various studies on classification (Rogers & Brame, 1982; Rogers & Brame, 1985; Nageswararao, 1999; Svarovsky, 2000; Mainza, 2006; Narasimha et al., 2014) have shown that the efficiency curve does not always start from the origin but meets the y-axis at the value of water split to the oversize (R_f). This is because during classification, there is a fraction of very fine particles that do not respond to classification forces and bypass to the oversize stream (Napier-Munn et al., 2006). Kelsall (1953) developed an equation that corrects for the bypass effect (Equation 2). The curve generated using Equation 2 is called the corrected efficiency curve. This curve is important in classification because it describes the efficiency due to classification only. The efficiency curve properties that are used as indicators for the performance of a classifier are extracted from the corrected curve. An example of the actual and corrected curves is shown in Figure 2.8.

$$E_{oc} = \frac{E_{ua} - R_f}{1 - R_f} \qquad 2$$

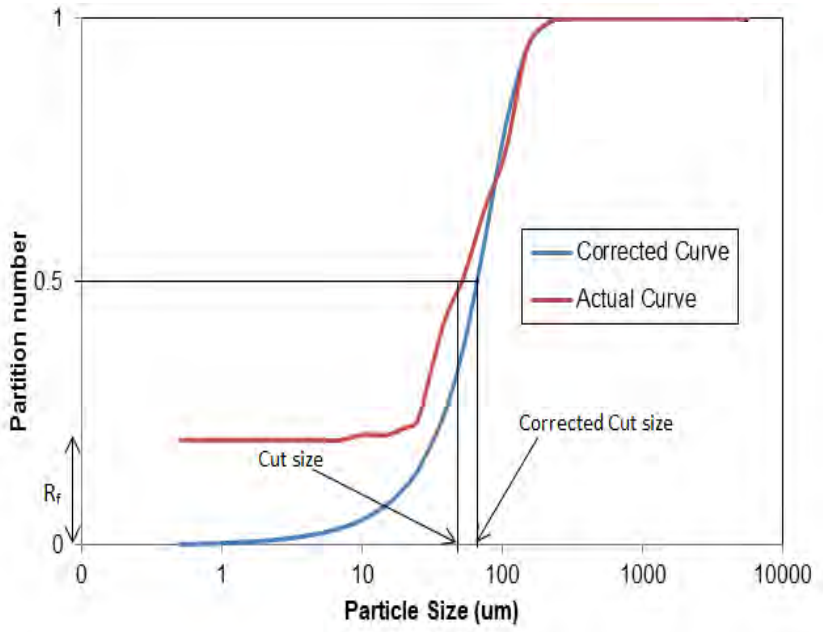

Figure 2.8: Partition curve for a classifier (Svarovsky, 2000)

2.5 Efficiency curve properties

The efficiency curve properties are used to quantify the performance of a classifier. The properties that are important include the corrected cut size (d_{50c}), sharpness of separation (α) and water recovery to the oversize (R_f) (Wills & Napier-Munn, 2006; Gupta & Yan, 2006; Napier-Munn et al., 2006).

2.5.1 Cut size (D50)

The cut size is one of the critical efficiency curve properties often used to assess the efficiency of a screen. It is defined as the size that has a 50 % chance of reporting to the undersize or oversize streams (Svarovsky, 2000). The D_{50c} is the cut size that corresponds to the particle size that has a 50 % probability of reporting to both the oversize and undersize for the corrected partition curve. The cut size is important because it indicate the point where separation occurs. In screens the cut size is always less than the aperture size (Wills & Napier-Munn, 2006). While cut size closer to the aperture size is desired in screening separation, the cut size alone does not indicate the effectiveness of the screening process. It has to be coupled with other efficiency curve properties discussed in the next sections.

2.5.2 Sharpness of separation (α)

The sharpness of separation (α) is a measure of the quantity of misplaced particles in the undersize and oversize streams (Majumder, et al., 2007). During classification, it is desirable to minimize the amount of misplaced material; a sharper cut means that less material is misplaced (Mainza et al., 2005). The sharpness of the cut is related to the general slope of the grade-efficiency curve. Gupta & Yan (2006) calculate the sharpness of separation using Equation 3. This is the slope of the curve between the d_{75} and d_{25} sizes and their respective partition coefficients (Gupta & Yan, 2006). For ideal conditions, the efficiency curve would be a vertical line at the cut size.

$$\text{Slope} = \frac{\mathrm{E}_{75} - E_{25}}{\mathrm{d}_{75} - d_{25}} \qquad 3$$

Where E_{75} and E_{25} are the partition coefficients of 0.75 and 0.25 respectively and d_{75} and d_{25} are their corresponding sizes.

2.5.3 Water recovery to the oversize (Rf)

Water recovery to the oversize is defined as the proportion of water in the feed stream that reports to the oversize (Kilavuz & Gulsoy, 2011). It is an important indicator of the efficiency of a separator particularly in classification that involves further processing before valuable minerals are recovered (Lusinga et al., 2009). Higher water recoveries to the oversize are associated with a decrease in the separation efficiency of the screen, as finer particles become entrained in the oversize stream (Roger & Brame, 1985).

A number of authors (Roger & Brame, 1985; Plitt, 1976; Lynch & Rao; 1968; Whiten, 1966) have developed equations for the corrected efficiency curve. The model that was used to analyse the results that were obtained in this work is shown in Equation 4. This expression is called the Whiten corrected efficiency model.

$$\mathrm{E}_{\mathrm{oc}} = 1 - \mathrm{C}\left(\frac{\exp(\alpha)-1}{\exp(\alpha \mathrm{x})-\exp(\alpha)-2}\right) \qquad 4$$

Where E_{oc} = corrected recovery to the oversize

$\mathrm{C} = \text{fraction of water to the undersize}$

$\mathrm{x} = \frac{\mathrm{d}}{\mathrm{d}_{50}}$

$\alpha = \text{sharpness of separation}$

The fraction of water to the oversize (Rf) was calculated from subtracting C from 1.

Sometimes the efficiency curve exhibits a hook at the fine particle sizes. This phenomenon is known as the fish hook effect. The fish hook has not largely been reported in literature, especially in screens. However, there have been attempts to describe the fish hook effect mostly in hydrocyclones (Nageswararao, 2000; Plitt, 1976; Lynch & Rao, 1968). Whiten used the parameter β to incorporate the fish hook into the model shown in Equation 4. The resulting Whiten fish hook model is given by Equation 5. This equation was used in the analysis of results obtained in this study to calculate the actual efficiency to the oversize. The corrected curves were generated by applying Equation 2.

$$E_{oa} = 1 - C\frac{(1+\beta\beta^{*}x)*(e^{\alpha}-1)}{e^{\alpha\beta^{*}x}+e^{\alpha}-2} \qquad 5$$

Where: E_{oa} = actual efficiency of size d_i particles to the oversize

C = water recovery to the undersize

$x = \frac{di}{D_{50c}}$

β = parameter that corrects for the fish hook effect

β* = a fitting value introduced to preserve the definition of D50c

2.6 Factors that affect screening efficiency

The performance of the screen is influenced by various variables. The variables that are known to affect the screen performance are often grouped into machine/design and operating variables. The design variables include the angle of inclination of the screen deck, screen length and width, screen open area, aperture size and shape and intensity of vibration (Fuerstenau & Han, 2003; Wills & Napier-Munn, 2006; Gupta & Yan, 2006). Operating varibles include the feed flow rate, particle size distribution, feed solids concentration and ore type (Gupta & Yan, 2006; Tsakalakis, 2001). Many of these factors are interrelated and the manner in which they affect the screening performance is complex (Kelly & Spottiswood, 1995). As a result quantitative information about the effect of these parameters on screen performance is often specific to a particular system (feed material and screen design) and some of the data available is contradictory (Hilden, 2006; Kelly & Spottiswood, 1995). This section reviews the literature conducted on the effect of the design and operating parameters on screening efficiency highlighting the variables that are relevant to this work.

2.6.1 Feed distribution and particle size on passage

During the screening process particles either pass through the screen aperture or are retained on the screen surface. In ideal situations all particles larger than the screen

aperture should be retained and recovered as the oversize product and all particles smaller than the screen aperture should pass through to the undersize product. However it has been shown that due to factors such as angle of repose, particle shape, fraction of near mesh particles in the feed, proportion of "small" and "small-to-large" particles, a fraction of particles although smaller than the screen aperture report to the oversize product stream (Gupta & Yan, 2006; Roberts & Beddow, 1968; Standish et al., 1986; Soldinger, 2000; Tsakalakis 2001; Trumic & Magdalinovic 2011).

The effect of particle size and angle of approach to the screen surface is illustrated in Figure 2.9. Particle A is larger than the aperture therefore it will not pass through, Particle B on the other hand will pass through since it is smaller than the aperture in any orientation. Elongated particle will pass through the screen aperture if it approaches the screen deck in an appropriate angle (Particle D), however it will be retained on the screen if the angle of approach is not appropriate (Particle C) (Gupta & Yan, 2006).

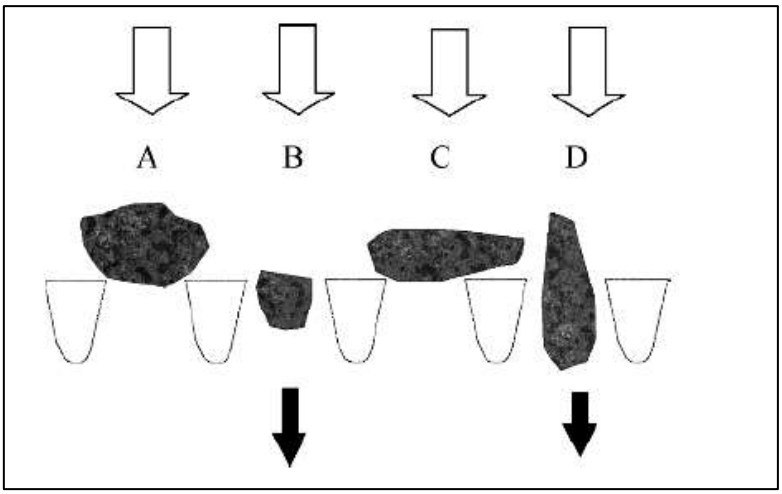

Figure 2.9: Behaviour of particle size and shape at screen surface (Gupta & Yan, 2006)

Effect of particle size on stratification

Stratification is the rate at which fine particles move from the top layers of the bed towards the screen surface. As the screen vibrates, it creates spaces between coarse particles which are then filled by the fine particles gravitating from the upper layers of the particle bed (Soldinger 1999). The effect of particle size and the fraction of fine particles in the feed on stratification has been investigated by various authors (Lawrence and Beddow, 1968; Standish et al., (1986); Subasinghe et al., 1989; Soldinger 1999).

Soldinger (1999) investigated the influence of particle size and bed thickness on stratification. It was observed that when the size of the particles in relation to the surrounding material in the upper layer was decreased, the rate of stratification also decreased. An increase in the rate of stratification was only observed when the bed

thickness was decreased or when the average diameter of coarse particles was increased. Standish et al. (1986) also indicated that the presence of oversize particles in the feed assists the stratification of fine particles.

Some of the factors that influence the stratification process are listed below (Soldinger, 1999):

- Stratification increases with increasing difference in particle size
- Stratification decreases when the overall particle size in a mixture becomes smaller
- Differences in particle density and shape are less important than differences in particle size
- Addition of liquids, such as water

The rate of stratification is also influenced by the proportion of fine particles in the feed material. A study by Lawrence & Beddow (1968) investigated the effect of different proportions of fine particles in a mixture on stratification. The results from this work (Figure 2.10) indicated that when the percentage of fine particles in the mixture was increased, the rate of stratification increased. A further increase in the fraction of fine particles caused a decrease in the rate of stratification. This was observed at fine particle percentages exceeding 60 %. Similarly, Soldinger (2000) highlighted that the share of fine material in a mixture has a considerable influence on the rate of stratification.

In wet fine screening the stratification of fine particles through the particle bed is mainly assisted by the amount of water in the feed. Studies by Valine & Wennen (2002), Albuquerque et al. (2008) and Valine et al. (2009) in wet screening have shown that more efficient screening performance is obtained at higher percentages of water in the feed.

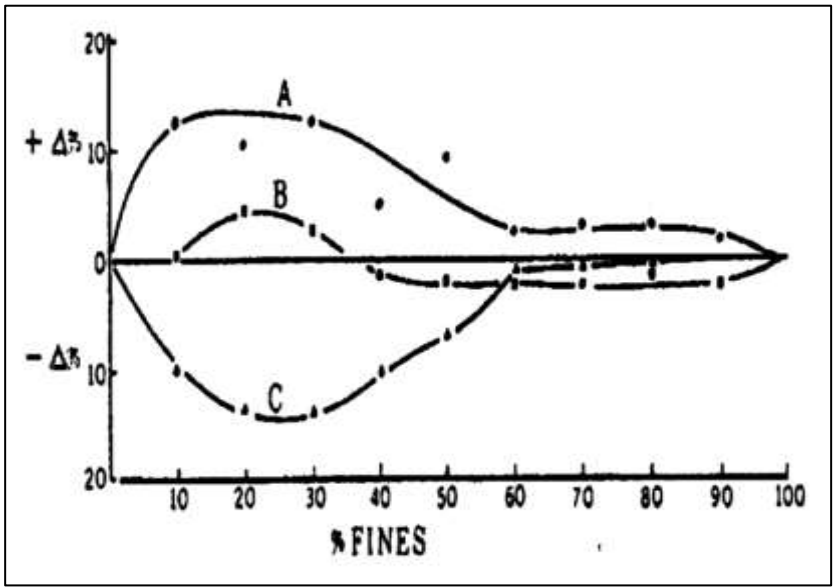

Figure 2.10: Results obtained by Lawrence & Beddow (1968), +Δ and -Δ denote excess of fine and coarse particles respectively

Effect of particle size on passage

For every presentation of particles on the screen surface there is a given probability that a particle of a given size will pass. Wills and Napier-Munn (2006) describe screening as a series of probabilistic events. The ratio of particle size to aperture size determines the probability of passage of particles through the screen. Additionally, the rate of passage is also determined by the amount of fine material in the bottom layer which is in contact with the surface of the screen (Soldinger, 1999).

A study by Standish et al. (1986) investigated the effect of operating variables on the efficiency of a vibrating screen. It was observed that particles of sizes 0.75 to 1.5 times the aperture (the near size particles) are the most difficult to screen. This confirms a well known fact that as the particle to aperture ratio increases, the probability of passage through the screen decreases rapidly (Wills & Napier-Munn, 2006). Tsakalakis (2001) also observed that the near size particles tend to blind the screen apertures which reduces the effective open area of the screen and the screen performance.

The probabilities of passage shown in Table 2.2 were calculated by Taggart (1945) using Equation 6. The figures were calculated for unresticted passage of spherical particles through a square meshed aperture. It can be seen that for every change in the particle-aperture ratio there is a rapid change in probability of passage.

$$p' = (1 - p)^n \qquad 6$$

Where p' = probability of passage for n presentations to the screen surface

n = number of times the particle gets presented to the screen surface

p = probability of passage for a single presentation to the screen surface

Table 2.2: Probability of passage (Wills & Napier-Munn, 2006)

Ratio of particle to aperture size	Chance of passage per 1000	Number of apertures required in path
0.001	998	1
0.01	980	2
0.1	810	2
0.2	640	2
0.3	490	2
0.4	360	3
0.5	250	4
0.6	140	7
0.7	82	12
0.8	40	25
0.9	9.8	100
0.65	2	500
0.99	0.1	10^4
0.999	0.001	10^6

Trumic and Magdalinovic (2011) investigated effect of particle shape on screening efficiency using gravel, metal balls coal, mica, magnesite and copper ores. Figure 2.11 shows the pictures illustrating the shape of particles used for the Trumic and Magdalinovic (2011) experiments. Gravel and metal balls were classified as round particles while coal, mica, magnesite and copper were classified as irregular particles. They noted that round particles gave better screening performance than the irregular particles. Roberts and Beddow (1968) also investigated the effect of particle shape on screening efficiency. They indicated that below 100 µm aperture the level of blinding was higher for spherically shaped particles than it was for irregularly shaped particles. This was attributed to the fact that irregular particles are able to rotate and dislodge from the apertures compared to spherical particles. These results were contrary to those obtained by Trumic and Magdalinovic (2011), as they obtained significantly higher screening rates for round particles compared to irregular particles.

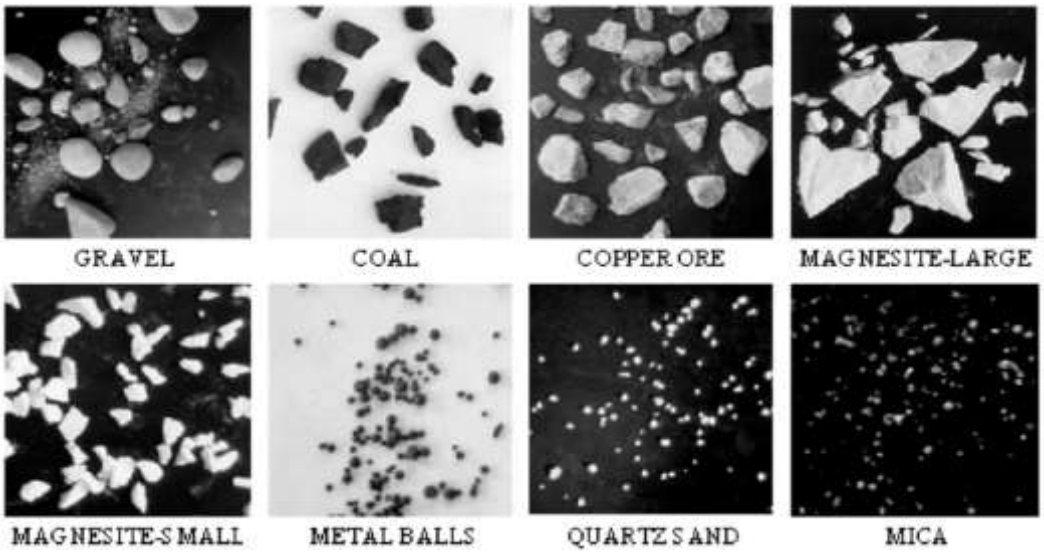

Figure 2.11: Particle shape of the raw materials used in experiments (Trumic & Magdalinovic, 2011)

2.6.2 Effect of Screen aperture size

The size and shape of the apertures are important in determining the capacity as well as the efficiency of the screen (Wills & Napier-Munn, 2006). A change in aperture size often affects the screen open area. Open area is defined as the total area of apertures available for passage of fine particles through the screen surface. To maintain the same open area for finer apertures, thinner wires have to be used. This makes the screen more fragile and result in higher wear rates. Therefore, for applications where the strength of the screen is maintained while reducing the aperture size, the capacity and efficiency of the screen decreases due to a decrease in open area (Fuerstenau & Han 2003). The probability of finer particles reaching and passing through the apertures decreases.

Tsakalakis (2001) studied the effect of aperture size on screening efficiency using crushed quartz. In this study four different screen aperture sizes of 0.6, 1.0, 2.0 and 4 mm were used. It was observed that when the feed particle size distribution is kept constant, higher recoveries where obtained at larger apertures. For instance, efficiencies of 45-50 % and 75-80 % were obtained for 0.6 and 1.0 mm apertures respectively. The significant decrease in efficiency was attributed to a higher content of the near size particles in the 0.6 mm feed (Tsakalakis 2001). This implies that as the aperture size is changed, the content of the oversize, undersize and near size particles in the feed is altered hence the efficiency is affected.

The difference between the aperture size and particle size is an important indicator of the efficiency of screening (Grozubinsky et al., 1998). Grozubinsky et al. (1998) studied the effect of screen slot size, particle size and duration screening on the screen performance. Grozubinsky et al. (1998) indicated that the screening efficiency increased significatly when there is a large difference between particle and aperture size. This was in agreement with what was observed by various authors (Lawrence and Beddow, 1968; Standish et al., 1986;

Subasinghe et al., 1989; Soldinger, 1999) as discussed in the previous section. Roberts and Beddow (1968) used atomised, electrolytic and flake copper powder to investigate the effect of aperture size on blinding during sieving. They observed that the blinding increased sharply as the aperture size was decreased, particularly for material with spherical particles.

2.6.3 Effect of feed flow rate

The feed flow rate is one of the factors that significantly affect the efficiency of the screen. In principle, low flow rates and longer screening times are preferable (Napier-Munn et al., 2005). However, this is not practical in the mineral processing industry due to relatively high feed flow rates required. At high flow rates, the rate of transport of material across the screen length is increased. In addition, there is more material that gets presented to the screen. This results in a thicker particle bed. A thicker particle bed reduces the efficiency of screening because finer particles have to percolate through the particle bed before they reach the screen surface. Depending on the thickness of the bed, some of the fine particles do not get to be presented to the screening surface and are carried over to the oversize stream.

Fuerstenau and Han (2003) indicated that the relationship between the bed thickness, D (in.) solids feed flow rate, M_f (stph), the rate of travel of the bed material T (ft/min) and the effective width of the screen (W) can be estimated using Equation 7. The bed depth at the discharge end of the screen should not exceed n times the screen opening; where n = 2 + (0.02 x bulk density) (Fuerstenau & Han 2003).

$$\mathrm{D} = \frac{400\mathrm{M}_f}{\mathrm{TW(bulk\ density)}} \qquad 7$$

The rate at which the bed material travels across the screen length (Equation 8) changes with the characteristics of motion and angle of inclination (A) of the deck. Therefore, the angle of inclination can be manipulated to achieve the desired bed thickness.

$$\mathrm{T} = 120 + 10\mathrm{A} \qquad 8$$

The effect of feed flow rate on the performance of the screen was investigated by Standish et al. (1986) using quaternary coke and ferrous sinter particles. In this study, it was observed that feed flow rate is one of the factors that affect the performance of the screen. An increase in flow rate resulted in a decrease in screening performance. However the effect of flow rate was very low for the feed containing abundant near mesh particles compared to

the one containing abundant fine particles. Wilkinson (1971) and Ferrara & Preti (1975) also indicated that an increase in feed flow rate decreased the screen performance.

Rogers and Brame (1985) analysed the high-frequency screening of fine slurries using coal, limestone and ore slurries. Contrary to the studies mentioned above, Rogers and Brame (1985) indicated that a variation in feed flow rate showed a negligible effect on the screening perfomance.

2.6.4 Effect of solids concentration

Most of the research done on screening performance has been done on dry applications. The effect of the amount of water in the feed has not been largely investigated in dry screening. It has been shown that the amount of moisture in the feed has a significant effect of the screening performance. Moisture causes fine particles to agglomerate or adhere the oversize particles (Fuerstenau & Han 2003). As a result, agglomerated fine particles either blind the screen apertures or are recovered in the oversize stream. The overall effect is lower screening efficiencies. Due to these complications, it was proposed that screening at less than around 5 mm aperture size must be conducted on perfectly wet material (Wills & Napier-Munn, 2006).

In wet fine screening applications, water is used to transport fine material to the undersize; therefore, the amount of water in the feed (or solids concetration) is crucial. The investigations by Valine and Wennen (2002) on using Derrick screens in wet fine screening applications tested the effect of feed solids concentration on the performance of the screen. The optimum feed solids concentration from which reasonable efficiencies are obtained is 20 % solids by volume (Valine & Wennen 2002). The water pass through the screen surface very quickly, which makes the completion of the screening process occur within a very short length. This is usually overcomed by installing water sprays along the screen or using multi feed screens.

Rogers and Brame (1985) investigated the effect of feed solids concentration on wet screening using limestone and coal slurries. It was observed that increasing the fraction of solids in the feed decreased the screening performance. The screening performance was assessed by developing the partition curves shown in Figure 2.12. The values of cut size (D50) and sharpness of separation (α) listed in Table 2.3 were calculated from the empiral equations developed by Rogers and Brame (1985).

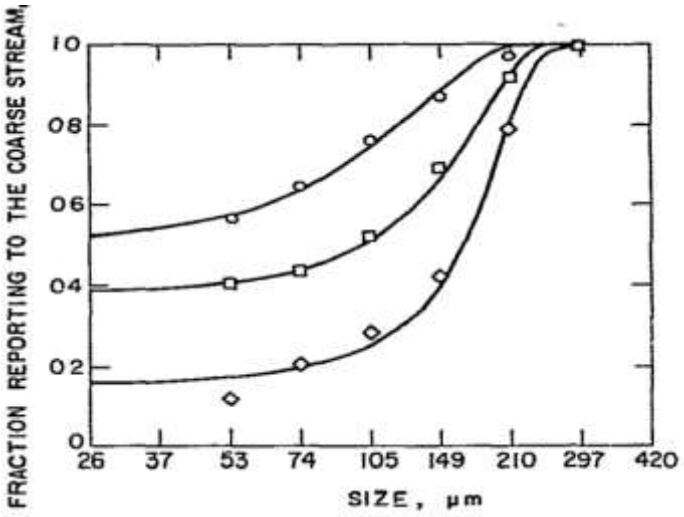

Figure 2.12: Effect of feed solids concentration on screening of coal slurry at 163 l/minm^2 (Rogers & Brame 1985)

As indicated by Figure 2.12 and Table 2.3, higher feed solids concentrations resulted in higher bypass values, finer cut sizes and lower sharpness of separation. This may be attributed to the combined effect of a decrease in water content and thicker particle bed presented at higher feed solids concetrations. The amount of water responsible for transporting fine particles to the undersize is reduced, thus a larger fraction of fine particles do not go through the screen surface but gets carried over to the oversize.

Table 2.3: : Effect of feed solids concentration on cut size and sharpness of separation (Rogers & Brame 1985)

	Vol. solids %	**D50 (µm)**	**α**
○	31.7	108	0.55
□	24.0	155	1.28
◊	16.5	178	1.82

Additionally, Rogers and Brame (1985) observed an increase in the fine particle bypass with increasing water split to the oversize. This confirms the fact that in fine screening, the fine particles follow the water (Wills & Napier-Munn, 2006; Barkhuysen, 2009). If most of the water goes to the oversize, the undersize particles are also carried over to the oversize, hence a poor sharpness of separation is observed.

2.6.5 Summary

Literature shows that the feed flow rate, solids concentration and aperture size have a significant effect on the screening efficiency. A decrease in aperture size has shown a decrease in screen efficiency as reported by most works reviewed. This has been attributed to the decrease in capacity of the screen at smaller apertures. The works indicated that a feed containing a lot of near size material was difficult to screen. This was explained by the fact that the near size particles tend to blind the screen apertures. Additionally, it has been shown that the content of fine particles in the feed critically affects the screen performance.

The effect of shape was not investigated in this study, however, literature showed that particle shape coupled with partcle size significatly affected the screen performance. Contradictory results were obtained with regards to the effect of particle shape. Feed solids concentration is among the important factors that affect the screen performance in wet fine screening applications. However most of the work reviewed was on dry applications. It was indicated that when the amount of moisture in the feed increases, the screening efficiency decreases. For wet screening, poor screen performance was observed at higher feed solids concentrations. Most of the work reviewed also showed that increasing the feed flow rate decreased the screen perfomance significantly. However, findings by (Roger and Brame 2005) showed no significant change in efficiency with increasing feed flow rate.

It is evident from the literature that most of the work published is on dry screening. The information available for wet screening applications is on aperture sizes greater than 150 µm. There is a gap in literature about the performance of screens in wet fine applications. The feed flow rate, solids concentration and aperture size have shown significant effects on screen performance. Therefore a model that incorporates these variables will be useful in simulation studies.

2.7 Screening models

Various authors have conducted extensive research in attempt to find the best way to describe the screening process and a lot of attention has been given mostly to developing and adjusting screen models that best describe the screening performance. The four screen models found in literature (Napier-Munn et al., 2005) can be categorized into the following classes:

1. Probability Models – incorporate the probability of a particle passing through the screen aperture.
2. Kinetic Models – assume that screening is defined by a rate process of a particular order.
3. Empirical Models – based on regression equations derived from experimental data, to predict the partition curve.
4. Capacity Models – used by equipment suppliers in specifying screen design for a given application.

2.7.1 Probability Models

Gaudin's probability model (1939), shown in Equation 9 forms the basis from which most of the probability models were developed. During the screening process, the fine particles may either pass through the screen aperture on their first encounter or may need repeated presentations before they pass through the screen surface. The model relates the probability of passage (p) of fine spherical particles through the screen to the particle diameter (x), aperture size (x_a) and wire diameter (x_w).

$$p = \left(\frac{x_a - x}{x_a + x_w}\right)^2 \qquad 9$$

The model developed by Whiten (1972), shown in Equation 10, extends the probability theory developed by Gaudin (1939). This model describes the partition curve based on the probability of passage of fine particles given by Equation 9 and the number of times the particles get presented to the screen surface. It allows for the possibility of undersize material reporting to the oversize. This is one of the models that are extensively used in modelling screening operations in mineral processing.

$$E(x) = \exp\left[-N\, f_o \left(1 - \frac{x}{x_a}\right)^2\right] \qquad 10$$

Where: E (x) = fraction of particles of size x in the feed that reports to the oversize.

N = number of times the particle gets presented to the screen surface.

$$f_o = \left(\frac{x_a}{x_a + x_w}\right)^2$$

The value of the exponent in the Whiten equation is not always 2. It can either be greater or smaller than 2 depending on different operating conditions (Hess, 1983; Pereira et al., 1993; Hilden, 2006). Therefore it can be replaced by the parameter σ as shown in Equation 11. Equation 11 is the well-known 2 parameter screen model developed by Whiten (1972).

$$E(x) = \exp\left[-Nf_o \left(1 - \frac{x}{x_a}\right)^{\sigma}\right] \qquad 11$$

The operating and design variables such as the feed flow rate, screen length, intensity of vibration and others affect the number of times the particle gets presented to the screen surface. An example of how flow rate affects the number of trials is illustrated in Figure 2.13. It can be seen that the type of screen surface significantly affects the number of trials parameter N. N increases with flow rate up to a certain level, thereafter decreases. N for steel is very high for low flow rates and decreases for high flow rates.

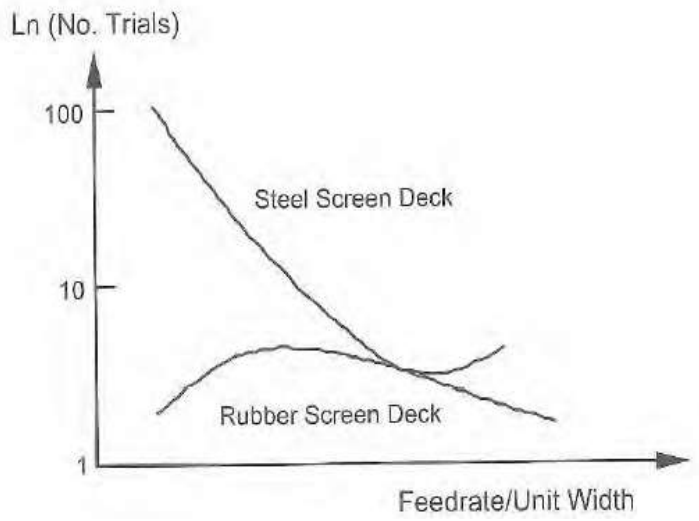

Figure 2.13: The relationship between flow rate and efficiency parameter (N) (Napier-Munn et al., 2005)

The σ parameter is related to the easiness of passage of particles through the screen surface. A value below 2 indicates a higher probability of passage of near size particles than predicted by the Gaudin model. A higher value indicates that the near size particles are less likely to pass through the screen surface (Hilden, 2006).

The restriction of the Whiten model is that it requires experimental data to allow for determination of the efficiency parameters. Therefore it cannot be used to predict the performance outside the experimental conditions. The model is not predictive unless the parameters N and σ are specified. The Whiten (1972) model was used as the basis for the modelling work done in this study and a further discussion of the Whiten model is given in the model development chapter (Chapter 5).

The Miwa (1960) model shown in Equation 12 was also derived from the Gaudin equation (1939). Unlike the Whiten model, the Miwa model does not include the open area into its development. The efficiency of separation is represented as a function of particle size (x), aperture size (x_a), and screen length (L).

$$E(x) = \exp\left[-nL\left(\frac{x_a - x}{x_a}\right)^2\right] \qquad 12$$

The n parameter is the number of trials per unit length that is empirically determined. n can be estimated using Equation 13 (Miwa, 1960). This expression shows the dependency of number of trials on screen length (L), diameter of wire (x_w), effective aperture length (x_{ae}) and cut size (d_{50}).

$$n = \frac{1}{L}\left(\frac{0.833\ (x_{ae} + x_w)}{x_{ae} + d_{50}}\right)^2 \quad 13$$

When equating Equation 12 to 0.5 and rearranging, the expression that can be used to calculate d50 given by Equation 14.

$$d_{50} = x_{ae} - \left(\frac{0.833\ x_{ae}}{\sqrt{Ln}}\right) \quad 14$$

2.7.2 Kinetic Models

Another approach to screening modelling is by kinetic and/or probabilistic approach. Ferrara and Preti (1975) developed a passage model that describes the two distinct types of screening (crowded and separated screening) that occur across the screening length. Crowded screening occurs near the feed end where the screen is heavily loaded. The particle bed is too thick, such that the undersize particles present in the top layers of the bed cannot be presented to the screen surface. The immediate particles on screen surface are the only particles that can pass through the screen aperture. This process was described by Equation 15.

The separated screening occurs near the discharge end where the screen is lightly loaded. At this point, there is no interference between particles and the particles behave like isolated particles. The rate at which particles are presented to the screen surface is directly proportional to the rate at which material passes through the apertures. Proposed equation for these conditions is given by the first order rate (Equation 16).

$$-\frac{dF_L}{dL} = k_c \quad 15$$

$$-\frac{dF_L}{dL} = k_c F_L \quad 16$$

Where: F_L = mass flow rate on the screen per unit width, at a distance L from the feed point

k_C = rate constant

Trumic and Madalinovic (2011) indicated that while the above screening kinetic model (Equation 16) has been widely used in literature it does not accurately describe the screening kinetics. This is due to the fact that Equation 16 assumes that the speed of

screening depends only on the composition of particles on the screen and does not account for the change of probability of screening through time. Trumic and Magdalinovic (2011) modified the kinetic model by introducing the screening probability coefficient (k_p) (Equation 17). The modification to the model appeared to describe the screen performance better.

$$\frac{dm}{dt} = -kmk_p \qquad 17$$

Where m = mass of a particle of size less than aperture size on the screen at time t

k = the screening rate constant

k_p = the change of the probability of screening coefficient

Similarly Standish et al. (1986) also used the kinetic constant that is related to the probability of passage as a measure of the rate of passage of fine particles through the screen surface. The observations showed that the kinetic rate constant was significantly affected by a change in particle size. Despite the fact that the the Trumic and Magdalinovic (2011) model showed improved results in terms of fitting and predicting the screening kinetics, it does not account for stratification of fine particles that happens along the screen length. Which is an important factor especially in dry screening application.

Subasinghe et al. (1989) describe the screening process using two rate constants k_s and k_p for stratification and passage respectively. The Subasinghe et al. (1989) model is given by Equation 18.

$$E(x) = \frac{[k_s \exp(-k_p L) - k_p \exp(-k_s L)\,]}{k_s - k_p} \qquad 18$$

The constants are solved for empiricaly from the experimental data obtained at different positions along the screen. These constants are similar to the k and c parameters used by Solidinger (1999). The Soldinger (1999) model was developed by incorportating both the stratification and passage processes simultaneously. The model captures changes in feed parameters, i.e. particle size distribution and feed rate and the machine parameters tested are the intensity of vibration (frequency and stroke), screen length and width, screen angle of inclination and aperture size. It also includes the bed flow model that interrelates the intensity of vibration and the angle of inclination (Soldinger,2000). The Soldinger model is implimented into a computer program which makes it easier to solve. It requires experimental data for fitting to solve for the model parameters.

The above models take into account several material and machine parameters which are important in describing the screen performance. However, they were all developed for dry screening applications. The mechaninsms for passage in wet screening are expected to be different from the onces in dry screening since in wet screening, passage of fine material is mainly due to the fluid.

2.7.3 Empirical Models

The main aim of the empirical models is to predict the fraction of particles in the feed that have passed through the screen surface (Wills & Napier-Munn, 2006). The Karra (1979) model (Equation 19) gives a relationship between the fraction of particles of size i in the feed that reports to oversize, the particle size and the cut size. Karra's model is restricted to the experimental data from which it was developed. This makes it difficult to apply it in other applications. In addition, it does not account for changes in the operating and design parameters such as the feed flow rate, aperture size and feed solids conentration.

$$E_{oi} = 100\left(1 - \exp\left(-0.693\left(\frac{x_i}{d_{50}}\right)^{5.846}\right)\right) \quad 19$$

Where E_{oi} = fraction of size i particles in the feed that reports to the oversize

x_i = geometric mean size

d_{50} = size corresponding to E_i = 50

The Hatch and Mullar model (1979) was developed using small particle statistics. This is a similar approach to the one used by Mohanty (2003) where statistical techniques were used for modelling the screening process. The model takes into account changes in the feed rate, aperture size and feed size distribution. It also allows for the calculation of the fraction of undersize particles carried over to the oversize. The efficiency of particles to the oversize is given by Equation 20.

$$E_{oi} = C_i + \frac{(1 - C_i)}{1 + \left(\frac{\exp\left({d_{50}}^3 - {x_i}^3\right)}{k}\right)} \quad 20$$

Where Ci = fraction of particles of size i that reports to the oversize

k = constant that depends on the feed rate, size distribution and aperture size

A modified version of the Hatch and Mullar (1979) model was developed by Batterham et al. (1980). In additon to changes in aperture size, feed flow rate and feed size distribution, Batterham et al. (1980) also investigated the effect of moisture content in the feed. The fraction of the oversize product for each size interval $-x_2 + x_1$ (Ea) is related to the constant k and the cut size by the expression given in Equation 21.

$$E_a = 1 + \frac{k}{x_2 - x_1} \ln \left\{ \frac{1 + \exp(\frac{x_{50} - x_2}{k})}{1 + \exp(\frac{x_{50} - x_1}{k})} \right\} \quad 21$$

The Batterham et al. (1980) efficiency equation does not explicitly have the aperture size. However, it is one of the models that can accurately predict the screening operation and is easy to implement (Napier-Munn et al., 2005).

Mohanty (2003) developed an empiral model that describes the efficiciency of a screen using statistical software. For a constant feed solids concentration, the screen efficiency (E) and imperfection functions (I) are given by Equations 22 and 23 respectively. The imperfection function calculates the sharpness of separation. This model was developed from experimental data using the Pansep screen. It accounts for changes in volumetric feed rate, linear velocity and spray angle. The model is only applicable within the experimental conditions from which it was developed.

$$E = 100.43 - 0.04A - 0.54B - 0.035C + 0.00012A^2 \quad 22$$

$$I = 0.28 + 0.0008A + 0.062B - 0.0014C - 0.000003A^2 + 0.00041AB \quad 23$$

Where A = volumentric feed rate (lpm)

B = screen linear velocity (m/min)

C = spray angle (^{0})

2.7.4 Capacity Models

The main aim of the capacity models is to determine the screen area required once the screen type has been established (Wills & Napier-Munn, 2006). These models are frequently used by the screen manufactures. The standard relationship used to calculate the theoretical area of the screen required is given by Equation 24.

$$\text{Theoretical area required} = \frac{\text{Total undersize in the feed (t/h)}}{\text{A x A1 x A2 x A3 x A4 x A5 x A6}} \qquad 24$$

Where A = flow rate (t/h) of the undersize per unit area

A1 = fraction of oversize in the feed

A2 = fraction of halfsize (particles less than half the aperture size) in the feed

A3 = deck location

A4 = wet screening

A5 = bulk density of material

A6 = percent open area

A7 = shape of aperture

The standard capacity model can be modified by incorperating other factors such as the type of screening used (either dry or wet screening), the size of the apertures, whether a top or a bottom deck screen etc. However the capacity-based models should be used with discretion as they are only guide (Olsen and Coombe, 2003).

2.7.5 Summary

The models that are discussed above were mostly developed for dry screening applications. This indicates that the models that can be used in wet fine screening applications are limited. Most models do not explicitly show how the model parameters are affected by changes in feed conditions. The model parameters have to be refitted for every change in feed and design conditions. There is therefore a need for a wet fine screen model that incorporates feed conditions while minimising the fitting process.

CHAPTER 3. EXPERIMENTAL METHODOLOGY

3.1 Introduction

This chapter presents a description of the experimental approach followed to assess the effect of feed solids concentration, feed flow rate and aperture size on the performance of a vibrating screen. The data was then used to develop a model for wet fine screens. The wet fine screen testwork was conducted at Mintek, Johannesburg using the Derrick single deck screen and the material used as feed was a mixture of the UG2 and Chromite ores. The samples were processed both at Mintek and University of Cape Town (UCT) Centre for Minerals Research (CMR) laboratories.

The chapter starts by explaining the major equipment used for feed ore preparation as well as the method followed to obtain the target feed particle size distribution. This is followed by a description of the Derrick screen test rig and the screening test procedure adopted for this study. The final section explains the sample processing procedure followed at the UCT CMR laboratories.

3.2 Feed ore preparation

3.2.1 Ore type

A combined ore consisting of Upper Group 2 (UG2) and Chromite ore samples was used for this work. UG2 is a platiniferous chromitite layer whose mineralogy varies depending on the geographic location within the complex (Nel et al., 2005). Its predominant constituents are the silicates and chromites. The chromite ore has chromium and iron as the main constituents. Table 3.1 shows the ore constituents as well as their relative densities.

Table 3.1: Main constituents of the ore taken from Mintek

Constituent	Relative Density
Chromite	4.97
Silicates	2.80

3.2.2 Equipment and materials

The particle size distribution of the feed to the screen is very important when conducting the testwork for screens because the amount of undersize in this stream determines the performance of the screen. The target was to produce the feed containing sufficient quantities of the minus 75 micron material (50 % passing 75 um) to ensure that there was sufficient undersize even for aperture sizes down to 45 microns. This was achieved by a series of continuous ore crushing and screening using a laboratory 2 ton cone crusher and a vibrating SWICO screen shown in Figure 3.1.

Figure 3.1: Pictures of the cone crusher and screen used during ore preparation

The initial step of ore preparation was to remove the inherent moisture from the ores by exposing the material to air and sun drying until the moisture content was below 5 % by weight. A 1 ton sample of the UG2 ore was crushed using the cone crusher. The crushed ore was then screened at 1 mm using the SWICO screen. The undersize material from the screen was collected and combined with the fine Chromite ore while the oversize product was sent back to the cone crusher for further size reduction. The procedure was repeated until the particle size of 80 % passing 1 mm was obtained.

A 1 ton sample of the chromite ore was screened at 600 µm. About 800 kg of the minus 600 micron was obtained from the 1 ton. The undersize products of both ores were thoroughly mixed using the mechanical blender. The ore was then split into 50 kg batches using the "coning and quartering" method as shown in Figure 3.2. The coning and quartering procedure was adopted from Schumacher et al. (1990).

A representative 10 kg sample was obtained from the bulk ore and split into 1 kg sub samples using a ten cup rotary splitter shown in Figure 3.3. Two random sub samples from the rotary splitter cups were then combined and sent to the analysis lab to determine the feed size distribution and specific gravity.

Figure 3.2: Pictures showing ore preparation process: a) Coning and quartering, b) Mechanical blending

Figure 3.3: A picture of a rotary splitter used during sample preparation

The particle size distributions from different batches were plotted and compared as shown in Figure 3.4. It can be seen that the particle size distributions from different batches are fairly similar, indicating homogeneity within the batches. It can further be noted that the feed contained a considerable amount of sub 75 µm material and this feed size distribution was generated to ensure that there was enough undersize material even for the 45 µm tests.

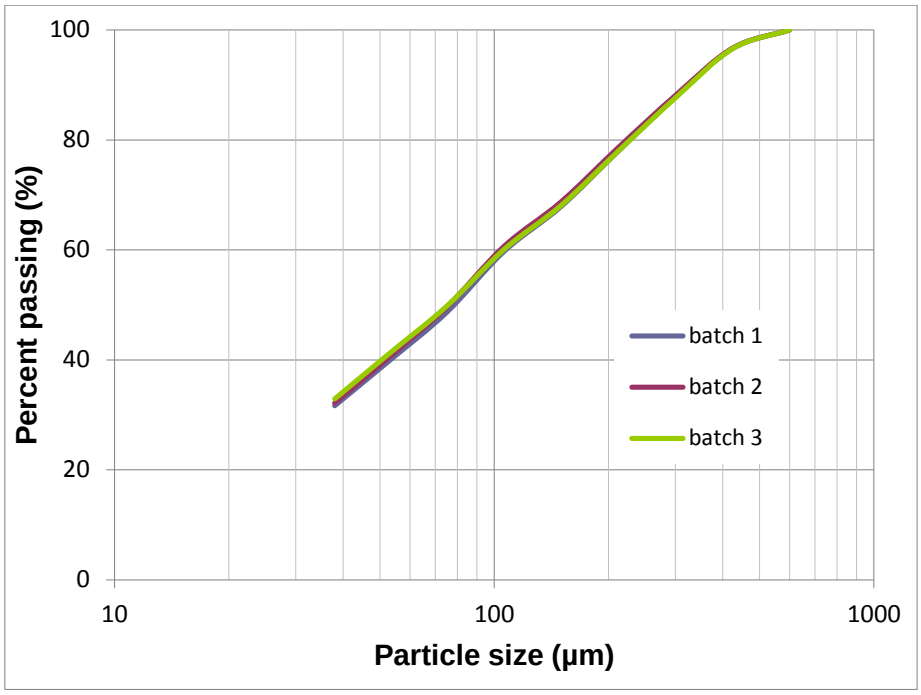

Figure 3.4: Feed size distribution for the UG2-Chromite ore used for the screen testwork

3.3 Description of the screen test rig

3.3.1 Derrick Screen

The screen that was used for the testwork is the single deck Derrick screen manufactured by Derrick Corporation. The major components of the screen are the feed box, dual vibrating motors, screen panels, oversize and undersize collection pans and spray pipes (Derrick Corporation, 2009). Figure 3.5 shows a labelled picture of the screen and the specifications are given in Table 3.2.

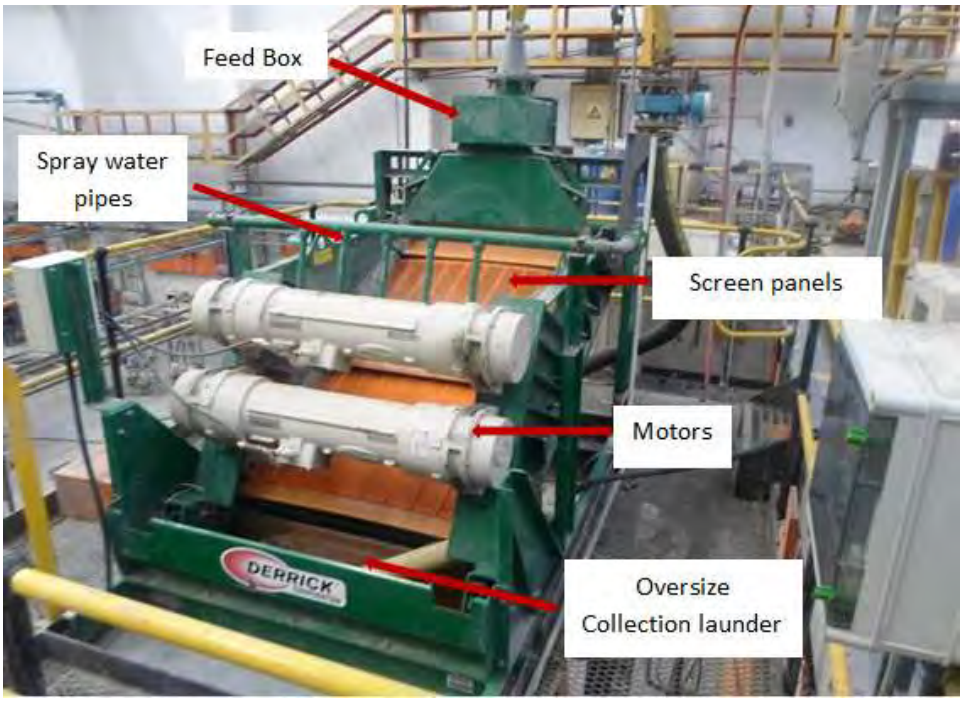

Figure 3.5: Single deck Derrick Screen used for the testwork

Table 3.2: Specifications of the Derrick screen given by Mintek

Screen model	MA017318
Number of decks	1
Angle of inclination (degrees)	17.5
Frequency of vibration (Hz)	42

The description of each component as described by Derrick Corporation (2009) is given below:

The feed box

The feed slurry from the sump is presented to the screen through the feed box. The feed box is used to distribute the slurry evenly across the screen width so as to allow for screening to occur.

Screening panels

The deck is equipped with two 1.22 m x 0.76 m polyurethane screen panels arranged in series. Undersize material passes through the panels into the undersize collection pan which discharges into the undersize chamber and the oversize remains on the screen surface and collected in the oversize chamber

Motors

The vibration is induced through rotating motors that produce a constant frequency and motion throughout the screen. This assists with stratification and passage of undersize particle as well as conveyance of oversize material across the screen

Repulping Section

In between the two panels, there is a rubber-lined trough available for repulping the material as shown in Figure 3.6. To repulp the slurry, water is sprayed on to the material from the first panel. The provision for repulping is available so that additional water is introduced to reproduce the slurry to promote the passage of undersize particles on the panels after the repulp zone.

Figure 3.6: Picture showing the repulping trough on the screen

3.3.2 Experimental set up

The screen test rig that was used for the test work is installed at Mintek. A schematic and picture of the screen rig is shown in Figure 3.7 and Figure 3.8, respectively. The major components of the circuit were a 300 litre sump used for preparing the feed slurry, a slurry pump for pumping the slurry from the sump, and a single deck Derrick screen. The feed valve and the bypass on the feed line are used to control the feed flow rate. There is a flow meter on the feed line located at a position after the feed valve and close to the screen that indicates the flow rate of the slurry presented to the screen. The flow rate measurements taken over a period of time at small intervals from the flow meter are used as an indicator of whether or not the system has reached steady state. The screen has two discharge ends for the undersize and oversize material. On the schematic, the sampling points for the undersize, oversize and feed are labelled 1, 2, and 3 respectively.

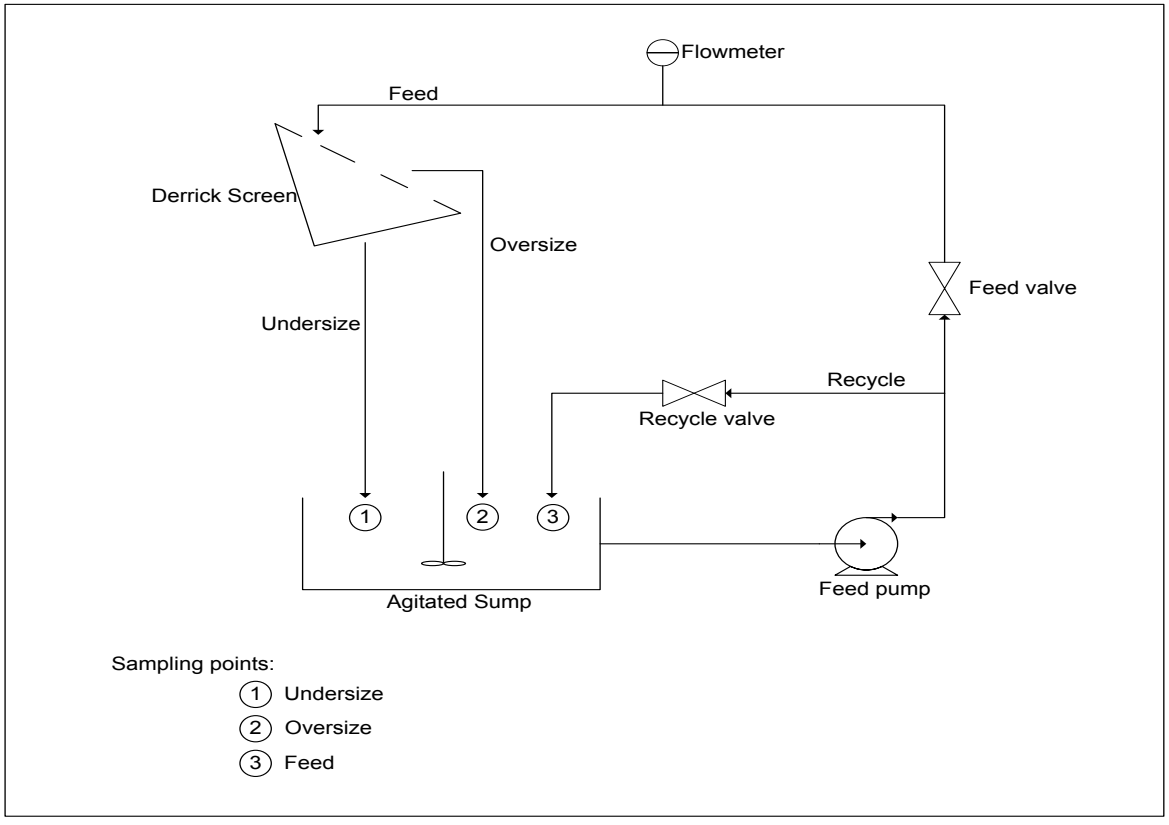

Figure 3.7: Schematic of the set-up of the experimental test rig

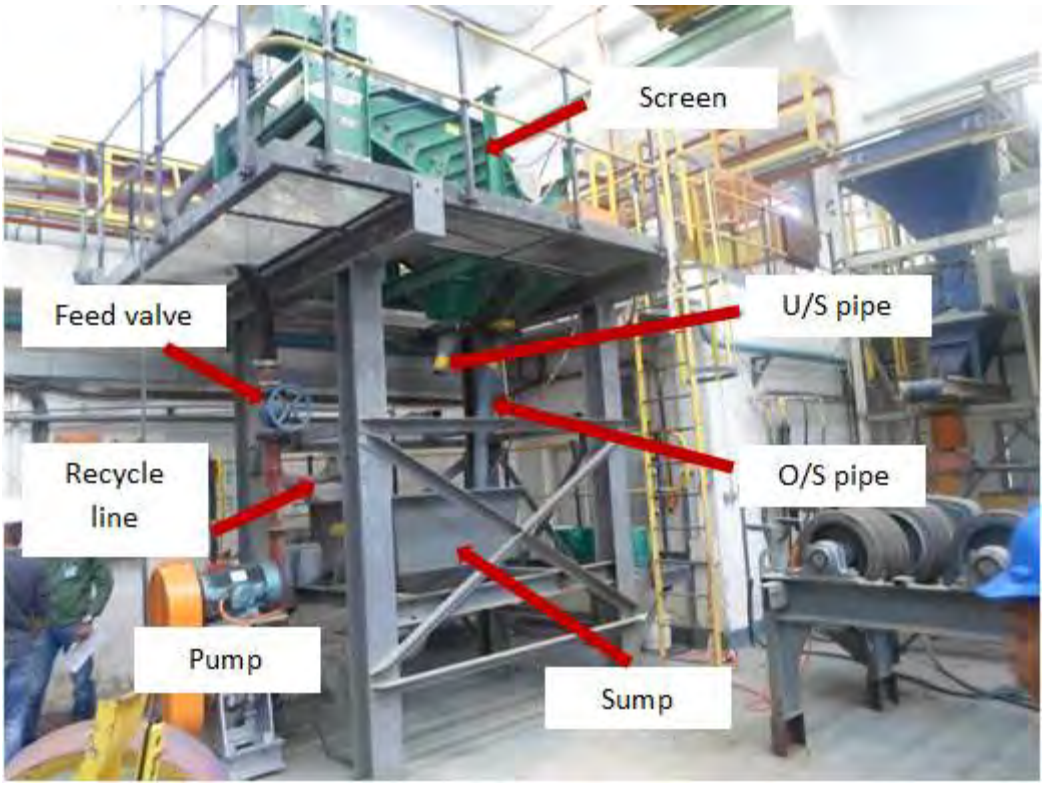

Figure 3.8: Picture of the experimental test rig

3.4 Experimental Test procedure

3.4.1 Test Matrix

The test matrix designed for this study is given in this section. Each variable was carefully selected with reference to conditions in real plant conditions. There was a slight difference in the flow rates tested for each aperture due to differences in open areas available for each screen panel. Smaller apertures have smaller open areas and lower capacities when compared to larger apertures. The open areas given for each aperture are presented in Table 3.3. It can be noted that as aperture size of the panels increased, the open areas also increases. An exception is observed for the 150 µm panel which has a larger open area than the 106 µm panel. Fine screens can have the same or greater open areas than coarse screens but the wires used have to be thinner and hence are more fragile" (Wills & Napier-Munn, 2006).

Table 3.3: Open area of the panels used in this study

Aperture (um)	Open area (%)
45	28
75	30.8
106	35.8
150	34.5

The experimental matrix shown in Table 3.3 gives the conditions that were tested in this study. For each aperture, a full factorial design was adopted using the Design Expert software. However, due to the restrictions presented by the ore type and the differences in capacities for each aperture, flow rates were allowed to vary slightly from the planned levels.

Table 3.4: Experimental Test Matrix

Aperture (µm)	% solids	Flow rate (t/h)						
		9	13	16	19	25	30	35
45	30	✓	✓					
75		✓	✓					
106		✓	✓					
150					✓			
45	40	✓	✓	✓	✓			
75		✓	✓	✓	✓			
106		✓	✓	✓	✓			
150			✓		✓			
45	50	✓	✓		✓	✓		
75		✓	✓		✓	✓		
106		✓	✓		✓	✓		
150			✓		✓	✓		
45	60		✓		✓	✓	✓	
75			✓		✓	✓	✓	✓
106			✓		✓	✓	✓	✓
150			✓		✓	✓	✓	✓

3.4.2 Selection of experimental variables

Feed solids concentration

For a given aperture, the feed solids concentration was varied from 30 to 60 % in increments of 10. This range of feed solids concentration was chosen because it captures the typical solids concentrations used in real plant operations. For example, in the case studies from Valine and Wheeler (2009) where Derrick screens were used in closed grinding circuits, the solids concentrations in those streams ranged from 30 – 55 %. This formed the basis of variation of solids concentrations in this study. Solids concentrations greater than 60 % are not encouraged for wet fine screens because the screen becomes problematic.

Feed flow rate

Similar approach as the one for solids concentration was taken when selecting the feed flow rates. Typical feed flow rates in industry for a single deck Derrick screen range from 20 to 40 t/h (Valine & Wheeler; 2009). This was taken into consideration when choosing the feed flow rates to test in this study. However, feed flow rate depends on both aperture size and the ore type and these limitations were taken into consideration when designing the text matrix.

Aperture size

The aim of the study was to assess the performance of a screen in wet fine screening applications. Therefore smaller apertures were chosen in order to fulfil the purpose of this study. The smallest aperture tested was determined by the smallest panels commercially available for Derrick screens. In this case Derrick screen Corporation could supply the 45 µm panels. The choice of the largest aperture was based on the fact that there is sufficient data in literature on apertures greater than 150 µm have been largely been tested in literature (Rogers & Brame 1985; Grozubinsky et al., 1998; Tsakalakis 2001).

3.4.3 Screening test procedure

Prior to conducting tests the screen panels with the desired aperture size were installed on the screen. The feed was then prepared by mixing a measured quantity of ore and water in the sump. The solids were kept in suspension by using an agitator. After ensuring that the suspension was well mixed, the screen feed pump was started up and feed flow rate adjusted to the required level. A feed sample was cut from the recycle line to measure the specific gravity using the Marcy scale. If the specific gravity was significantly higher or lower than the desired level, more water or solids were added in the sump. The system was allowed to stabilise at the desired feed flow rate. Steady state was achieved when there were minimal fluctuations in the flow rate indicated by the flow meter. The screen was operated with both the undersize and oversize reporting to the feed sump as shown in Figure 3.9.

Samples of the feed, oversize and undersize were cut after the system had reached steady state. For each sample, an A sample for processing and B sample for back-up were obtained and stacked in pre-weighed plastics. The time taken to cut the oversize and undersize samples was recorded to obtain the flow rate measurements. The samples were weighed immediately after the test to obtain the wet masses. They were then filtered and dried in an oven overnight.

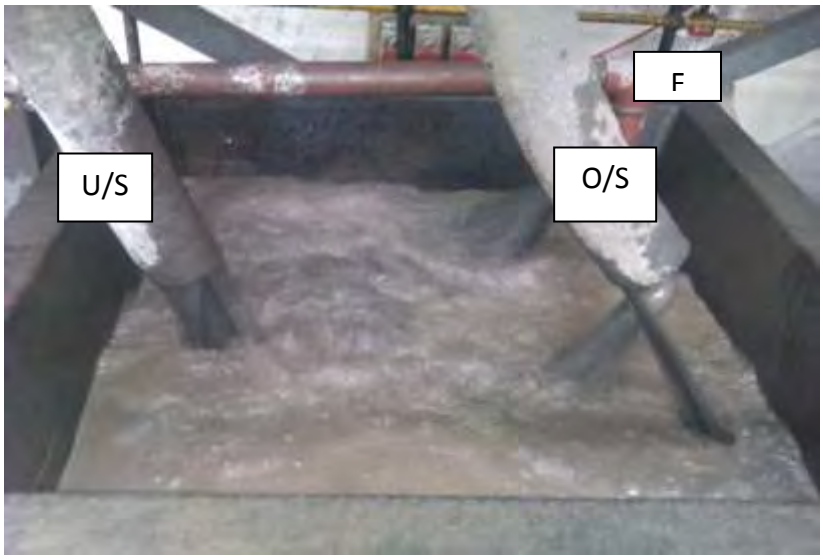

Figure 3.9: Sampling points for Feed (F), Undersize (U/S) and Oversize (O/S)

3.5 Sample Processing

Wet samples of the feed, oversize and undersize were filtered using the filter press shown in Figure 3.10 and dried overnight. The dry samples were weighed and the actual solids concentration for each sample was calculated from the wet and dry masses of the respective sample. The flow rate of the oversize and undersize for each sample was calculated from the dry masses and the sampling times recorded for that particular sample. To obtain particle size measurements, the sample was prepared by delumping the material from the sample using a 1 mm screen and splitting to obtain sub sample of 300 g using a 10 way rotary splitter. The 300 g sub samples were then packed and processed at the Centre for Minerals research laboratories.

Figure 3.10: Picture of a Filter press used during sample processing

The particle size distributions were obtained using the Malvern MasterSizer 2000 particle size analyser available at the Centre for Minerals Research laboratories. Prior to obtaining the particle size measurements, the 300 g samples from the testwork were further split to obtain 1.2g sub samples using the micro rotary splitter. Each sub sample was then analysed using the Malvern particle analyser to obtain the particle size distributions of the respective samples.

3.6 Assessing the reproducibility of results

Selected tests were conducted in duplicates to assess the reproducibility of the results by using the standard deviation (SD) and standard error (SE) indicators of reproducibility. The standard deviation, calculated by Equation 25, indicates the difference between the results obtained from the repeated tests. Low values of standard deviation means that there are minor differences between the results while larger values indicate significant differences. Standard error on the other hand is calculated by Equation 26 and indicates the deviation of result from the mean.

$$SD = \sqrt{\sum_{x=i}^{N} \frac{(x_i - \bar{x})^2}{N-1}} \qquad 25$$

$$SE = \frac{1}{\sqrt{N}} \sqrt{\sum_{x=i}^{N} \frac{(x_i - \bar{x})^2}{N-1}} \qquad 26$$

Where SD = Standard deviation

SE = Standard error

N = Number of tests

Table 3.5 shows the standard deviation and standard error with reference to the feed, oversize and undersize for tests done at 45, 75m 106 and 150 µm aperture size for different flow rates and aperture sizes. The corresponding efficiency curves are shown in Figure 3.11. It can be seen that the standard deviations and standard errors for all the variables are low indicating that the result was reproducible. The minor variations were expected because of the errors introduced during sampling in this kind of operation.

Table 3.5: Reproducibility of results based on the solids and water flow rates and the % solids

Ap. (µm)		solids rate (t/h)				Water flow rate (t/h)				% solids			
		Run 1	Run 2	SD	SE	Run 1	Run 2	SD	SE	Run 1	Run 2	SD	SE
	Feed	23.7	22.4	0.9	0.6	41.9	40.8	0.8	0.5	36.1	35.4	0.5	0.3
	U/S	9.3	8.5	0.6	0.4	24.5	26.7	1.6	1.1	27.6	24.1	2.5	1.7
45	O/S	14.3	13.9	0.3	0.2	17.4	14.1	2.3	1.7	45.2	49.6	3.2	2.2
	Feed	35.5	32.9	1.8	1.3	23.6	25.8	1.5	1.1	60.0	56.0	2.8	2.0
	U/S	12.1	13.5	1.0	0.7	4.3	5.7	1.0	0.7	73.9	70.3	2.5	1.8
75	O/S	23.4	19.4	2.8	2.0	19.4	20.1	0.5	0.4	54.7	49.1	3.9	2.8
	Feed	8.7	9.5	0.6	0.4	17.5	16.4	0.7	0.5	33.2	36.7	2.5	1.7
	U/S	5.4	4.9	0.4	0.3	16.8	15.5	0.9	0.6	24.4	24.0	0.3	0.2
106	O/S	3.3	4.6	0.9	0.7	0.7	0.9	0.1	0.1	82.2	83.6	1.0	0.7
	Feed	21.8	22.7	0.6	0.4	21.8	22.5	0.5	0.3	50.0	50.2	0.2	0.1
	U/S	13.8	12.8	0.7	0.5	19.3	17.0	1.6	1.1	41.7	43.0	0.9	0.6
150	O/S	8.0	9.9	1.3	0.9	2.6	5.5	2.1	1.5	75.8	64.3	8.2	5.8

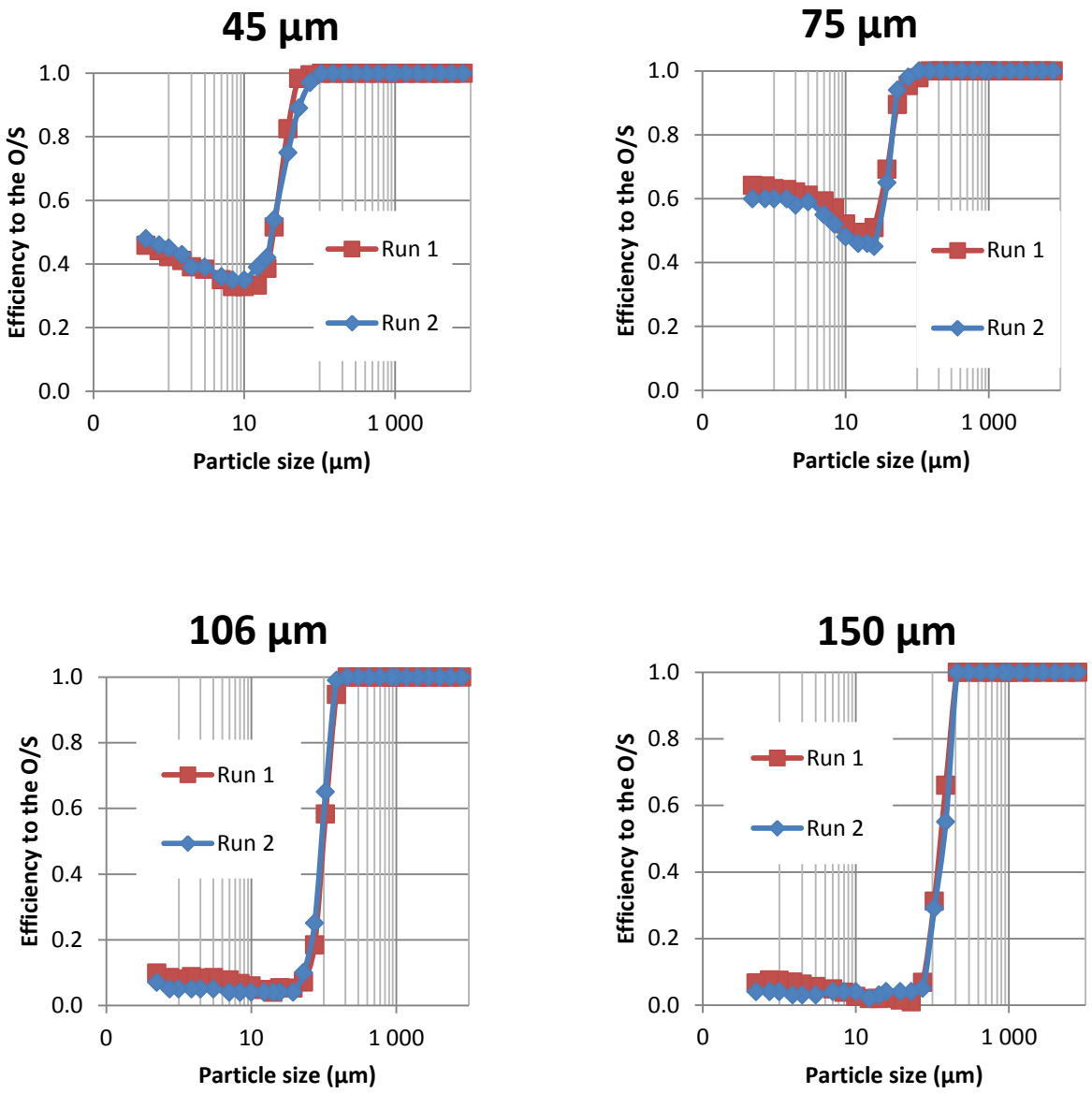

Figure 3.11: The efficiency curves obtained for the repeat tests at 45, 75, 106 and 150 µm apertures

CHAPTER 4. RESULTS AND DISCUSSION

4.1 Introduction

The purpose of this work is to develop a model for wet fine screening based on experimental data. The experiments were performed to investigate the influence of feed flow rate, solids concentration and aperture size on wet fine screening performance. While there are many ways of assessing the screen performance, only the analytical approach that contributed to the model developed in this work is presented. The chapter is divided into seven main sections: Section 4.2 discusses the mass balance results obtained as part of the assessment of the reliability of the experimental data generated from the test work; Section 4.3 presents a discussion of the effect of feed conditions and aperture size on the actual and corrected efficiency curves; Section 4.4 discusses salient properties of the efficiency curve as extracted from the Whiten model. The reproducibility of results is assessed in Section 4.5; and lastly, in Section 4.6, the overall summary of the results is presented.

4.2 Mass balance

The variations in operating conditions and errors introduced when sampling during operation are inevitable. Mass balancing aims to assess the consistency and integrity of the experimental data collected and to provide information on missing data (Napier-Munn, 2005). Prior to analysing the data from the testwork, mass balancing was performed using Microsoft Excel software. Table 4.1 summarizes the experimental and mass balanced results pertaining to the water and solids flow rates, the solids concentration and P80 values in the feed, undersize and oversize streams for three test conditions. The results are for screens operating at 45, 75 and 150 µm apertures at a range of feed flow rates and solids concentrations. Minor differences were observed between the experimental and balanced results suggesting that the data is reliable and can be used for further analysis. A comparison of the balanced and experimental particle size distributions for a screen operated at 13 t/h, 40 % solids and 106 µm aperture is illustrated by Figure 4.1. It can be seen that the mass balanced data matches the experimental data well. The data from all the tests was found to be consistent through the mass balance analysis undertaken. Therefore, the trends observed were accepted as a reflection of how wet fine screens perform under the conditions tested. These were in turn used in the model development discussed later.

Table 4.1: Mass balancing results for tests done at 45, 75 and 150 µm at different solids % and flow rates

Aperture (µm)	Stream	Solids flow rate (t/h)		Water flow rate (t/h)		% Solids		P80 (µm)	
		Exp.	Bal.	Exp.	Bal.	Exp.	Bal.	Exp.	Bal.
45	Feed	9.56	9.56	22.30	22.30	30.0	30.0	53.59	53.60
	U/S	5.41	5.43	19.28	19.26	21.9	22.0	25.35	26.16
	O/S	4.14	4.12	3.02	3.04	57.9	57.6	75.33	75.35
75	Feed	16.63	16.63	24.95	24.95	40.0	40.0	54.12	54.20
	U/S	8.55	8.57	20.30	20.28	29.6	29.7	25.99	26.01
	O/S	8.08	8.06	4.65	4.67	63.5	63.3	212.2	212.1
150	Feed	25.24	25.24	16.83	16.83	60.0	60.0	53.80	51.37
	U/S	15.07	15.09	13.42	13.40	52.9	53.0	39.25	38.34
	O/S	10.17	10.16	3.41	3.43	74.9	74.8	212.70	212.45

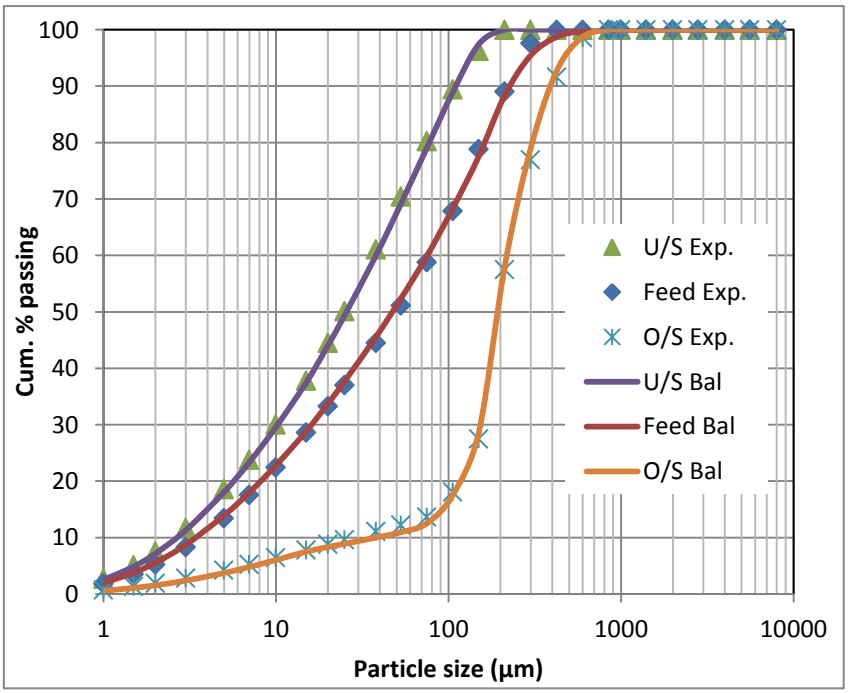

Figure 4.1: The experimental and balanced particle size distributions at 13 t/h, 40 % solids and 106 µm aperture size

4.3 Efficiency Curves

The efficiency/partition curve gives the probability that a particular size class in the feed will separate or leave with the fluid and is often used as an indicator of the performance of a separator (Svarovsky 2000). The curve is developed from calculating the fraction of each particle size class present in the feed that reports to either the screen oversize or undersize stream. It is generally accepted that most classifier efficiency curves do not reach 0 % for oversize curves due to the fact that fine particles will not respond to classification forces and will follow the fluid flow (Napier-Munn et al., 2005). As a result, the curve will meet the y axis at the value that corresponds to the water split to the oversize (Kelsall, 1953). This type of curve is called the uncorrected or actual efficiency curve. Kelsall (1953) proposed that the actual efficiency can be corrected for bypass by applying Equation 28. The corrected curve expresses the efficiency of particles recovered through true classification only. For each test conducted in this study, both the actual and corrected efficiency curves were established. The actual efficiency of particles of size d_i to the oversize was calculated using Equation 27while the correction was done by applying Equation 28. The three parameters that were extracted are the corrected cut size (D50c), sharpness of separation (α) and water recovery to the oversize (R_f). These are the parameters used to assess the performance of the screen.

$$E_{oa} = 1 - C\left[\frac{(1 + \beta\beta^{*}x) * (e^{\alpha} - 1)}{e^{\alpha\beta^{*}x} + e^{\alpha} - 2}\right] \quad 27$$

$$E_{oc} = \frac{E_{ua} - R_f}{1 - R_f} \quad 28$$

Where E_{oa} = actual efficiency of size d_i particles to the oversize

E_{ua} = actual efficiency to the undersize

E_{oc} = corrected efficiency to the oversize

C = water recovery to the undersize

R_f = 1- C

$x = \frac{di}{D_{50c}}$

β = parameter that corrects for the fish hook effect

β* = a fitting value introduced to preserve the definition of D50c

An example of the actual and corrected curves developed after applying Equations 27 and 28 for the test performed using a 45 µm screen aperture at 19 t/h and 60 % feed solids concentration is shown in Figure 4.2 and Figure 4.3 respectively.

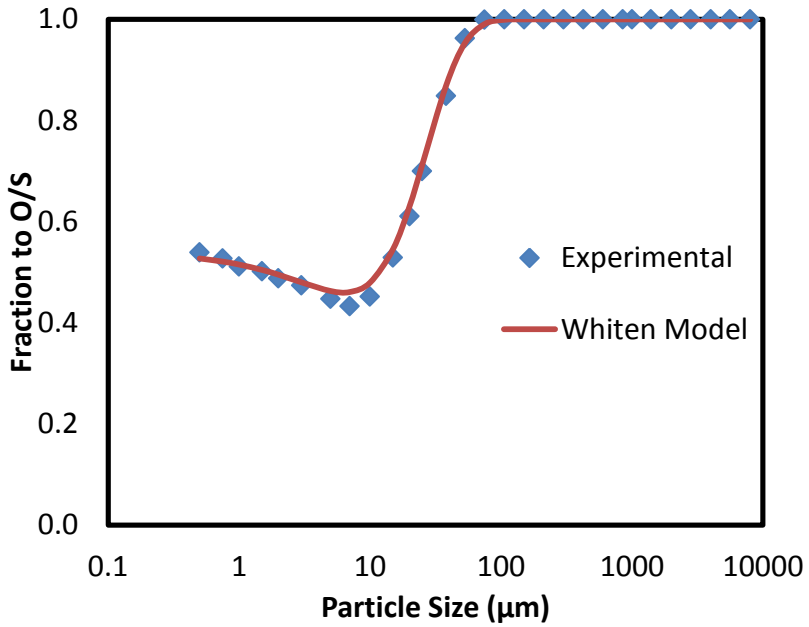

Figure 4.2: Actual efficiency curve at 45 µm, 60 % solids and 19 t/h

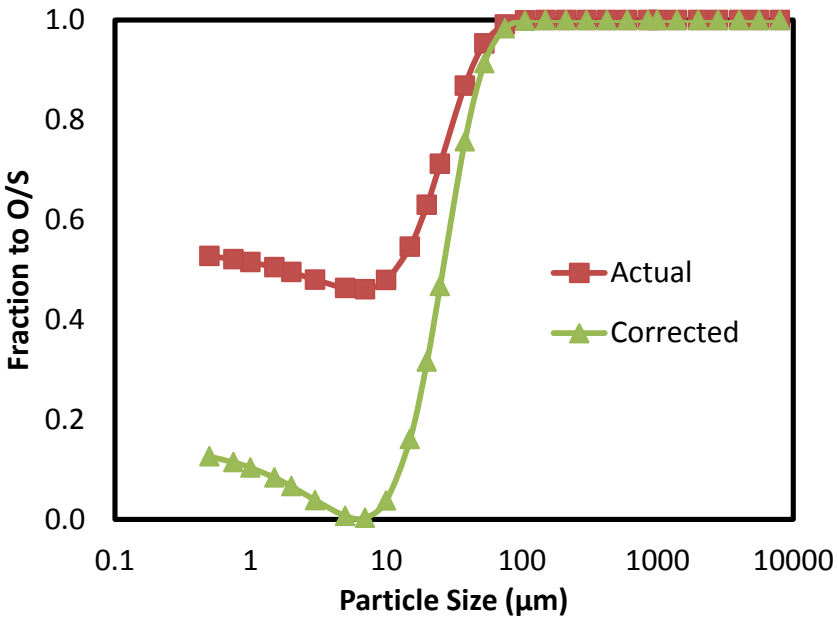

Figure 4.3: The actual and corrected curves at 45 µm, 60 % solids and 19 t/h

The efficiency curves were generated for each dataset and compared. Figure 4.4 shows an example of the actual efficiency curves obtained at different feed flow rates (a), solids concentrations (b) and aperture sizes (c). It can be seen from Figure 4.4 (a) that increasing the feed rates results in a shift of the efficiency curve towards finer sizes and upwards indicating higher bypass fractions. A similar effect was observed when the aperture size is decreased (Figure 4.4 (c)). In Figure 4.4 (c) increasing the solids concentration did not appear to influence the shift on the size axis but showed an increase in the bypass fraction.

The bypass fraction in many classifiers corresponds to the value of water recovery to the oversize where water is used as a fluid as discussed by Rogers and Brame (1982). Table 4.2 shows the corresponding water split for the three main variables. It can be seen that increasing the feed rate results in higher water recovery to the oversize. This effect has been observed from previous works on fine classification (Rogers & Brame, 1982; Rogers & Brame, 1985; Nageswararao, 1999; Mainza, 2006; Narasimha et al., 2014).

The water recovery to the oversize increased with an increase in solids concentration (Table 4.3) and a decrease in aperture size (Table 4.4). At higher feed flow rates, higher solids concentrations and smaller apertures, higher water recoveries to the oversize are expected due to a thicker closely packed particle bed presented to the screen at these conditions (King, 2001; Wills & Napier-Munn, 2006; Gupta & Yan, 2006). As a result of a thick and packed bed, there is restriction of flow of water through and a large amount of water reports to the oversize. Hence high water recovery of about 95 % was obtained at 45 µm, 30 t/h feed flow rate and 60 % feed solids concentration as shown in Figure 4.5 (c).

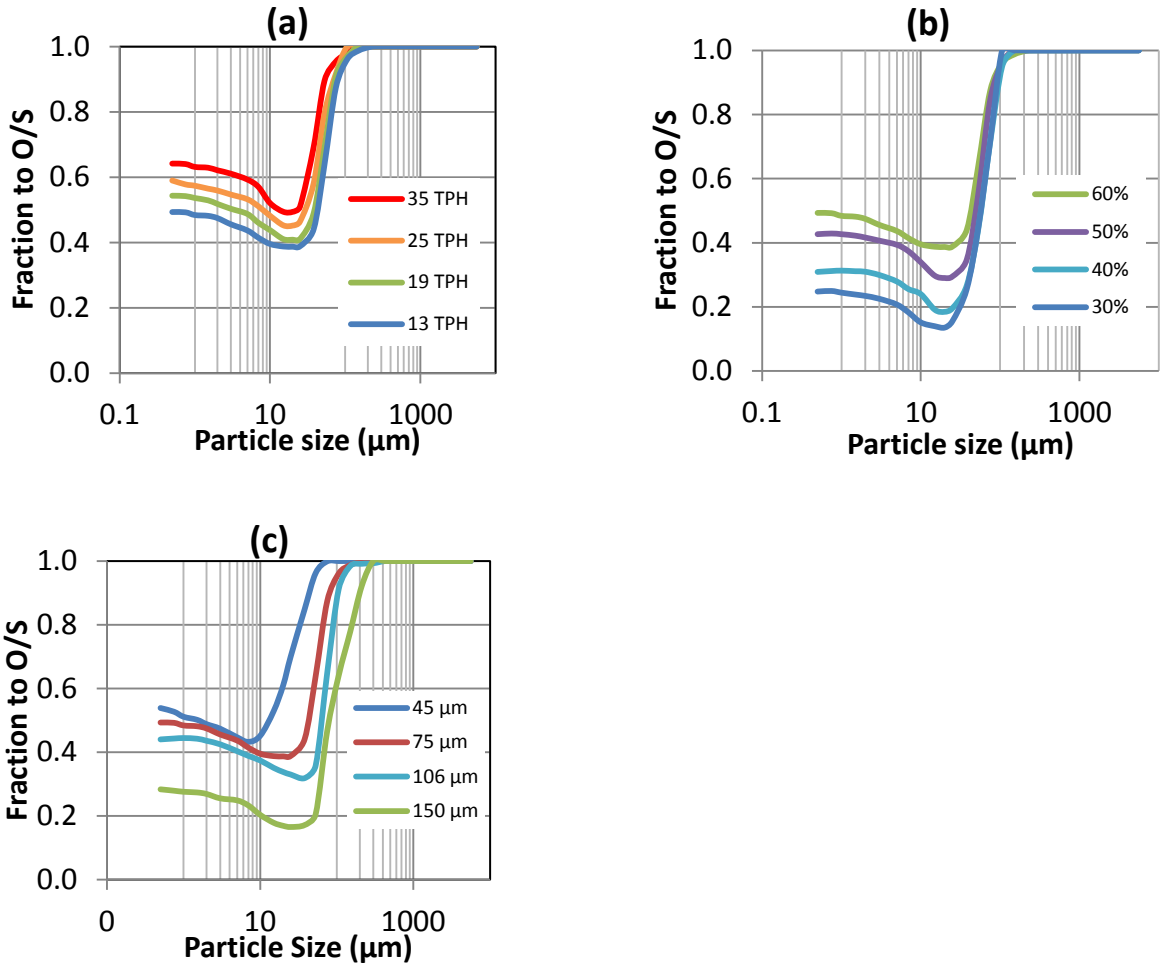

Figure 4.4: Effect of operating conditions on the efficiency curve: flow rate (a), solids concentration (b), aperture size (c)

Table 4.2: Effect of flow rate on water recovery to oversize

Feed rate (t/h)	Aperture (µm)	% solids	Water to Oversize
13	75	60	0.52
19	75	60	0.59
25	75	60	0.67
35	75	60	0.82

Table 4.3: Influence of solids concentration on water recovery to oversize

% solids	Aperture (µm)	Feed rate (t/h)	Water to Oversize
30	75	13	0.09
40	75	13	0.16
50	75	13	0.31
60	75	13	0.52

Table 4.4: Variation of water recovery to oversize with aperture size

Aperture (µm)	Feed rate (t/h)	% solids	Water to Oversize
45	13	60	0.59
75	13	60	0.52
106	13	60	0.25
150	13	60	0.14

The mass split, also known as the total efficiency is defined as the ratio of the mass of all particles separated to the mass of all solids fed into the classifier (Svarovsky, 2000). In applications such as closed grinding circuits, the mass split is important in assessing the classifier performance as it indicates how much material gets recirculated to the mill. The mass splits to the undersize for the tests done at solids concentrations close to 60 % for different aperture sizes are summarised in Table 4.5. It can be seen that when the feed flow rate is increased from around 13 to 30 t/h the mass split to the undersize decreases. From the particle size distribution of the feed, the true undersize of the 45, 75, 106 and 150 µm screen apertures are 60, 70, 80, and 85 % respectively. Comparing these to the mass splits obtained at each aperture in Table 4.5, it can be seen that there is a large difference between the mass splits and the true undersize values. This indicates that the factors chosen in this work affect classification and that separation at these conditions deviates from the ideal case.

Table 4.5: Mass splits at 60 % feed solids concentration

Flow rate (t/h)	Mass split the U/S (%)			
	45 µm	**75 µm**	**106 µm**	**150 µm**
12.40	35.24	44.38	51.45	69.97
19.97	33.59	42.94	47.51	66.88
25.73	32.30	39.20	45.51	59.70
28.87	29.46	36.73	40.39	56.50

4.4 The influence operating conditions on the efficiency curve properties

Variations in the feed rate, solids concentration and aperture size have a significant effect on the screen performance. This section analyses the screen performance measured by the influence of these variables on the efficiency curve properties. These properties were extracted using the Whiten model shown in Equation 27.

4.4.1 Effect of flow rate on the efficiency curve properties

Since the feed flow rate is one of the critical operating variables, an assessment was performed to evaluate its influence on the partition curve properties at different aperture sizes. Figure 4.5 shows the effect of feed flow rate on the sharpness of separation (α), corrected cut size (D50c) and water recovery to the oversize (R_f) at 60 % solids for a range of aperture sizes.

Sharpness of separation

The sharpness of separation is a measure of the amount of misplaced particles in the undersize or oversize streams (Majumder, et al., 2007). During classification, a good separation is achieved when there is a minimum amount of misplaced material. A higher value of sharpness of separation (α>4) suggests that a classifier is efficient (Napier-Munn, 2005). The influence of feed flow rate on the sharpness of separation is shown in Figure 4.5 (a). It can be seen that for very close solids concentrations the sharpness of separation decreased with an increase in the feed flow rate for the 75, 106 and 150 µm aperture sizes. The decrease in sharpness of separation can be explained by higher amounts of undersize particles carried over to the oversize at increased flow rates. At higher flow rates, the rate of transport of material across the screen is increased. Therefore, the undersize particles do not get the opportunity to be presented to the screen surface resulting in lower sharpness of separation. The results obtained for the 45 µm aperture on the other hand show no significant change in sharpness of separation with an increase in flow rate. This is can be attributed to the fact that effective separation happens when the screen capacity is not

exceeded. It is further observed that for all apertures, the sharpness of separation is less than 4. This indicates that the separation at solids concentrations close to 60 % is poor.

Valine and Wennen (2002) indicated that increasing the feed flow rate, the amount of fine material misplaced to the oversize increased, which in turn decreased the sharpness of separation. However, a study by Rogers and Brame (1985) on the effect of feed rate on efficiency curve parameters revealed no significant change in sharpness of separation with increasing flow rate despite the fact that the capacity of the screens tested were not exceed. The results obtained for the 45 µm aperture at 60 % solids were expected since the panel open area is smaller compared to larger apertures. At higher feed solids concentration, the particle bed on the screen surface builds up faster and the capacity of the screen is exceeded even at lower feed flow rates. Beyond the flow rate of 9 t/h, most of the material fed to the screen is carried over to the oversize without being classified and most of the water is recovered in the oversize.

Corrected cut size (D50c)

The cut size is the size that has a 50 % probability of reporting to the undersize or oversize streams (Svarovsky, 2000). It indicates the size at which separation occurs and is commonly used to quantify the efficiency of a classifier. For screens, a cut size closer to the screen aperture is desired. Larger deviations from the aperture size indicate poor screening performance.

The effect of feed flow rate on the corrected cut size is shown in Figure 4.5 (b). Increasing the feed flow rate from 13 to 30 t/h decreases the cut size for the 75, 106 and 150 µm aperture sizes. There is no significant change in cut size with increasing feed flow rate for the 45 µm aperture size. The decrease in cut size observed at larger apertures can be attributed to the higher load of material presented to the screen surface at higher feed flow rates. When the particle bed is thicker, the finer particles first have to percolate through the spaces between coarser particles before reaching the screen surface, the effective aperture size of the screen is reduced.

Water recovery to oversize (R_f)

The water recovery to the oversize is a critical indicator of the efficiency of a classifier. It is defined as the ratio of the water recovered in the oversize to the water in the feed (Kilavuz & Gulsoy, 2011). A higher water recovery to the oversize is not desired because it is often associated with higher carryover of fine particles to the oversize. It has been shown that the water split gives a good approximation for the fraction of undersize particles that get carried over to the oversize (Rogers & Brame, 1985). Figure 4.5 (c) shows the effect of flow rate on water recovery. It can be seen that increasing the feed flow rate results in an increase in water recovery to the oversize for all apertures. An increase in feed rate reduces the

residence time of slurry on the screen and presents thicker particle bed on the screen surface. As the slurry is transported faster across the screen, most of the water bypasses to the screen oversize. A study on testing the Derrick Stack Sizer as the classifier by Delgado et al. (2007) supports the results obtained in this work. Delgado et al. (2007) observed an increase in water recovery to the oversize when the flow rate was varied from 126 to 143 t/h.

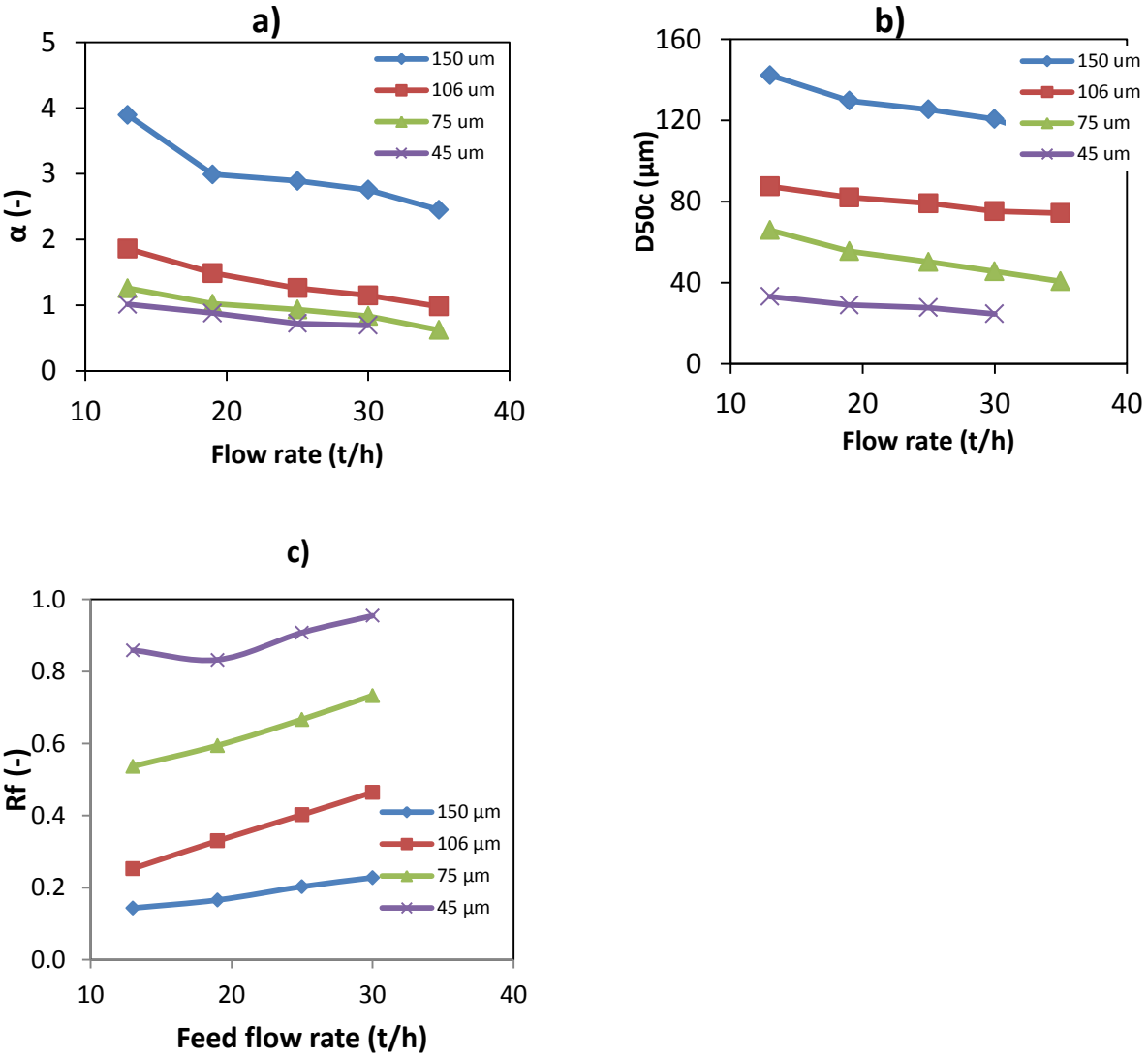

Figure 4.5: Effect of flow rate on partition curve properties: a) α, b) d50c, c) R_f

4.4.2 Effect of solids concentration on efficiency curve properties

The feed solids concentration is the easiest operating variable to manipulate on the plant although it is not practical to operate at very high dilute levels due to the influence on downstream processes and the volume limitations on the equipment design. Figure 4.6

shows the effect of solids concentration on the sharpness of separation (α), corrected cut size (D50c) and water recovery to the oversize (R_f) at 13 t/h for different apertures.

Sharpness of separation (α)

The influence of solids concentration on the sharpness of separation is shown in Figure 4.6 (a). It can be seen that at constant feed flow rate, an increase in the solids concentration from 30 to 50 % results in a sharp decrease in the sharpness of separation over the range of apertures tested. A further increase in solids concentration (50-60 %) resulted in a gradual decrease in sharpness of separation. The reduction in sharpness of separation could be due to the high restriction of flow of fine particles through the particle bed. As the solids concentration is increased, the particle bed becomes closely packed and fine particles do not get to be presented to the screen surface. At this point the material fed to the screen bypasses to the oversize without being separated. The decrease in sharpness of separation with increasing solids concentration was also observed by Firth et al. (1999) who performed tests on fine coal classification using the Derrick screen. Similarly, de Korte (2005) also revealed that at higher solids concentrations "the ultra-fine particles become trapped in the particle bed and are discharged with the oversize material".

Corrected cut size (D50c)

Figure 4.6 (b) shows the effect of solids concentration on corrected cut size. It was observed that increasing the solids concentration led to a decrease in cut size. The cut size closer to the aperture size is observed at the lowest solids concentration for all aperture sizes indicating a good separation at those conditions. The decrease in cut size can be attributed to the bed becoming closely packed at higher solids concentration and reducing the effective aperture size. This is in accordance with findings of Rogers and Brame (1985) where they tested the Derrick screen using limestone and coal slurries.

Water recovery to oversize (R_f)

The influence of solids concentration on water recovery is shown in Figure 4.6 (c). It can be seen that at constant feed flow rate, the water recovery to the oversize increase with an increase in solids concentration. A gradual increase is observed when the solids concentration is increased from 30 to 40%, after which the increase in water recovery to the oversize becomes sharper. This effect has also been observed by Albuquerque et al. (2008) and Valine and Wennen (2002) and has been attributed to restriction of flow of water through the thicker particle bed presented on the screen surface at higher solids concentration. An increase in the solids concentration reduces the particle bed porosity until only a small amount of water can pass through the bed. Beyond this point most of the water will bypass to the screen oversize. This explains the sharp increase in water recovery observed when the solids concentration is increased beyond 50 %.

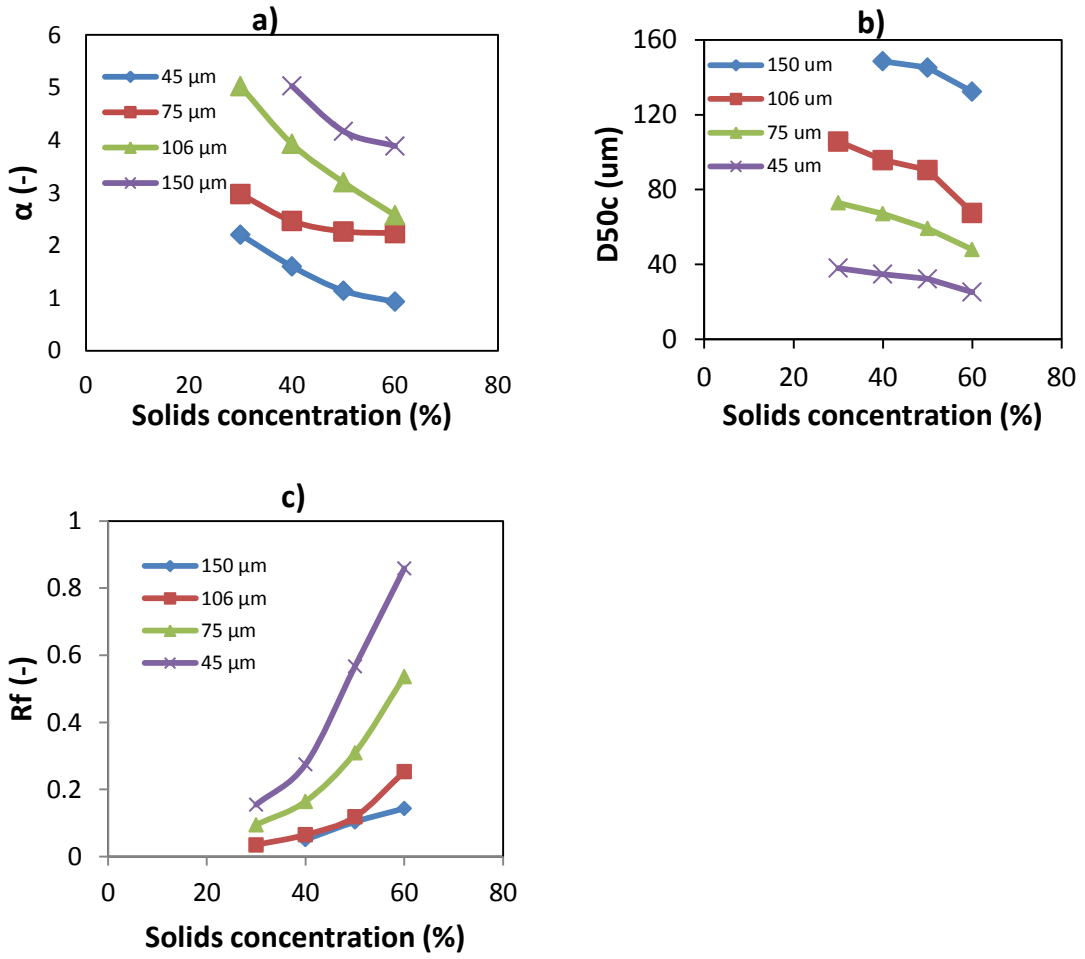

Figure 4.6: Effect of solids concentration on partition curve properties: a) α, b) d50c, c) R_f

4.4.3 Effect of aperture size on efficiency properties

The aperture size is one of the parameters that significantly affect the efficiency of the screen. Figure 4.7 shows the influence of the aperture size on the efficiency curve properties.

Sharpness of separation (α)

An assessment of the effect of aperture size on sharpness of separation is shown in Figure 4.7 (a). The results are for the 60 % solids tests at three different flow rates. It can be seen that there is a non-linear increase in the sharpness of separation with increasing aperture size over all the feed flow rates investigated. The highest sharpness of separation of about 3.25 is obtained at 13 t/h flow rate and 150 µm aperture size. The increase in sharpness of separation can be attributed to thinner particle beds presented on the screen at larger

aperture sizes. Since the apertures are larger the rate at which the particles build up on the surface of the screen is lower resulting in more fine particles getting presented to the screen surface without being trapped in between the coarser particles.

Corrected cut size (D50c)

Figure 4.7 (b) shows the influence of aperture size on corrected cut size. It can be seen that an increase in aperture size results in an increase in cut size. The comparison was done by observing the difference between the cut sizes and their respective apertures size. It was observed that the cut size approaches the aperture size at 150 µm and 13 t/h feed flow rate. At larger apertures sizes, the particle bed is thinner and loosely packed. Therefore the effective aperture size is close to the actual aperture size.

Water recovery to oversize (R_f)

The water recovery to the oversize increases with decreasing aperture size as shown in Figure 4.7 (c). Decreasing the screen aperture size while maintaining the screen strength will reduce the screen capacity and open area (Fuerstenau & Han, 2003; Tsakalakis, 2001). At smaller open area, there is a higher particle build up on the screen surface resulting in smaller effective apertures, higher fine particle bypass and higher water recoveries to the oversize. The results obtained with regards to the influence of aperture size on these efficiency curve properties are in line with what was observed by Firth et al. (1999), Valine and Wennen (2002), and de Korte (2005).

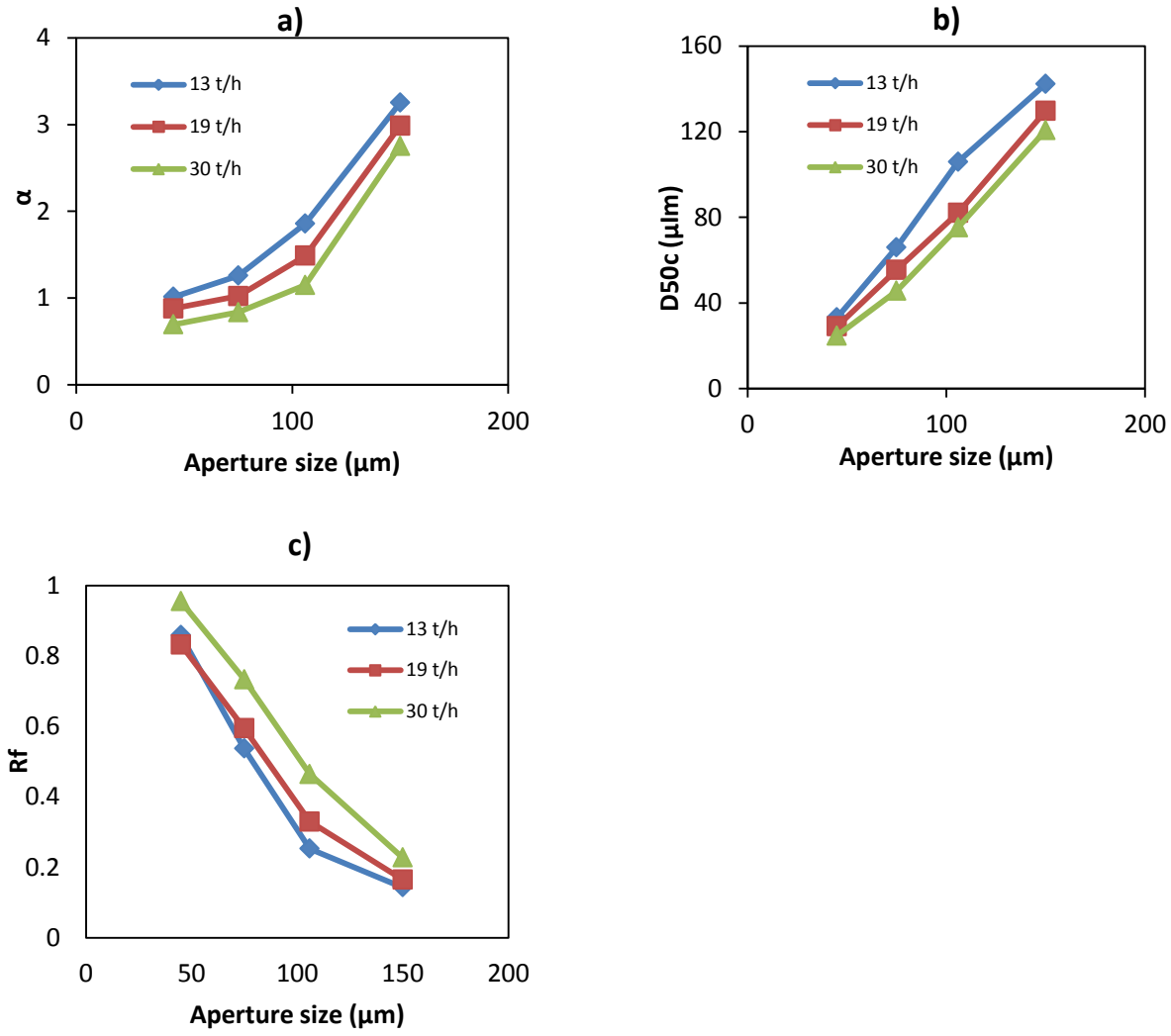

Figure 4.7: Effect of aperture size on efficiency curve properties a) α, b) d50c, c) R_f

4.4.4 Influence of operating conditions on the beta (β) parameter

For all the conditions tested in this work, the efficiency curves exhibited fish hooks at finer particle sizes. The fish hook phenomenon has been observed in screens and cyclones employed to treat very fine multi-density ores (Rogers & Brame, 1985; Plitt, 1971; Flintoff et al., 1987). Authors who studied this phenomenon have proposed different hyphotheses for the occurrence of the fish hook in classifiers. Rogers and Brame (1985) as well as Plitt (1971) assumes that the fraction of undersize particles bypassed is directly proportional to the water recovery to the oversize while Flintoff et al. (1987) attributes the fish hook to fine particles adhering to the coarse particles. In this study, pronounced fish hook was observed at higher feed tonnages, higher solids concentrations and smaller apertures. The fish hooks appeared to be closely related to the proportion of water recovered to the oversize which is in agreement with Rogers and Brame (1985), and Flintoff et al. (1987).

While it has been shown that in some cases this phenomenon can be due to experimental errors (Nageswararao, 2000), different models incorporating the fish hook have been developed (Plitt, 1971; Flintoff et al., 1987; Roldan-Villasan, 1993). The Whiten model shown in Equation 27 uses the Beta (β) parameter to describe the fish hook. The β parameter in the Whiten expression controls the initial rise in the curve. Higher values of β correspond to more pronounced fish hooks while a value of 0 corresponds to the condition when there is no fish hook present. Figure 4.8 illustrates the effect of β on the efficiency curve for a hydrocyclone overflow taken from Napier-Munn et al. (2005).

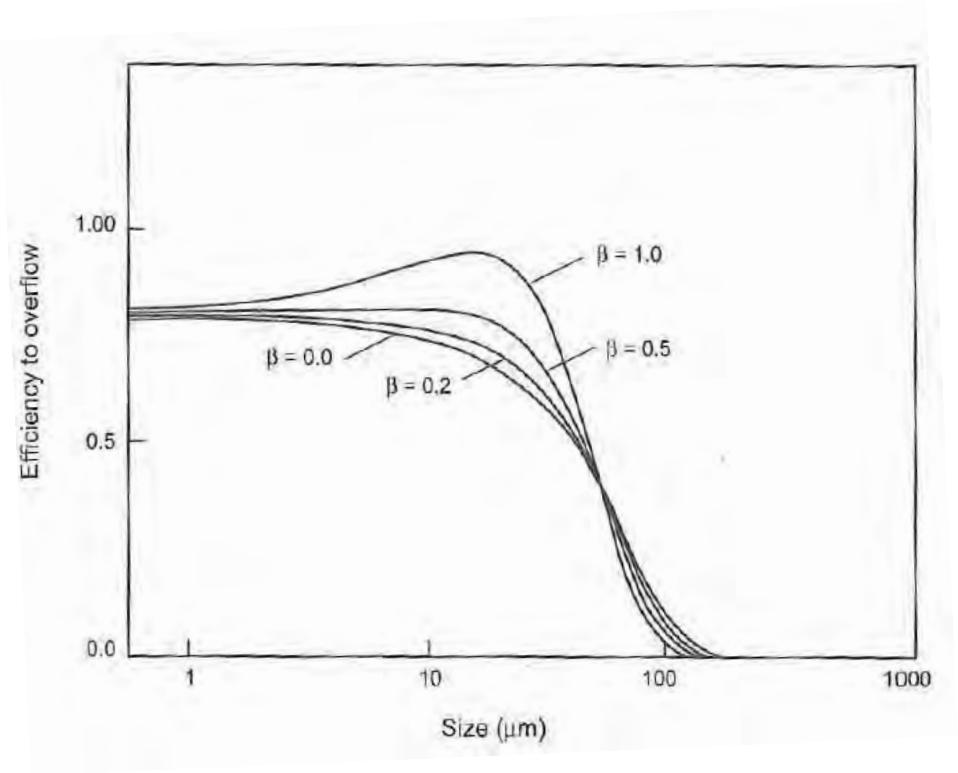

Figure 4.8: Variation of efficiency curve with at α = 2 (Napier-Munn et al., 2005)

The effect of feed flow rate, solids concentration and aperture size on β from this study is shown in Figure 4.9 (a), (b) and (c) respectively. From Figure 4.9 a) no discernible change in the fish hook parameter was observed with increasing feed rate for the 45 µm aperture screen. However, the fish hook parameter had a high value for all tests performed at 45 µm indicating that it was very pronounced. The fish hook parameter increased with feed flow rate for tests performed using the 75, 106 and 150 µm apertures. The fish hook parameter value increased with feed solids concentration for all the aperture sizes evaluated as shown in Figure 4.9 (b). For the same feed solids concentration, the fish hook parameter was more pronounced for the smallest aperture and diminished with an increase in aperture size. Figure 4.9 (c) shows the trend for the β value against aperture size for different solids concentration. The fish hook parameter values decreased with increase in aperture size for

the same flow rate indicating that the resistance to flow of the aperture plays a role in the existence of this phenomenon.

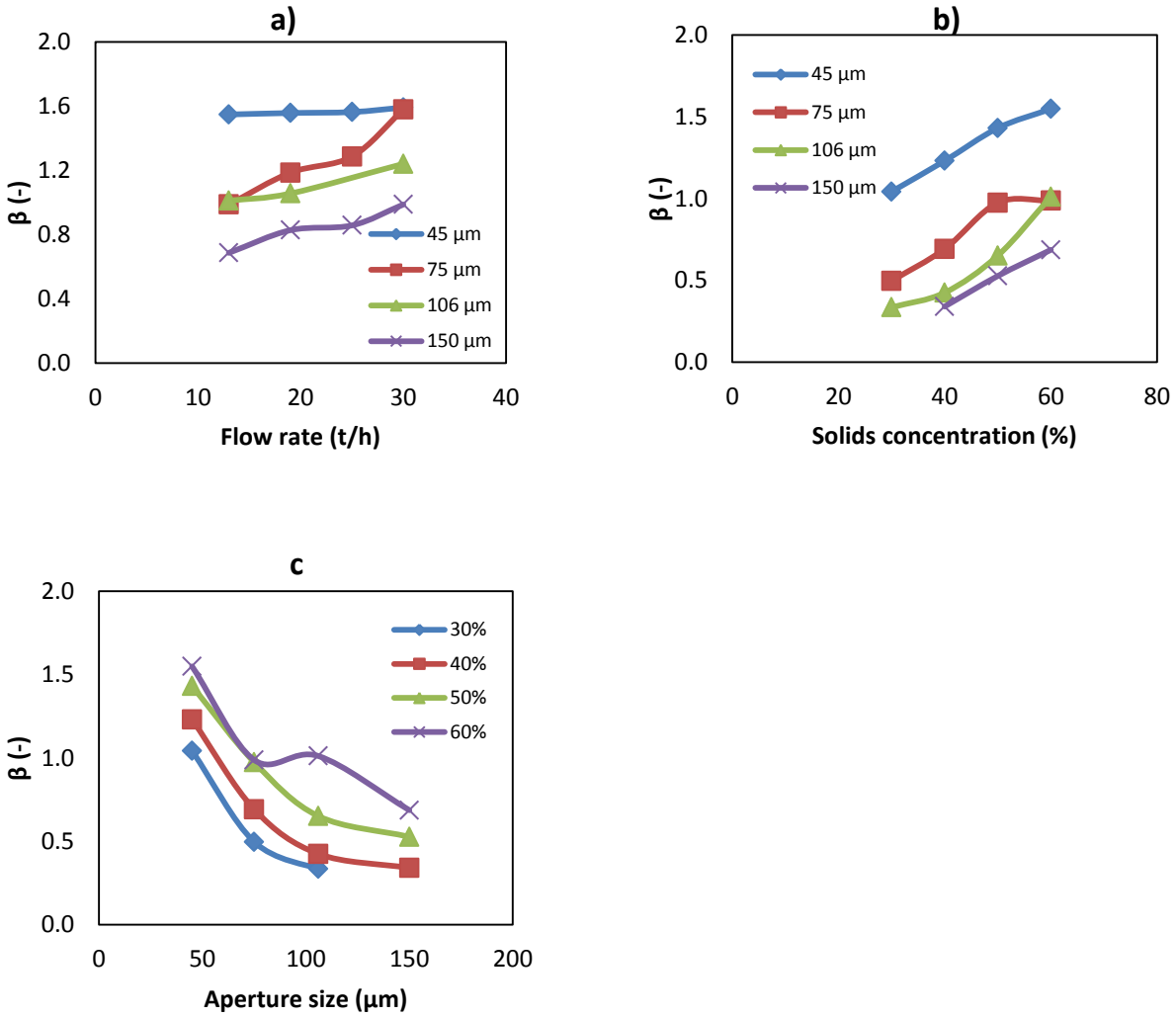

Figure 4.9: The effect of operating conditions on the β parameter

4.5 Summary

The experimental results show that the feed flow rate, solids concentration and aperture size have a significant influence on the wet fine screen performance. Higher feed flow rates and solids concentration are accompanied by lower cut sizes and sharpness of separation and higher water recovery to the oversize. The solids concentration seemed to affect the sharpness of separation and water recovery to the oversize more than it does the cut size. The fraction of undersize particles carried over to the oversize is also increased with increasing flow rate and solids concentration and reducing aperture size. At smaller apertures, the efficiency curves exhibit more pronounced fish hooks as a result of increased fine particle bypassed to the oversize. Similar trends were observed at increased feed flow

rates and solids concentrations. In general, the results obtained for all conditions tested in this study have shown the influence of different variables on the performance of the wet fine screen that was used in developing the model reported in Chapter 5.

CHAPTER 5. MODEL DEVELOPMENT

5.1 Introduction

This chapter reports the steps taken to develop a model for wet fine screens. The model is based on the general screen model developed by Whiten (1972). The data used in the development of the model was obtained from the experiments performed by the author of this thesis and for a thesis submitted by Mwale (2015). The model developed for the wet fine screen by Mwale (2015) is given in Equation 29. After developing the primary model, Mwale (2015) extended the model to account for the fish hook effect using Equation 30. The main difference between Mwale (2015) and the work reported here is the approach taken in the models developed from the same data. Mwale (2015) used the kinetic approach to develop the general screen model and modified for the fish hook effect using the Karra (1979) model as the basis.

$$E_{io} = 100exp\left[-\frac{A_o K}{F_f s\left(\frac{d_i}{a}\right)^{\alpha}}\right] \quad 29$$

$$E_{io} = 100exp\left[-\frac{A_o K}{F_f s\left(\frac{d_i}{a}\right)^{\alpha}}\right] + \frac{\delta F_f}{\omega}\left[\exp\left(-\frac{d_i}{a}\right)\right]^{\alpha} \quad 30$$

Where E_{oi} = efficiency to the oversize

F_f = mass flow rate of solid in the feed

A_o = screen open area

K = model constant

s = solids content

d_i = particle size

a = aperture size

α = sharpness of separation

δ = fish hook parameter

ω = water content

The Whiten (1972) screen model shown in Equation 31 which incorporated the Gaudin (1939) probability function was used as a basis for modelling in this study. The fraction of particles of size x in the feed that are recovered in the oversize product, E(x) is calculated from the fraction screen open area, f_o and the aperture size, x_a. N is the parameter representing the number of trials or presentations to the screen surface and σ is an empirical parameter used for fitting.

The Whiten model was chosen as the basis because it provides a good description of the shape of the efficiency curve obtained from screen and has few parameters. Together with the Ferrara and Preti (1975) model, the Whiten model is considered the most accurate mathematical model for screens compared to other models (Hilden, 2006; Wills & Napier-Munn, 2006). It has been available since early 1970's and has been incorporated into the JKSimMet computer simulation software with a few modifications since then.

$$E(x) = \exp\left[-Nf_o\left(1 - \frac{x}{x_a}\right)^{\sigma}\right] \qquad 31$$

Where N = number of trials at passage

σ = the parameter that affects the ratio of passage probabilities

fo = fraction open area of the screen

x = particle size

xa = aperture size

Napier-Munn et al. (2005) describes a typical efficiency curve by a three region curve shown in Figure 5.1. The size classes above the aperture size are described by Region 1. Region 2 represents the size classes below the aperture size in which the probability of passage of fine particles is directly dependent on the size of the particle. This region is the most important region for modelling purposes (Napier-Munn et al., 2005). Region 3 describes the ultra-fine particles that are carried over to the oversize stream. The Whiten (1972) model shown in Equation 31 was developed to describe Region 2.

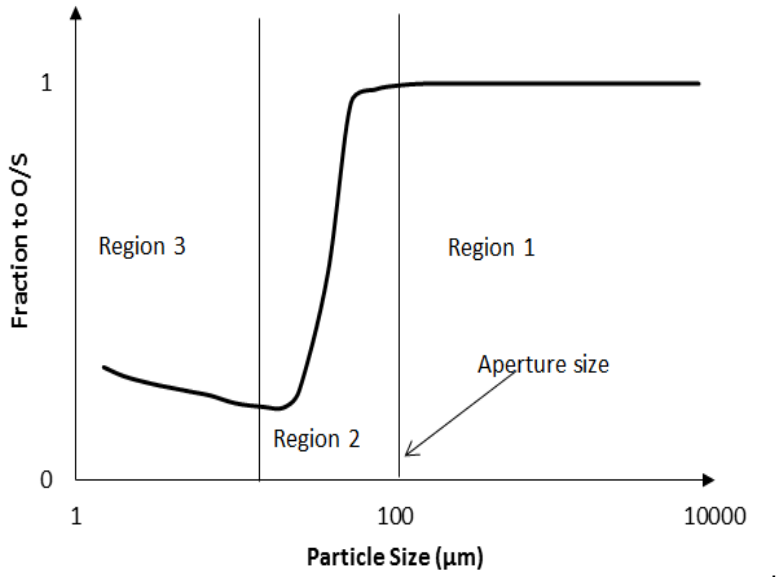

Figure 5.1: A typical efficiency curve for a vibrating screen (Napier-Munn et al., 2005)

The restriction to the Whiten model is that it does not explicitly show how the model parameters are affected by varying operating and design variables. Thus, the parameters have to be refitted for every change in operating conditions. There are some regression equations that have been developed in an attempt to calculate the parameter N; However, it has been noted that these equations are extensive and make the screen model difficult to fit compared to other models (Napier-Munn et al., 2005). The model was modified by inserting terms to account for the influence of key operating and design variables directly. Additionally, a model that describes the ultra-fine region is necessary for data that exhibits the fish hook effect.

In the modelling work performed in this thesis, the N and σ parameters were replaced with equations developed using dimensionless terms generated from the factors affecting screen performance obtained from the experimental data. Using this approach, equations that integrate the variation of these model parameters with operating conditions were developed.

5.2 Significance of the N and σ parameters

As discussed in previous chapter, the shape and properties of the partition curve are affected by various screening conditions. It is noted that for every change in operating and design factors the N and σ parameters in the Whiten model have to be re-evaluated. This indicates that these parameters are affected by variations in operating conditions. Understanding the significance of these parameters and studying their effect on the shape

of the efficiency curve at different screening conditions provided useful insights when developing the relationship between the operating conditions and model parameters.

5.2.1 The N parameter

The parameter N corresponds to the number of trials at passage of a particle through the screen slots. It is alternatively referred to as the efficiency parameter by Napier-Munn et al. (2005). For the undersize particles to pass through the screen they first have to be presented to the screen surface. As these particles meet the screen surface more frequently (higher values of N), their chances of passing through to the undersize stream are increased and the screening performance is improved. The manner in which the N parameter affects the efficiency of the screen was studied by examining the shape of the efficiency curve produced at different N values.

The effect of N on the shape of the efficiency curve is shown in Figure 5.2. The curve is a graphical representation of Equation 31 obtained when fixing the σ parameter at 2 and arbitrarily varying N between 0.05 and 10 for a 45 µm screen with 28 % fraction open area. It can be seen that with constant σ, a change in N affected the separation efficiency. Increasing the N value increased the slope of the curve, thus the sharpness of separation. Additionally, the cut size shifted closer to aperture size with increasing N.

The number of presentations parameter is affected by the load on the screen surface (Napier-Munn et. al., 2005). When the screen is heavily loaded, fine particles are presented to the screen less frequently and this gives rise to small N values. Operating conditions such as the feed rate, parameters characterizing the screening surface (open area, aperture size, shape and type), screen vibration characteristics and the screen deck angle of inclination have an effect on the number of presentations of particles to the screen surface (Whiten, 1972; Ferrara & Preti, 1975; Soldinger, 1999; Napier-Munn et al., 2005;). From the factors that were investigated in this study, higher sharpness of separation and cut sizes were observed at lower feed solids concentrations and flow rates and larger apertures.

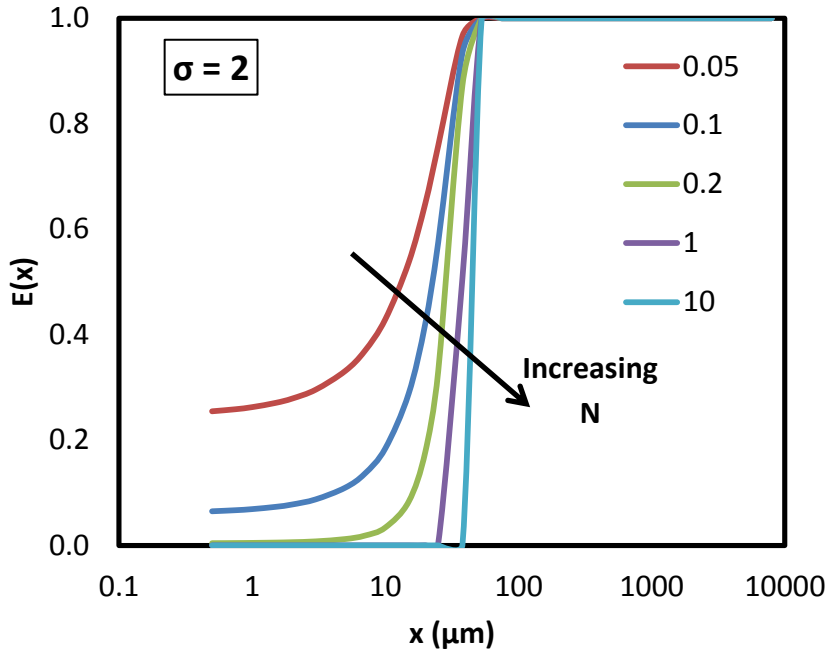

Figure 5.2: The effect of the N parameter on the shape of the efficiency curve

5.2.2 The σ parameter

Ferrara & Preti (1975) describes σ as the parameter that "affects the ratio of passage probabilities for particles of different sizes". It gives an indication of relative easiness at passage of near size particles compared to fine particles. The σ parameter is dependent on the type of screening material and the apparent size and shape of the aperture as "seen" by the particle approaching the screen surface (Hilden, 2006). The value of σ was approximated to be 2 by Gaudin (1939) for square apertures; however, different authors (Hess, 1983; Pereira et al., 1993) have obtained values smaller or greater than 2 depending on the screening conditions employed in each study.

The factors that were varied in this study are the feed rate and solids concentration and aperture size. For a fixed aperture, intensity of vibration and angle of inclination, a change in feed rate and/or solids concentration is expected to affect the σ parameter. These factors are responsible for the thickness of the bed and the rate of flow of material on the screen surface. When there is a thicker particle bed on the screen, fine particles on the top layers of the bed have to first percolate through smaller spaces between coarse particles. The effective aperture size is reduced; hence the value of σ should be affected.

The effect of σ on the shape of the efficiency curve is shown in Figure 5.3. The curves were generated from fixing N at 0.2 and randomly varying σ between 0.5 and 10 for a 45 µm screen with 28 % fraction open area. It can be seen that higher values of σ shift the efficiency curve away from the aperture size, indicating poorer separation efficiency.

Additionally, it can also be noted that the sharpness of separation is not affected by the changes in the σ value.

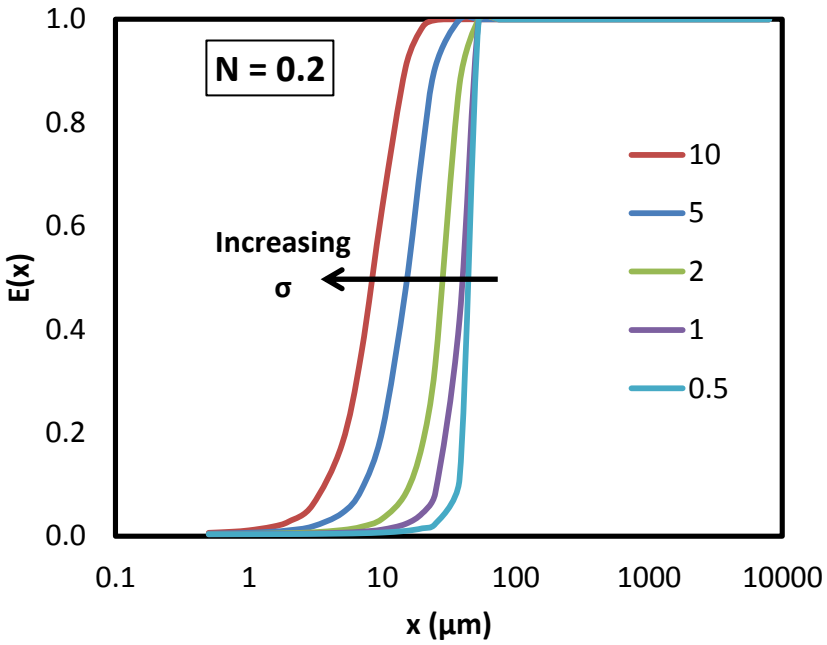

Figure 5.3 The effect of the σ parameter on the shape of the efficiency curve

The above discussion indicates that the Whiten model parameters, N and σ affect the shape of the efficiency curve, consequently the overall efficiency of the screen. The N parameter changes both the cut size and sharpness of separation while σ affects only the cut size. It has been shown that these parameters are dependent on screening conditions; however the Whiten model does not explicitly show how these conditions affect the model parameters and relies on refitting to obtain new parameter values for every change in operating and design factors. Developing Sub models for N and σ that capture changes in feed conditions will improve the model and reduce the fitting process.

5.3 Model development approach

5.3.1 Developing the dimensionless groups

As discussed in previous sections, there are a number of factors that affect the screening efficiency. The equation for the Whiten parameters N and σ were defined using the dimensional analysis approach by considering variables that affect the screening efficiency. The most important variables that apply to wet screening operations listed in literature (Fuerstenau & Han, 2003; Wills & Napier-Munn, 2006; Rogers & Brame, 1985; Tsakalakis,

2001) are the: mass flow rate of the feed (m_f), mass flow rate of undersize particles ($m_{u,f}$), pulp density (ρ_p), feed slurry viscosity (μ_s), particle size (x), aperture size (x_a), screen open area (A_o), gravitational acceleration (g), vibration angular frequency (ω) and amplitude (a). According to Buckingham's PI theorem, seven dimensionless groups (PI numbers) can be used to define the system with 10 variable and 3 reference dimensions (Mass, Length and Time). After making several combinations the π numbers that were developed are:

- $\pi_1 = \frac{m_{u,f}}{m_f}$
- $\pi_2 = \frac{{m_f}^2}{{\rho_p}^2 g {x_a}^5}$
- $\pi_3 = \frac{x}{x_a}$
- $\pi_4 = \frac{{A_o}^2}{{x_a}^2}$
- $\pi_5 = \frac{\mu_{sl} x_a}{m_f}$
- $\pi_6 = \frac{a}{x_a}$
- $\pi_7 = \frac{x_a \omega^2}{g}$

The dimensionless groups were reduced by combining π_1 and π_2 to get ${\pi_1}^*$ as well as π_6 and π_7 to get ${\pi_6}^*$:

- ${\pi_1}^* = \frac{{m_u}^2}{{\rho_p}^2 g {x_a}^5}$
- ${\pi_6}^* = \frac{a\omega^2}{g}$

The above expression (${\pi_6}^*$) is the Froude number (Fr) for a vibrating screen, also known as the throw number. This number is frequently used in industrial screening to define the vibration characteristics of a screen by relating the gravitational acceleration to the frequency and amplitude of vibration, **f** and **a** respectively. It was however excluded from the model development in this study since the frequency and amplitude of vibration were kept constant for all the conditions tested. Therefore, the π numbers that were investigated when developing equation for N and σ are:

- ${\pi_1}^* = \frac{m_u}{{\rho_p}^{0.5} g {x_a}^{2.5}}$
- $\pi_3 = \frac{x}{x_a}$
- $\pi_4 = \frac{A_o}{{x_a}^2}$
- $\pi_5 = \frac{\mu_{sl} x_a}{m_f}$

The discussion in section 5.2 showed that the Whiten model parameters are affected by the operating conditions and have an effect on the cut size and sharpness of separation. The above terms were selected from the operating and design factors that have shown an influence on the efficiency in previous works but limited to the factors that were tested in this study. The viscosity of the slurry obtained from the work done by Muzanenhamo (2014) was introduced as an additional term even though it was not tested in this study. This is because Muzanenhamo (2014) used a similar ore type and slurry conditions.

5.3.2 The N and σ parameter models

Equations that describe Regions 2 and 3 in Figure 5.1 were developed separately. For Region 2, equations 32 and 33 were investigated for N and σ respectively.

$$N = f_N\left(\frac{A_o}{{x_a}^2}, \frac{\mu_{sl} x_a}{m_f}, \frac{m_u}{\rho_p g^{0.5} {x_a}^{2.5}}\right) \quad 32$$

$$\sigma = f_\sigma\left(\frac{{A_o}^2}{{x_a}^2}, \frac{\mu_{sl} x_a}{m_f}, \frac{m_u}{\rho_p g^{0.5} {x_a}^{2.5}}\right) \quad 33$$

The first step to developing the function forms of f_N and f_σ was to fit the Whiten model to the experimental data to obtain the N and σ values. The fitting process was done using EXCEL SOLVER multiple linear fitting routine by minimizing the sum of the squares of the deviations from each experimental data (y_i) to the predicted outcome (Y'_i):

$$\mathrm{SSE} = \sum_i^n (y_i - {Y'}_i)^2 \quad 34$$

In formulating the relationship between the parameter and the dimensionless groups, the graphs of fitted model parameter values against each dimensionless group were plotted and the curve fitting tool in EXCEL was used to obtain the function form that describes the data. The data followed a power function between for all conditions tested. It was therefore assumed that the equations that describe the relationship between the model parameters and operating conditions follow the power function as shown in Equations 35 and 36. Similar function forms of models were used by other authors (Narasimha et al., 2014; Nageswararao et al., 2004) when developing the models that describe the hydrocyclone

performance. All the operating/design variables that were kept constant were lumped together in the constants K_N and K_σ.

$$N = K_N \left(\frac{\mu_{sl} x_a}{m_f}\right)^{C1} \left(\frac{m_u}{\rho_p g^{0.5} {x_a}^{2.5}}\right)^{C2} \left(\frac{A_o}{{x_a}^2}\right)^{C3} \quad 35$$

$$\sigma = K_\sigma \left(\frac{\mu_{sl} x_a}{m_f}\right)^{C4} \left(\frac{m_u}{\rho_p g^{0.5} {x_a}^{2.5}}\right)^{C5} \left(\frac{A_o}{{x_a}^2}\right)^{C6} \quad 36$$

All the model constants were evaluated using the experimental data from all the 55 tests conducted in this study. The sums of the squares of the deviations from the experimental data to the predicted outcome were minimized for each aperture using EXCEL SOLVER multiple linear fitting routine. The constants C1 to C6 are the same for all the apertures while the K values vary according to the aperture size. After testing different combinations of the dimensionless terms, the resulting equations that explained the data well are given in Equations 37 and 38 with the K values for each aperture given in Table 5.1.

The results show that K_N decreases with increasing aperture size while an opposite effect is observed for Kσ. The range for K_N values is from 0.70 for larger apertures and 2.860 for smaller apertures. A value of 0.024 is obtained for the smaller apertures and 0.149 for the largest apertures.

$$N = K_N \left(\frac{\mu_{sl} x_a}{m_f}\right)^{-0.78} \left(\frac{m_u}{\rho_p g^{0.5} {x_a}^{2.5}}\right)^{-1.25} \left(\frac{A_o}{{x_a}^2}\right)^{0.25} \quad 37$$

$$\sigma = K_\sigma \left(\frac{\mu_{sl} x_a}{m_f}\right)^{0.53} \left(\frac{m_u}{\rho_p g^{0.5} {x_a}^{2.5}}\right)^{0.91} \left(\frac{A_o}{{x_a}^2}\right)^{-0.16} \quad 38$$

Table 5.1: The K values obtained for different apertures

Aperture size (µm)	K_N	K_σ
45	2.86	0.024
75	1.33	0.029
106	0.82	0.054
150	0.70	0.149

The efficiency curves shown in Figures 5.4 were generated using the Whiten Model (Equation 31). The curves represent the model-fits obtained for the 75 and 106 µm aperture screens operated at 50 % solids and 13 t/h flow rate. The N and σ parameter values were calculated from Equations 37 and 38 respectively using the modified model while the fitted values were used for the Whiten model. It can be noted that the modified model gives the results that are visually similar to the Whiten model. Both models fit the experimental data reasonably well in Region 2 except for the region where there is a pronounced fish hook.

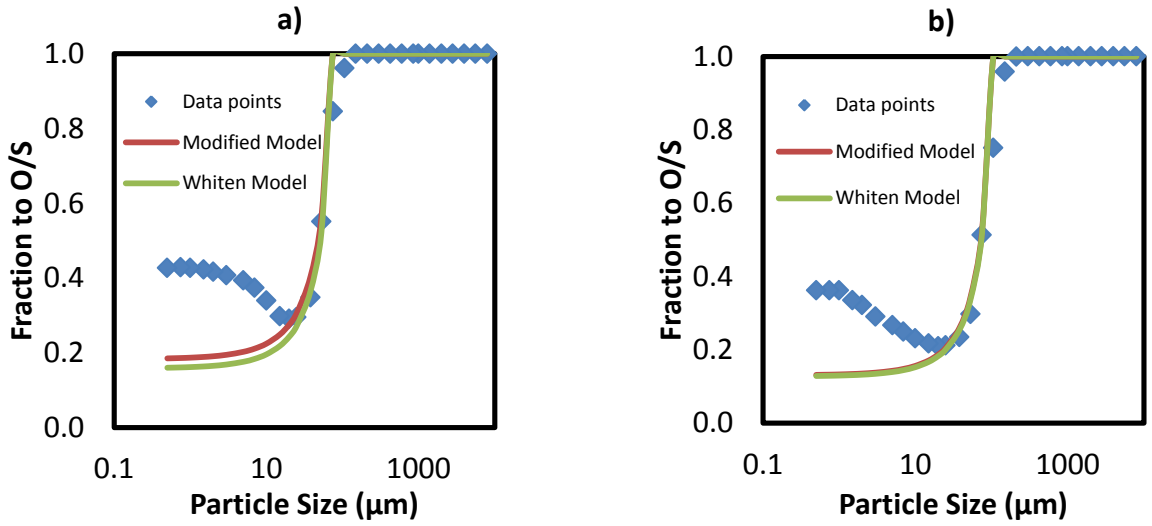

Figure 5.4: Model fits for the tests done at 50 % and 13 t/h at aperture of a) 75 µm and b) 106 µm

In assessing how well the modified model predicts the Whiten model parameters, the model parameter values obtained for all tests were compared. Similarly, fitted N and σ values were used to obtain for the Whiten model. For the modified model the N and σ were calculated using Equations 37 and 38. It can be seen from Figure 5.5 that there is a reasonably good

relation between the models. This is measured by the R^2 value obtained for both parameters. The σ parameter seems to have a better prediction compared to the N parameter. This is indicated by high R^2 values close to unity. Further explanation of the R^2 value is given in section 5.5.

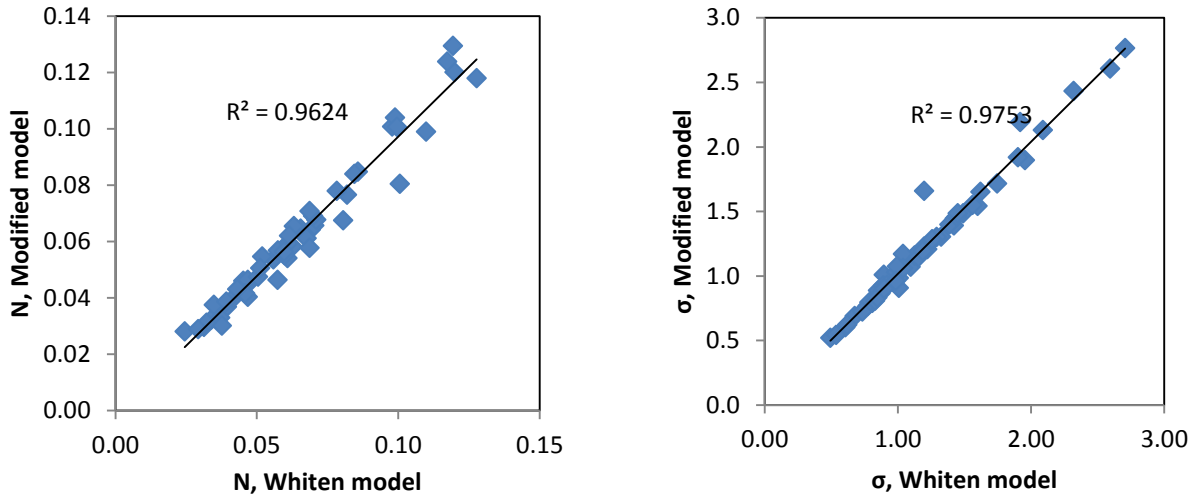

Figure 5.5: A comparison of the Whiten and modified model parameters

5.3.3 The fish hook model

All the partition curves generated in this study had a pronounced fish hook. Nageswararao (2000) indicates that although the fish hook has been infrequently reported in literature, it has been observed in both screens and hydrocyclones when treating very fine material and ores with density differences. In this study, exaggerated fish hook was observed at smaller apertures, higher flow rates and solids concentrations. A model that does not account for this would have inaccuracies in predicting the screen performance. To describe the fish hook behaviour shown as region 3 in Figure 5.1, the equation was extended using the function delta (δ). δ is a function dependent on operating conditions as shown in Equation 39. The approach of using dimensionless terms was also adopted when extending the model to incorporate the fish hook effect.

$$\delta(x) = f_\delta\left(\frac{x}{x_a}, \frac{\mu_{sl} x_a}{m_f}, \frac{m_u}{\rho_p g^{0.5} {x_a}^{2.5}}\right) \qquad 39$$

The function form of the equation was assumed to be exponential based on the fish hook models available in literature (Frachon and Cilliers, 1999; Roldan-Villasan et al., 1993, Mwale, 2015). Different combinations of equations were tested using the experimental data

from all the 55 tests by means of the EXCEL solver multiple linear fitting routine. The simplicity of the model and the minimum error calculated from the sum of the squares of the deviations were used as the standard for choosing the final model. The expression used to account for the fish hook is given in Equation 40. Where K_δ is the model constant that varies with aperture size as shown in Table 5.2. The range of K_δ is 8.93 x 10^{-6} for smaller apertures and 3.23 x 10^{-5} for larger apertures. The value of δ varies with operating conditions even though the model constant remains constant for a fixed aperture.

$$\delta\,(x) = K_\delta \left(\frac{m_u}{\rho_p g^{0.5} {x_a}^{2.5}} \right)^{0.35} \exp\left(-\left(\frac{\mu_{sl} x_a}{m_f} \right)^{-0.16} \left(\frac{x}{x_a} \right)^{1.13} \right) \qquad 40$$

Table 5.2: The fish hook constants at different apertures

Aperture (µm)	K_δ
45	8.93E-06
75	2.01E-05
106	2.98E-05
150	3.23E-05

5.4 Influence of operating conditions on the model parameters

For a particular aperture size, the model is fitted once to obtain the model constants K_N, K_σ, and $K_{\delta.}$ The screen performance at other operating conditions can then be predicted using the same model constants without the need to refit the model. The effect of flow rate, solids concentration on model parameters for each aperture size is shown in Figures 5.6 and 5.7 respectively.

It can be seen that these operating conditions have an effect on the screen parameters. Increasing the feed flow rate and solids concentration decreases the number of trials parameter and increases. These results are consistent with what is expected since at higher flow rates particles do not reside longer on the screen surface they move faster and do not get to be presented to the screen surface more frequently. At high solids concentration there is a thicker bed on the screen surface. Fine particles on the top layers are prevented from reaching and screen surface more repeatedly since they first have to travel through the particle bed.

The σ parameter is related to the shape and size of the aperture. For a constant aperture size, increasing the flow rate and solids concentration increases the σ parameter. This is consistent to what would be expected. At higher flow rates and solids concentration there is more material presented to the screen surface. A thicker and closely packed particle bed affects the apparent aperture size and shape. The spaces between the coarse particles act as the aperture to the fine particles on the top layers of the particle bed. This means that the effective aperture is narrower and less like a square aperture.

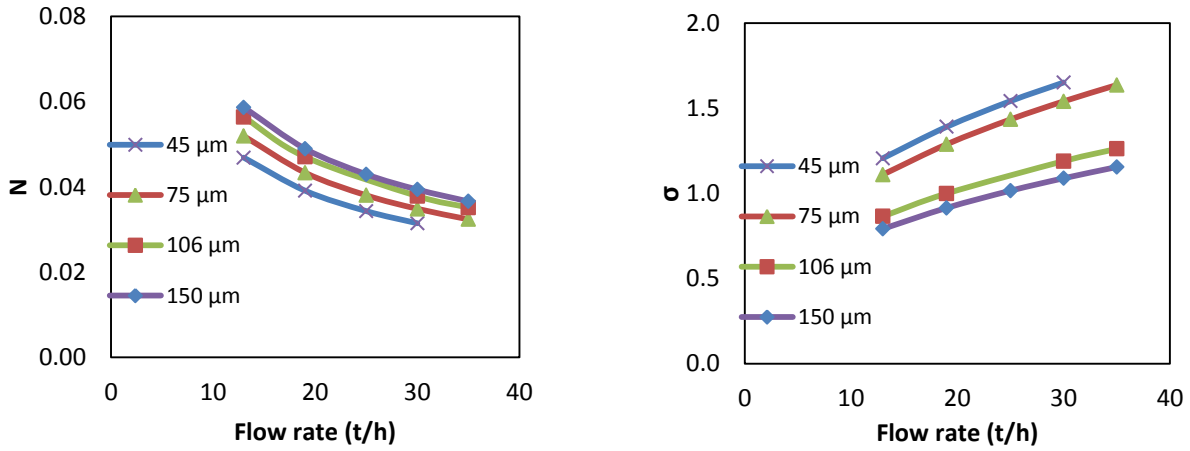

Figure 5.6: Effect of flow rate on model parameters at 60 % solids concentration

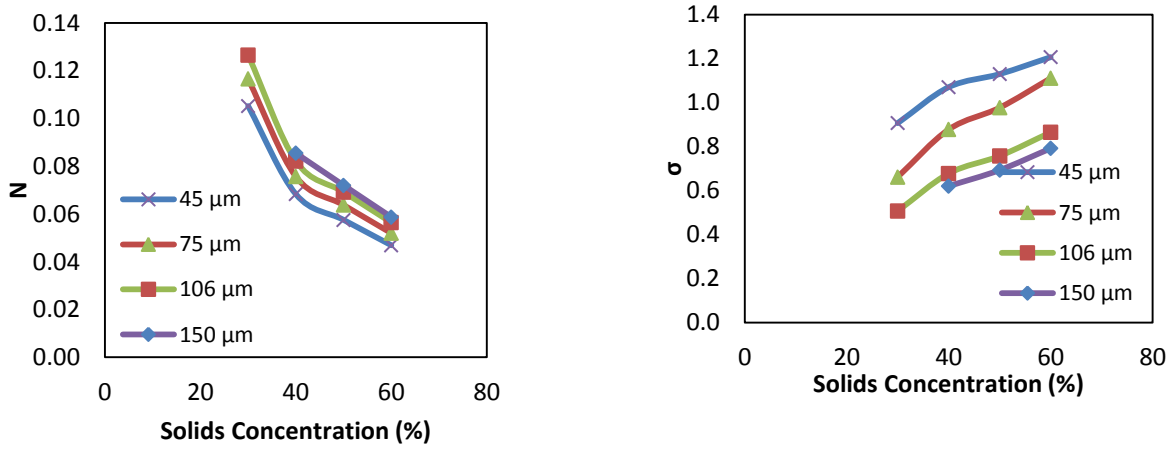

Figure 5.7: Effect of solids concentration on model parameters at 13 t/h feed flow rate

5.5 The modified Whiten Model:

The two equations for Regions 2 and 3 were then combined to give the modified Whiten model that incorporates the fish hook effect. This expression is given by Equation 41.

$$E(x) = exp(-N\, f_o(1 - \frac{x}{x_a}))^{\sigma} + \delta \qquad 41$$

The modified screen model in Equation 41 was used to fit the data obtained for each aperture in order to assess the goodness of the fit. The model fits for tests done at 40 % solids concentration and 19 t/h for four different apertures are shown in Figures 5.8. It can be seen that at these operating conditions, the model (red lines) visually fits the data (data points) reasonably well. Similar trends were observed in other conditions.

The statistical goodness of fit was assessed by comparing the sum of squares error

s (SSE) and the coefficient of determination correlation coefficients (R^2). The SSE measures the total deviation of the experimental response from the predicted response. A smaller value of SSE (closer to 0) indicates a smaller error. Thus the model fit is good and can be used for prediction. The R^2 value shows the closeness of the data to the fitted regression line. A value closer to 1 indicates that the model correlates to the data well. The equation used to calculate R^2 is given by Equation 42. Where y_i, $\hat{y}$ are the observed and predicted values respectively and $\bar{y}$ are the average observed values.

$$R^2 = \frac{\sum(y_i - \bar{y})^2 - \sum(y_i - \hat{y})^2}{\sum(y_i - \bar{y})^2} \qquad 42$$

The R^2 and SSE values obtained for the model fits shown in Figure 5.8 are given in Table 5.3. For all the apertures, the R^2 values are above 0.95 and the SSE values are low which indicates that there is a good correlation between the data and the model. It is noted that the model fits better for smaller apertures compared to larger apertures.

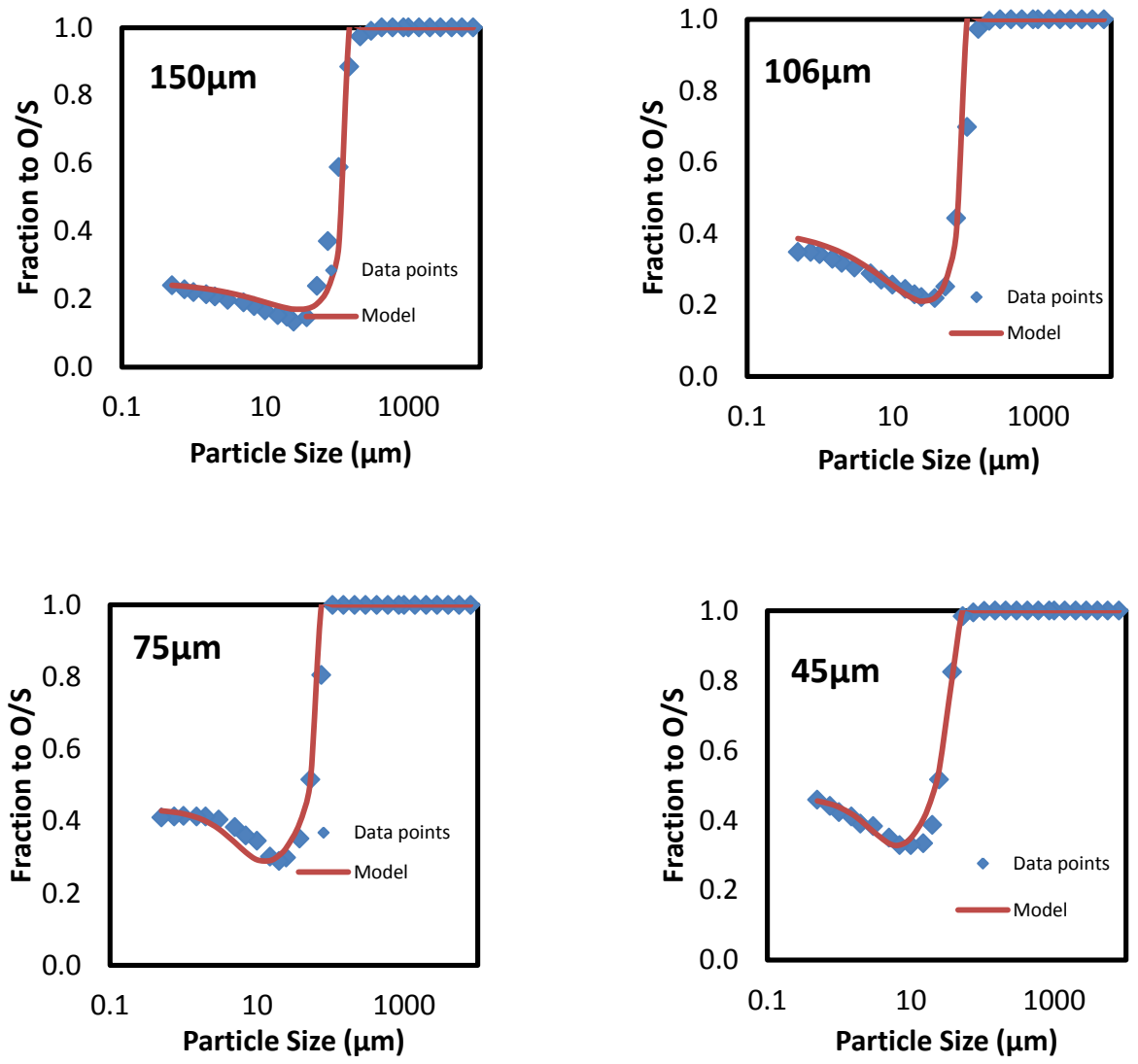

Figure 5.8: Model fits at 19 t/h and 40 % solids for different screen apertures

Table 5.3: The statistical values corresponding to the model fits at 19 t/h and 50 % solids concentration

Aperture (µm)	N	σ	R^2	SSE
45	0.057	1.15	0.993	0.02
75	0.063	0.85	0.984	0.05
106	0.069	0.78	0.971	0.08
150	0.071	0.72	0.978	0.08

5.6 Summary

The existing Whiten (1972) model excludes the operating and design parameters from the model. In this study, the Whiten model was modified and a model that captures changes in operating and design conditions was developed using the dimensional analysis approach. In addition, dimensional analysis was further applied to develop the model describing the fish hook as the experimental data exhibited pronounced fish hooks. The N and σ parameters were described in terms of the feed flow rate, feed viscosity, pulp density, aperture size, undersize flow rate and screen open area. Other changes in operating conditions such as, frequency, amplitude, amount of near size particles in the feed and gravitational acceleration are not incorporated in the model.

It has been shown that the operating conditions have an effect on the Whiten model parameters. For a constant aperture, higher flow rates and solids concentrations results in lower N values and higher σ values which is consistent to what was expected. The improvement to the Whiten model is that, for the modified model, once the model constants K_N, K_σ and K_δ are fitted for a particular aperture and particle size distribution, the model can predict the performance of the screen for other operating conditions. The model constants are only refitted if the particle size distribution or aperture size is changed.

The model fits the experimental data reasonably well with the R^2 values above 0.97. It appears to fit better at finer apertures than larger apertures. This is indicated by higher R^2 values of 0.99 obtained at smaller apertures. Therefore it can be used to assess the screen performance.

CHAPTER 6. Conclusions and Recommendations

The aim of this project was to assess the performance of a screen at aperture sizes below 150 µm and to develop a screen model that captures the influence of changes in feed conditions on wet fine screen performance. This chapter summarizes the main observations and conclusions drawn from the test work.

6.1 Key observations from test work

The key observations that were made from the test work include the following:

- For all the conditions tested, increasing the feed flow rate from 13 t/h to 30 t/h decreased the cut size and sharpness of separation and increased the recovery of water to the oversize. The influence of flow rate appeared to be more apparent at larger apertures. The highest cut size and sharpness of separation and lowest water recovery to the oversize were attained at 13 t/h feed flow rate.

- Increasing the feed solids concentration resulted in lower cut sizes and sharpness of separation and higher water recovery to the oversize. The influence on sharpness of separation and water recovery to the oversize appeared to be sharper than the one on the cut size. Solids concentration of 30 % produced the best performance with regards to all the partition curve properties.

- The feed solids concentration appeared to have a significant effect on cut size than feed solids flow rate.

- A decrease in aperture size reduced the cut size and sharpness of separation and increased the water recovery to the oversize. The cut size was closer to the aperture size at 13 t/h flow rate and 30 % solids concentration for all apertures.

- The fraction of fine particles bypassed to the oversize increased with increasing feed solids concentration and flow rate and decreasing aperture size.

- All efficiency curves exhibited fish hooks at finer particle size (< 38µm). The fish hooks became more exaggerated at higher feed flow rates and solids concentration and smaller apertures.

6.2 Modelling

The Whiten 2- parameter screen model was modified by applying the dimensional analysis approach using factors that affect the vibrating screen performance. The modified model demonstrates that the **N** and **σ** parameters in the Whiten model can be described using different operating and design variables. The **N** parameter describes the number of trials at passage of fine particles and it significantly changes both the sharpness of separation and cut size. The **σ** parameter on the other hand affects the rate of passage of fine particles through the screen apertures and it mainly affects the cut size. The effect of operating conditions on the Whiten model parameters was evaluated and sub models that capture changes in operating conditions were developed. The variables that were used to develop the sub-models were the feed flow rate, solids concentration, viscosity and aperture size. All variables that were not varied in this study but are important in describing the screening performance were lumped together in the model constants K_N and K_σ. The model that accounts for the fish hook was developed and incorporated into the Whiten model. The dimensional analysis approach was also applied when developing the fish hook model. Generally, the modified model describes the efficiency curve reasonably well for all the conditions tested in this work.

6.2.1 Advantages of the modified model

The modified model has the following advantages:

- For a constant aperture size, the model has the ability to predict the performance of the screen at different conditions without the need to perform more experiments. This is because the feed conditions are captured in the model.

- The model constants are fitted once for every change in aperture size. Thus, there is no requirement to refit the model when the feed rate or solids concentration are varied. This has reduced the fitting process initially required for the original Whiten model.

- The model captures the fish hook effect, making it more accurate for data that exhibits the fish hook. This phenomenon is not incorporated in most of the screen models available.

6.2.2 Limitations of the model

The limitations of the model are as follows:

- The model was developed for wet fine screening and has not been tested for dry screening conditions.

- A particular particle size distribution was used to develop the model. However, the model constants can be refitted easily once the particle size distribution is changed.

Despite the limitations, the model gives a good prediction of the wet fine screen performance and can be useful in the simulation of comminution circuits incorporating wet fine screening.

6.3 Conclusions

The conclusions that were drawn in addressing the objectives of this work with regards to the test work and modelling are given below:

6.3.1 Test work

- For the same solids concentration and aperture size, increasing the feed flow rate decreases the cut size and sharpness of separation and increases the amount of water recovered to the screen oversize.

- Higher feed solids concentrations are associated with lower cut sizes, lower sharpness of separation and higher water recoveries.

- The carryover of undersize material to the oversize increases with increasing feed flow rate, increasing solids concentration and decreasing aperture size.

- The fish hook becomes more pronounced at higher flow rates and solids concentrations and smaller aperture sizes.

6.3.2 Modelling

- A model that captures changes in operating and design conditions has been developed. This was achieved by using the dimensional analysis approach to develop sub-models for the efficiency parameters **N** and **σ** in the Whiten 2-parameter screen model. These parameters affect both the cut size and sharpness of separation which are used as indicators of screening performance.

- The model that describes the fish hook effect was also incorporated in the modified model.

- The wet fine screen model predicts the performance reasonably well and reduces the fitting process required in the original Whiten model.

6.4 Recommendations

The recommendations proposed for future work on investigating the effect of operating and design conditions on wet screening efficiency are as follows:

- A function that relates the cut size and sharpness of separation to **N** and **σ** parameters would be useful as it will allow for direct calculation of these parameters without the need to draw the efficiency curve.

- The feed conditions have shown significant effect on the water recovery to the oversize; therefore the development of the water recovery to the oversize model is recommended for future work.

- Additional tests on screen performance using other feed and design conditions are recommended to allow for a more robust model encompassing more screen conditions.

CHAPTER 7. References

Ahmed, J., Al-Foudari, M., Al-Salman, F. & Almusallam, A. S. 2014. Effect of particle size and temperature on rheological, thermal, and structural properties of pumpkin flour dispersion. *Journal of Food Engineering*. 124, pp.43–53.

Albuquerque, L.G., Wheeler, J., Valine, S., & Ganahl, B. 2008. Application of high frequency screens in closing grinding circuits. In International Mineral Processing Seminar–Gecamin.

Barkhuysen, N.J. 2009. Implementing strategies to improve mill capacity and efficiency through classification by particle size only. *The South African Institute of Mining and Metallurgy*, pp.101–114.

Batterham, R.J., Weller, K.R., Norgate, T.E. & Birkett, C.J. 1980. Screen performance and modelling with special reference to iron-ore crushing plants. *European Symposium on Particle Technology*, 57, pp.73–81.

Beerkircher, G. 1997. Banana screen technology. In *Communition Practices*. SME, pp. 37–40.

Chatterjee, A. 1998. Role of particle size in mineral processing at Tata Steel. *International Journal of Mineral Processing*, 53, pp.1–14.

Chen, Y. & Tong, X. 2010. Modeling screening efficiency with vibrational parameters based on DEM 3D simulation. *Mining Science and Technology (China)*, 20(4), pp.615–620. Available at: http://linkinghub.elsevier.com.

Cleary, P.W., Sinnott, M.D. & Morrison, R.D. 2009. Separation performance of double deck banana screens - Part 1: Flow and separation for different accelerations. *Minerals Engineering*, 22(14), pp.1218–1229. Available at: http://dx.doi.org/10.1016/j.mineng.2009.07.002.

de Korte, G.J. 2005. De-Sliming of Fine Coal. *CSIR*. pp. 1-23.

Delgado M., Diaz G. & Chambi R. 2007. Expansión de Producción de Condestable com Innovaciones Tecnologicas de Clasificación de Molienda (XXVIII Convención Minera Extemin 2007 – Perú).

Derrick Corporation, 2009. Wet Screening Machine-Maintenance & Operation Manual Available:http://www.derrickcorp.com/Images/Wet%20Screening%20Machine%20Manual%20-%20E3%20Motor.pdf.

Derrick Corporation, 2012. Dry Screening Technology. Available: http://www.derrickcorp.com/Images/Documents/DryScreening.pdf [2015, November 20].

Drzymala, J. 2007. *Mineral Processing, Foundations of theory and practice of minerallurgy*, Wroclaw.

Ferrara, G. & Preti, U. 1975. A contribution to screening kinetics, 11th International Minerals Processing Congress, pp.1–35.

Ferrara, G., Preti, U. & Schena, G.D. 1987. Modelling of screening operations. *Modelling of screening operations*, 22, pp.193–222.

Firth, B., O'Brien, M., Edward, D. and Clarkson, C. 1999. Fine coal classification – final report. Acarp Project C3084.

Flintoff, B.C., Plitt, L.R. & Turak, A.A. 1987. Cyclone modelling a review of present technologies. CIM Bulletin, 80(905), pp. 39– 50.

Frachon, M. & Cilliers, J.J. 1999. A general model for hydrocyclone partition curves. *Chemical Engineering Journal*, 73, pp.53–59.

Fuerstenau, M.C. & Han, K.N. 2003. *Principles of Mineral Processing*, Colorado: SME.

Gaudin, A.M. 1939. *Principles of Mineral Dressing*, McGraw Hill.

Grozubinsky, V., Sultanovitch, E. & Lin, I.J. 1998. Efficiency of solid particle screening as a function of screen slot size, particle size, and duration of screening: The theoretical approach. *International Journal of Mineral Processing*, 52(4), pp.261–272.

Gupta, A. & Yan, D. 2006. *Mineral Processing Design and Operation*, Elsevier Science and Technology.

Hatch, C.C. & Mular, A.L. 1979. Simulation of the Brends Mines Ltd secondary crushing plant. *Mining Engineering*, 34, pp.1354–1362.

He, X.M. & Liu, C.S. 2009. Dynamics and screening characteristics of a vibrating screen with variable elliptical trace. *Mining Science and Technology*, 19(4), pp.508–513.

Hess, F.W. & Whiten, W.J. 1983. A one step method to mass balance data and fit screen models, Aus.I.M.M. Illawarra Branch Symposium on Coal and Mineral Sizing. Symposia Series. *Australasian Inst of Mining & Metallurgy*. Wollongong, Australia.

Hilden, M.M. 2006. *A dimensional Analysis Approach to the Scale-up and Modelling of Industrial Screens*. University of Queensland.

Irannajad, M. 2009. Validation of proposed methods. *Mining and Metallurgical Engineering*.

Karra, V.K. 1979. Development of a model for predicting the screening performance of a vibrating screen. *CIM Bulletin*, 72, pp.167–171.

Kelley, C. 2007. Fine dry screening with urethane screen surfaces. In *The 6th International Heavy Minerals Conference "Back to Basics."* The Southern African Institute of Mining and Metallurgy.

Kelley, C.P. & Mckeon, T.J., 2005. Application of Derrick High Frequency Fine Screening Technologies in Kelsey Jig Zircon Tailings Recovery (DuPont , Starke , Florida), pp.1–5.

Kelly, E.G. and Spottiswood, D.J. 1995. Introduction to mineral processing. *The Australian Mineral Foundation.* pp. 169-198.

Kelsall, D.F. 1953. A further study of the hydraulic cyclone. *Chemical Engineering Science*, 2, pp. 254–272.

Kilavuz, F.S. & Gulsoy, O.Y. 2011. The effect of cone ratio on the separation efficiency of small diameter hydrocyclones. *International Journal of Mineral Processing*, 98, pp.163–167.

King, R.P. 2001. *Size Classification, Modelling & Simulation of Mineral Processing Systems*, Butterworth-Heinemann.

Krause, M. 2005. Horizontal versus inclined screens. *Quarry*, pp.26–27.

Lawrence, J. & Beddow, J.K. 1968. Powder Segregation during Die Filling. *Powder Technology*, 2, pp.253–259.

Li, J., Webb, C., Pandiella, S. S. & Campbell, G. M. 2003. Discrete particle motion on sieves - A numerical study using the DEM simulation. *Powder Technology*, 133(1-3), pp.190–202.

Lim, S.C. 1958. *PhD. Thesis*. University of Sydney.

Lusinga, D., Angombe, J. & Mainza, A.N. 2009. Assessing the effects of the cone force ratio on the performance of hydrocyclone. *The South African Institute of Mining and Metallurgy*, 109, pp.239–244.

Lynch, A. J. & Rao, T. C. 1968. Studies on the operating characteristics of hydrocyclone classifier. *Mining and metallurgical engineering,* 6, pp. 106-114.

Mainza, A. N. 2006. *Contribution to the understanding of the three product cyclone on the classification of a dual density platinum ore,* Cape Town: University of Cape Town.

Mainza, A., Powell, M.S. & Knopjes, B. 2005. A comparison of different cyclones in addressing challenges in the classification of the dual density UG2 platinum ore. *Journal of the South African Institute of Mining and Metallurgy*, 105(5), pp.341–348.

Mainza, A., Powell, M. S. & Knopjes, B. 2004. Differential classification of dense material in a three product cyclone. *Minerals Engineering,* pp. 537-579.

Majumder, A.K., Shah, H., Shukla, P. & Barnwal, J.P. 2007. Effect of operating variables on shape of fish hoek curves in cyclones. *Minerals Engineering*, 2(20), pp.204–206.

Matthews, C.W. 1985. General Classes of Screens. In *SME Mineral Processing Handbook*. Society of Mining Engineers, pp. 3E1–13.

Meinel, A. 1998. Classification of fine, medium-sized and coarse particles on shaking screens. *Aufbereitungs-Technik/Mineral Processing*, 39(7), pp.317–327.

Miwa, S. 1960. Proposal of a new index for expressing the performance of screens. *Kagaku Kogaku*, 24, pp.150–153.

Mohanty, M.K. 2003. Fine coal screening performance enhancement using the Pansep screen. *International Journal of Mineral Processing*, 69(1-4), pp.205–220.

Muzanenhamo, P., 2014. *Assessing the effect of cone ratio, feed solids concentration and viscosity on hydrocyclone performance*. University of Cape Town.

Mwale, A. 2015. *A Mathematical Model for Predicting Classification Performance in Wet Fine Screens*. University of Cape Town.

Nageswararao, K. 2000. Reduced efficiency curves of industrial hydrocyclones-an analysis for plant practice. *Minerals Engineering,* 5(12), pp. 517-544.

Nageswararao, K. Wiseman, D. M. & Napier-Munn, T. J., 2004. Two empirical hydrocyclonemodels revisted. *Minerals Engineering,* Volume 17, pp. 671-687.

Nakahira, K., Hotta, T., Naito, M., Shinohara, N., Cho, Y., Katori, S., Emoto, H., Yamada, T. and others. 2003. Characterization of coarse particles in alumina powders by a wet sieving method. *Journal of the European Ceramic Society*, 23(10), pp.1661–1666.

Napier-Munn, T. J., Morrell, S. & Morrison, R. D. 2005. *Mineral Comminution Circuits Their Operation and Optimisation*, Queensland: Julius Kruttschnitt Mineral Research Centre.

Narasimha, M., Mainza A.N., Holtham P.N., Powell, M.S. & Brennan M.S. 2014. A semi-mechanistic model of hydrocyclones-Developed from industrial data and inputs from CFD. *International Journal of Mineral Processing,* 133, pp. 1-12.

Nel, E., Valenta, M. & Naude, N. 2005. Influence of open circuit regrind milling on UG-2 ore composition and mineralogy at Impala's UG-2 concentrator. *Minerals Engineering*. 18, pp.785–790.

Pereira. M.J., Durao, F.O., & Guimaraes, C.A. 1993. Contribution to the validation and development of the kinetic industrial screening model. In: J. Elbrond and X. Tang (Editors), APCOM 24, International Symposium on the Application of Computers and Operations Research in the Minerals Industries. pp. 243-250.

Plitt, I.R. 1976. A mathematical model of the hydrocyclone classifier. *CIM Bull*. 114–122.

Plitt, L.R. 1971. The analysis of solid–solid separations in classifiers. CIM Bulletin. 64 (708), pp.42– 47.

Olsen, P. & Coombe, A. 2003. Is screening a science or art? *Quarry*, 11(8), pp.20–25.

Roberts, T.A. & Beddow, J.K. 1968. Some Effects of Particle Shape and Size upon Blinding During Sieving. *Powder Technology*, 2, pp.121–124.

Rogers, R.S.C. 1982. A Classification Function for Vibrating Screens. *Powder Technology*, 31, pp.135–137.

Rogers, R.S.C. & Brame, K.A. 1985. An analysis of the High-Frequency Screening of Fine Slurries. *Powder Technology*, 42, pp.297–304.

Roldan-Villasana, E.J., Williams, R.A. & Dyakowski, T. 1993. The origin of the fish-hook effect in hydrocyclone separators. *Powder Technology*. 77, 243– 250.

Santos, W.P.C., Hatje, V., Lima, L. N., Trignano, S. V. and others. 2008. Evaluation of sample preparation (grinding and sieving) of bivalves, coffee and cowpea beans for multi-element analysis. *Microchemical Journal*, 89(2), pp.123–130.

Schumacher, B.A., Shines, K.C., Burton, J.V. & Papp, M.L. 1990. A comparison of soil sample homogenization techniques. *Lockheed Engineering and Sciences Company, Inc.*

Soldinger, M. 2000. Influence Of Particle Size and Bed Thickness On The Screening Process. *Minerals Engineering*, 13(3), pp.297–312.

Soldinger, M. 1999. Interrelation of stratification and passage in the screening process. *Minerals Engineering*, 12(5), pp.497–516.

Standish, N., Bharadwaj, a. K. & Hariri-Akbari, G. 1986. A study of the effect of operating variables on the efficiency of a vibrating screen. *Powder Technology*, 48(2), pp.161–172.

Steckel, H., Markefka, P., TeWierik, H . & Kammelar, R. 2006. Effect of milling and sieving on functionality of dry powder inhalation products. *International Journal of Pharmaceutics*, 309(1-2), pp.51–59.

Subasinge, G.K.N.., Schaap, W. & Kelly, E.G., 1989. Modelling the screen process - an empirical approach. *Minerals Engineering*, 2(2), pp.235–244.

Svarovsky, L. 2000. *Solid-Liquid Separation.* 4th ed. Oxford: Butterworth-Heinemann.

Taggart, A.F., 1945. Screen sizing, Handbook of Mineral Dressing: Ores and Industrial Minerals. In New Yourk: John Wiley and Sons, pp. 1–72.

Tinke, A.P., Govoreanu, R., Weuts, I., Vanhoutte, K. and others. 2009. A review of underlying fundamentals in wet dispersion size analysis of powders. *Powder Technology*, 196, pp.102–114.

Trumic, M. & Magdalinovic, N. 2011. New model of screening kinetics. *Minerals Engineering*, 24(1), pp.42–49.

Tsakalakis, K. 2001. Some basic factors affecting screen performance in horizontal vibrating screens. *The European Journal of Mineral Processing and Environmental Protection*, 1, pp.42–54.

Valine, S.B. & Wennen, J.E. 2002. *Mineral Processing Plant Design, Practice, and Control* A. L. Mular, D. N. Halbe, & D. J. Barratt, eds., SME.

Valine, S.B., Wheeler, J.E. & Albuquerque, L.G. 2009. Fine sizing with the derrick stack sizer screen. In *Recent Advances in Mineral Processing Plant Design*. SME, pp. 433–443.

Vorster, W., Hinde, a. & Schiefer, F. 2002. Increased screening efficiency using a Kroosher unit coupled with a Sweco screen (Part 1). *Minerals Engineering*, 15(1-2), pp.107–110.

Whiten, W.J. 1966. Lecture notes for winter school on mineral processing. Dept Min & Met Eng, University of Queensland (JKMRC).

Whiten, W.J. 1972. *Simulation and model building for mineral processing*. University of Queensland, Australia.

Wilkinson, H.N. 1971. H.N. Wilkinson. *J. Iron Steel Inst.*, 209, pp.178.

Wills, B.A. 1997. *Mineral Processing Technology*, London: Butterworth-Heinemann.

Wills, B.A. & Napier-Munn, T. 2006. *Mineral Processing Technology* 7th ed., UK: Elsevier Science and Technology Books.

Xiao, J. & Tong, X. 2013. Characteristics and efficiency of a new vibrating screen with a swing trace. *Particuology*, 11(5), pp.601–606.

Appendix

Experimental Data

A 1: Actual feed flow rates and solids concentration for the 45 and 75 µm aperture sizes

Apt. (µm)	Feed rate (t/h)	Feed % solids	Water in Feed (t/h)	O/S rate (t/h)	Water in O/S (t/h)	O/S % solids	U/S rate (t/h)	Water in U/S (t/h)	U/S % solids	Water split to O/S	Mass split to O/S	Mass split to U/S
45	29.2	41.7	40.9	20.3	19.7	50.7	8.9	21.1	29.6	0.5	0.7	0.3
	22.4	42.2	30.7	14.6	13.6	51.8	7.8	17.2	31.3	0.4	0.7	0.3
	17.2	41.2	24.6	10.7	9.5	52.9	6.5	15.1	30.2	0.4	0.6	0.4
	11.3	40.3	16.7	6.7	6.5	51.0	4.5	10.2	30.7	0.4	0.6	0.4
	23.7	36.1	41.9	14.3	17.4	45.2	9.3	24.5	27.6	0.4	0.6	0.4
	17.7	35.8	31.7	10.2	11.6	46.9	7.4	20.1	27.0	0.4	0.6	0.4
	12.7	41.5	18.0	7.2	7.2	49.9	5.6	10.8	34.0	0.4	0.6	0.4
	8.2	36.2	14.4	4.3	4.0	52.4	3.8	10.4	26.8	0.3	0.5	0.5
	17.9	29.7	42.6	9.7	9.8	49.9	8.2	32.8	20.0	0.2	0.5	0.5
	15.6	28.9	38.5	8.3	7.6	52.2	7.4	30.9	19.2	0.2	0.5	0.5
	10.4	25.3	30.9	4.8	5.3	47.6	5.6	25.6	18.0	0.2	0.5	0.5
	9.5	10.5	80.3	4.6	3.9	54.0	4.9	76.4	6.0	0.0	0.5	0.5
	10.7	19.6	43.9	4.9	3.9	55.8	5.8	40.1	12.7	0.1	0.5	0.5
	8.9	19.4	36.8	3.8	2.8	57.8	5.0	34.0	12.9	0.1	0.4	0.6
75	35.5	60.0	23.6	23.4	19.4	54.7	12.1	4.3	73.9	0.8	0.7	0.3
	28.3	60.0	18.9	17.7	13.7	56.4	10.6	5.2	67.2	0.7	0.6	0.4
	24.3	60.0	16.2	14.8	10.8	57.8	9.5	5.4	63.8	0.7	0.6	0.4
	16.9	60.0	11.3	9.6	6.7	59.0	7.3	4.6	61.4	0.6	0.6	0.4
	10.2	60.0	6.8	5.6	3.6	60.8	4.6	3.2	59.0	0.5	0.5	0.5
	22.0	50.0	22.0	12.6	8.4	59.9	9.5	13.6	41.0	0.4	0.6	0.4
	15.1	50.0	15.1	8.3	5.2	61.5	6.8	9.9	40.7	0.3	0.6	0.4
	12.3	50.0	12.3	6.4	3.8	62.5	6.0	8.5	41.2	0.3	0.5	0.5
	8.7	50.0	8.7	5.4	3.2	63.2	3.3	5.5	37.1	0.4	0.6	0.4
	18.1	40.0	27.2	9.4	5.7	62.3	8.7	21.5	28.9	0.2	0.5	0.5
	14.3	40.0	21.5	6.9	4.0	63.4	7.4	17.5	29.7	0.2	0.5	0.5
	10.0	40.0	15.0	4.6	2.5	64.9	5.5	12.6	30.3	0.2	0.5	0.5
	9.1	40.0	13.7	4.1	2.1	65.7	5.1	11.6	30.5	0.2	0.4	0.6
	12.2	30.0	28.5	5.3	2.7	66.0	7.0	25.8	21.2	0.1	0.4	0.6
	7.6	30.0	17.8	3.1	1.4	69.0	4.5	16.4	21.6	0.1	0.4	0.6

A 2: Actual feed flow rates and solids concentration for the 106 and 150 µm aperture sizes

Apt. (µm)	Act. Feed rate (t/h)	Feed % solids	Water in Feed (t/h)	O/S rate (t/h)	Water in O/S (t/h)	O/S % solids	U/S rate (t/h)	Water in U/S (t/h)	U/S % solids	Water split to O/S	Mass split to O/S	Mass split to U/S
106	30.9	60.0	20.6	19.5	10.6	64.9	11.4	10.0	53.2	0.5	0.6	0.4
	28.4	60.0	18.9	16.1	7.6	67.9	12.3	11.3	52.1	0.4	0.6	0.4
	22.8	60.0	15.2	13.8	7.1	66.2	9.0	8.2	52.5	0.5	0.6	0.4
	12.9	60.0	8.6	6.7	2.8	70.3	6.2	5.8	51.8	0.3	0.5	0.5
	9.1	60.0	6.1	4.5	1.5	74.3	4.7	4.6	50.8	0.3	0.5	0.5
	23.8	53.9	20.4	13.0	5.6	70.0	10.9	14.8	42.3	0.3	0.5	0.5
	19.7	52.5	17.8	9.0	3.5	72.0	10.7	14.3	42.8	0.2	0.5	0.5
	17.2	52.1	15.8	7.1	2.0	77.8	10.1	13.8	42.3	0.1	0.4	0.6
	12.4	49.8	12.5	4.5	1.1	81.1	7.9	11.4	40.8	0.1	0.4	0.6
	20.0	43.7	25.7	10.4	3.5	74.7	9.6	22.2	30.2	0.1	0.5	0.5
	14.5	32.1	30.7	6.8	2.1	76.5	7.7	28.6	21.2	0.1	0.5	0.5
	10.8	39.4	16.6	4.4	1.1	80.7	6.4	15.6	29.1	0.1	0.4	0.6
	5.8	36.0	10.2	2.1	0.4	83.8	3.7	9.8	27.1	0.0	0.4	0.6
	8.7	33.2	17.5	3.3	0.7	82.2	5.4	16.8	24.4	0.0	0.4	0.6
	8.5	27.5	22.5	2.3	0.4	85.3	6.2	22.1	21.9	0.0	0.3	0.7
150	28.9	60.0	19.3	12.6	4.4	74.1	16.3	14.9	52.3	0.2	0.4	0.6
	25.7	60.0	17.2	12.8	4.6	73.5	12.9	12.5	50.7	0.3	0.5	0.5
	21.5	60.0	14.3	8.7	2.9	74.9	12.8	11.4	52.9	0.2	0.4	0.6
	15.0	60.0	10.0	5.0	1.7	75.0	10.0	8.4	54.6	0.2	0.3	0.7
	11.3	60.0	7.5	3.4	1.1	75.8	7.9	6.5	55.0	0.1	0.3	0.7
	21.8	50.0	21.8	8.0	2.6	75.8	13.8	19.3	41.7	0.1	0.4	0.6
	14.4	50.0	14.4	4.4	1.4	76.0	10.0	13.0	43.5	0.1	0.3	0.7
	18.9	40.0	28.4	5.2	1.6	77.0	13.7	26.9	33.8	0.1	0.3	0.7
	19.6	30.0	45.8	3.1	0.8	78.9	16.6	45.0	26.9	0.0	0.2	0.8

PSDs for the 45 µm aperture

Size (um)	45 um, 60 %									45 um, 50 %								45 um, 40 %								45 um, 30 %			
	Feed	30 t/h		25 t/h		19 t/h		13 t/h		25 t/h		19 t/h		13 t/h		9 t/h		19 t/h		16 t/h		13 t/h		9 t/h		13 t/h		9 t/h	
		U/S	O/S	U/S	O/S	U/S	O/S	U/S	O/S	U/S	O/S	U/S	O/S	U/S	O/S	U/S	O/S	U/S	O/S	U/S	O/S	U/S	O/S	U/S	O/S	U/S	O/S	U/S	O/S
8000	100.0	100.0	100.0	100.0	100.0	100.0	100.0	100.0	100.0	100.0	100.0	100.0	100.0	100.0	100.0	100.0	100.0	100.0	100.0	100.0	100.0	100.0	100.0	100.0	100.0	100.0	100.0	100.0	100.0
5600	100.0	100.0	100.0	100.0	100.0	100.0	100.0	100.0	100.0	100.0	100.0	100.0	100.0	100.0	100.0	100.0	100.0	100.0	100.0	100.0	100.0	100.0	100.0	100.0	100.0	100.0	100.0	100.0	100.0
4000	100.0	100.0	100.0	100.0	100.0	100.0	100.0	100.0	100.0	100.0	100.0	100.0	100.0	100.0	100.0	100.0	100.0	100.0	100.0	100.0	100.0	100.0	100.0	100.0	100.0	100.0	100.0	100.0	100.0
2800	100.0	100.0	100.0	100.0	100.0	100.0	100.0	100.0	100.0	100.0	100.0	100.0	100.0	100.0	100.0	100.0	100.0	100.0	100.0	100.0	100.0	100.0	100.0	100.0	100.0	100.0	100.0	100.0	100.0
2000	100.0	100.0	100.0	100.0	100.0	100.0	100.0	100.0	100.0	100.0	100.0	100.0	100.0	100.0	100.0	100.0	100.0	100.0	100.0	100.0	100.0	100.0	100.0	100.0	100.0	100.0	100.0	100.0	100.0
1400	100.0	100.0	100.0	100.0	100.0	100.0	100.0	100.0	100.0	100.0	100.0	100.0	99.9	100.0	100.0	100.0	100.0	100.0	100.0	100.0	100.0	100.0	100.0	100.0	100.0	100.0	100.0	100.0	100.0
1000	100.0	100.0	100.0	100.0	100.0	100.0	100.0	100.0	100.0	100.0	100.0	100.0	99.8	100.0	100.0	100.0	100.0	100.0	100.0	100.0	100.0	100.0	100.0	100.0	100.0	100.0	100.0	100.0	100.0
850	100.0	100.0	100.0	100.0	100.0	100.0	100.0	100.0	100.0	100.0	100.0	100.0	99.7	100.0	100.0	100.0	100.0	100.0	100.0	100.0	100.0	100.0	100.0	100.0	100.0	100.0	100.0	100.0	99.9
600	100.0	100.0	100.0	100.0	100.0	100.0	100.0	100.0	100.0	100.0	100.0	100.0	99.6	100.0	100.0	100.0	99.7	100.0	99.7	100.0	99.9	100.0	99.9	100.0	99.8	100.0	99.9	100.0	99.9
425	100.0	100.0	100.0	100.0	99.9	100.0	99.8	100.0	99.9	100.0	99.8	100.0	99.2	100.0	99.9	100.0	98.0	100.0	98.6	100.0	99.3	100.0	99.2	100.0	99.0	100.0	99.7	100.0	99.7
300	99.7	100.0	99.5	100.0	99.1	100.0	98.9	100.0	99.2	100.0	98.6	100.0	98.1	100.0	99.0	100.0	95.5	100.0	95.9	100.0	97.4	100.0	97.4	100.0	96.9	100.0	98.8	100.0	98.8
212	98.8	100.0	97.7	100.0	96.6	100.0	96.2	100.0	96.9	100.0	95.5	100.0	95.4	100.0	96.1	100.0	92.0	100.0	91.7	100.0	93.0	100.0	94.8	100.0	93.2	100.0	96.3	100.0	96.3
150	96.5	100.0	93.3	100.0	93.4	100.0	90.2	100.0	94.6	100.0	89.7	100.0	92.3	100.0	92.3	100.0	87.4	100.0	84.6	100.0	86.6	100.0	91.3	100.0	87.5	100.0	93.0	100.0	92.8
106	91.7	99.8	89.1	100.0	91.1	99.8	83.8	100.0	89.6	100.0	86.2	100.0	86.1	100.0	89.2	100.0	80.6	100.0	83.8	100.0	86.0	100.0	88.5	100.0	86.1	100.0	91.3	100.0	90.9
75	84.2	99.3	81.7	99.8	85.4	99.2	73.2	100.0	85.1	100.0	81.2	99.9	78.8	100.0	81.1	100.0	73.5	100.0	79.0	100.0	81.6	99.8	81.9	100.0	80.9	99.9	81.3	99.8	76.7
53	74.3	98.3	72.3	99.3	76.6	97.3	59.8	99.6	79.1	99.6	73.1	99.2	66.1	99.6	68.4	99.2	59.0	99.8	68.7	99.7	71.8	99.0	66.0	100.0	61.3	98.9	51.1	98.6	44.8
38	63.4	96.1	62.2	97.3	66.9	94.1	49.5	96.7	68.0	96.4	56.8	95.8	49.6	95.9	50.5	95.5	45.5	95.6	52.2	92.0	45.9	92.6	46.7	92.2	42.6	89.2	33.5	90.7	33.6
25	49.8	89.9	51.1	90.6	54.9	85.3	39.4	88.9	55.6	89.9	46.8	84.8	37.9	80.2	35.3	83.8	36.4	80.9	38.9	80.2	36.9	79.0	37.6	75.9	33.8	75.3	27.8	77.4	28.6
20	43.2	85.9	46.3	86.3	49.7	79.9	35.1	84.1	50.6	82.6	40.5	70.9	29.5	67.9	28.4	73.3	31.7	72.4	34.4	69.3	31.4	68.7	32.9	65.3	29.5	60.0	23.1	64.6	24.9
15	35.9	78.1	40.4	78.1	43.1	70.6	29.9	75.5	44.0	72.8	35.6	53.6	23.3	54.0	23.2	62.5	27.7	57.7	28.1	60.0	27.9	60.4	29.6	55.1	25.8	44.5	18.5	54.2	21.8
10	27.7	60.8	31.9	54.3	30.5	53.3	23.1	53.8	32.0	58.1	29.7	39.4	18.6	39.4	18.0	45.4	21.4	43.1	22.1	45.7	22.7	46.1	24.0	42.3	21.1	37.5	16.3	45.8	19.2
7	21.7	46.7	25.5	39.5	23.1	39.9	18.1	39.2	24.5	46.4	24.6	30.1	14.9	29.7	14.2	35.8	17.6	32.2	17.6	35.6	18.6	35.8	19.5	32.7	17.3	29.0	13.2	34.6	15.2
5	16.9	35.7	20.2	29.2	17.7	29.9	14.1	29.0	18.9	29.8	17.6	22.7	11.8	22.2	11.2	26.4	13.6	24.3	14.0	26.7	14.6	25.6	14.8	24.2	13.6	21.8	10.3	26.1	12.0
3	10.8	21.4	12.8	15.8	10.2	17.9	8.8	16.1	11.1	19.3	12.2	13.5	7.7	13.1	7.0	16.7	9.1	15.6	9.4	16.6	9.7	15.1	9.5	15.3	9.2	12.5	6.3	14.3	7.0
2	7.2	13.2	8.2	9.3	6.3	10.9	5.6	9.6	6.9	10.6	7.3	8.3	5.0	8.0	4.5	9.9	5.7	9.7	6.2	10.7	6.6	9.1	6.0	9.7	6.1	6.6	3.5	7.6	4.0
2	5.3	8.9	5.7	6.2	4.3	7.3	3.9	6.4	4.8	6.7	4.8	5.6	3.5	5.4	3.2	6.4	3.8	6.7	4.4	7.4	4.7	6.2	4.3	6.7	4.4	0.0	0.0	0.0	0.0
1	3.3	4.5	3.0	3.1	2.3	3.7	2.0	3.2	2.5	2.9	2.2	2.9	1.9	2.8	1.7	2.8	1.8	3.5	2.4	4.0	2.6	3.3	2.3	3.6	2.4				
1	2.2	2.3	1.5	1.6	1.2	1.9	1.1	1.6	1.3	1.5	1.1	1.5	1.0	1.5	0.9	1.5	1.0	1.8	1.3	2.1	1.4	1.7	1.3	2.0	1.3				
1	1.0	0.0	0.0	0.0	0.0	0.0	0.0	0.0	0.0	0.0	0.0	0.0	0.0	0.0	0.0	0.0	0.0	0.0	0.0	0.0	0.0	0.0	0.0	0.0	0.0				

PSDs for the 75 µm aperture

Size (um)	75 um, 60 %								75 um, 50 %								75 um, 40 %								75 um, 30 %			
	35 t/h		**30** t/h		**19** t/h		**13** t/h		**25** t/h		**19** t/h		**13** t/h		**9** t/h		**19** t/h		**16** t/h		**13** t/h		**9** t/h		**13** t/h		**9** t/h	
	U/S	**O/S**	**U/S**	**O/S**	**U/S**	**O/S**	**U/S**	**O/S**	**U/S**	**O/S**	**U/S**	**O/S**	**U/S**	**O/S**	**U/S**	**O/S**	**U/S**	**O/S**	**U/S**	**O/S**	**U/S**	**O/S**	**U/S**	**O/S**	**U/S**	**O/S**	**U/S**	**O/S**
8000	100.0	100.0	100.0	100.0	100.0	100.0	100.0	100.0	100.0	100.0	100.0	100.0	100.0	100.0	100.0	100.0	100.0	100.0	100.0	100.0	100.0	100.0	100.0	100.0	100.0	100.0	100.0	100.0
5600	100.0	100.0	100.0	100.0	100.0	100.0	100.0	100.0	100.0	100.0	100.0	100.0	100.0	100.0	100.0	100.0	100.0	100.0	100.0	100.0	100.0	100.0	100.0	100.0	100.0	100.0	100.0	100.0
4000	100.0	100.0	100.0	100.0	100.0	100.0	100.0	100.0	100.0	100.0	100.0	100.0	100.0	100.0	100.0	100.0	100.0	100.0	100.0	100.0	100.0	100.0	100.0	100.0	100.0	100.0	100.0	100.0
2800	100.0	100.0	100.0	100.0	100.0	100.0	100.0	100.0	100.0	100.0	100.0	100.0	100.0	100.0	100.0	100.0	100.0	100.0	100.0	100.0	100.0	100.0	100.0	100.0	100.0	100.0	100.0	100.0
2000	100.0	100.0	100.0	100.0	100.0	100.0	100.0	100.0	100.0	100.0	100.0	100.0	100.0	100.0	100.0	100.0	100.0	100.0	100.0	100.0	100.0	100.0	100.0	100.0	100.0	100.0	100.0	100.0
1400	100.0	100.0	100.0	100.0	100.0	100.0	100.0	100.0	100.0	100.0	100.0	100.0	100.0	100.0	100.0	100.0	100.0	100.0	100.0	100.0	100.0	100.0	100.0	100.0	100.0	100.0	100.0	100.0
1000	100.0	100.0	100.0	100.0	100.0	100.0	100.0	100.0	100.0	100.0	100.0	99.9	100.0	100.0	100.0	100.0	100.0	100.0	100.0	100.0	100.0	100.0	100.0	100.0	100.0	100.0	100.0	100.0
850	100.0	100.0	100.0	100.0	100.0	100.0	100.0	100.0	100.0	100.0	100.0	99.9	100.0	100.0	100.0	100.0	100.0	100.0	100.0	99.9	100.0	100.0	100.0	100.0	100.0	100.0	100.0	100.0
600	100.0	99.8	100.0	100.0	100.0	100.0	100.0	100.0	100.0	100.0	100.0	99.8	100.0	100.0	100.0	100.0	100.0	100.0	100.0	98.9	100.0	100.0	100.0	99.6	100.0	99.4	100.0	99.9
425	100.0	98.9	100.0	100.0	100.0	99.9	100.0	100.0	100.0	99.6	100.0	99.2	100.0	99.9	100.0	98.4	100.0	99.2	100.0	96.7	100.0	99.7	100.0	98.6	100.0	96.0	100.0	98.7
300	100.0	97.2	100.0	100.0	100.0	99.0	100.0	100.0	100.0	97.3	100.0	96.4	100.0	97.8	100.0	93.4	100.0	95.5	100.0	90.1	100.0	96.0	100.0	93.9	100.0	88.0	100.0	93.6
212	100.0	94.9	100.0	100.0	100.0	97.2	100.0	100.0	100.0	92.0	100.0	88.1	100.0	88.5	100.0	84.2	100.0	87.2	100.0	77.8	100.0	84.5	100.0	83.2	100.0	75.7	100.0	82.7
150	100.0	93.0	99.9	97.1	100.0	94.7	99.9	97.5	100.0	83.9	100.0	71.3	100.0	66.7	100.0	38.6	100.0	75.5	99.9	62.9	100.0	64.8	100.0	67.7	100.0	39.8	100.0	37.3
106	99.9	90.3	99.6	90.0	98.4	72.1	98.6	77.2	100.0	73.3	99.9	67.4	99.8	62.0	100.0	27.5	100.0	63.4	99.7	56.5	99.4	52.8	99.7	45.3	100.0	27.3	100.0	22.2
75	99.1	82.2	97.4	69.5	91.6	42.2	91.8	48.7	98.9	64.6	98.7	59.5	98.5	55.1	98.8	24.0	97.6	54.2	96.5	46.5	96.1	43.0	96.8	35.5	97.0	21.4	96.2	17.0
53	95.7	66.9	87.6	44.4	80.6	31.3	81.1	37.1	94.7	57.2	93.0	52.3	92.9	48.7	92.6	20.6	91.5	48.1	90.1	40.3	90.3	37.4	90.6	31.0	91.2	17.9	89.7	14.1
38	85.2	54.7	75.7	36.1	69.5	26.5	70.3	31.9	85.3	51.0	82.8	46.6	83.0	43.7	83.4	18.6	82.9	43.8	81.1	36.3	82.9	34.2	82.3	28.0	84.2	16.0	83.1	12.9
25	62.3	42.4	59.9	29.9	55.7	22.2	57.3	26.9	70.5	44.0	68.5	40.4	69.5	38.4	72.3	16.7	69.6	38.6	65.8	31.2	71.4	30.8	69.0	24.7	74.2	14.7	74.5	12.0
20	55.4	38.9	53.0	27.2	49.3	20.2	51.4	24.6	62.6	40.3	60.7	37.0	61.3	35.3	64.5	15.5	62.0	35.7	58.8	29.1	63.9	28.8	61.6	23.0	67.1	13.8	68.0	11.5
15	46.6	34.4	44.5	24.0	41.6	17.8	44.3	21.8	53.1	35.8	51.5	32.9	51.8	31.5	55.9	14.0	52.8	32.0	50.3	26.3	54.9	26.2	52.7	21.0	58.7	12.8	60.4	10.7
10	34.9	27.9	33.7	19.4	32.0	14.4	35.3	18.3	40.9	29.6	40.6	27.5	41.2	26.3	46.1	12.1	42.3	26.8	40.1	22.0	45.2	22.5	42.6	18.3	48.7	11.4	51.4	9.7
7	26.9	22.4	25.8	15.5	24.9	11.7	28.6	15.4	31.3	24.1	31.7	22.8	32.7	21.6	37.4	10.3	33.6	22.2	32.2	18.3	36.8	19.1	34.2	15.3	40.0	9.9	43.2	8.6
5	20.6	17.6	19.6	12.1	19.1	9.3	23.0	12.7	23.3	19.0	24.4	18.3	25.5	17.2	29.7	8.4	26.2	17.9	25.4	14.8	29.4	15.6	27.0	12.4	32.0	8.3	35.3	7.4
3	12.5	11.0	11.8	7.5	11.7	5.9	15.8	9.1	14.1	12.1	15.5	12.0	16.7	11.5	20.9	6.0	16.6	11.9	16.4	9.7	19.6	10.6	17.5	8.2	22.4	6.2	25.9	5.8
2	7.8	7.0	7.3	4.7	7.3	3.8	11.3	6.6	8.6	7.7	9.7	7.8	10.8	7.5	14.3	4.2	10.7	8.0	10.5	6.3	13.0	7.1	11.4	5.3	15.3	4.6	18.4	4.4
1.5	5.3	4.9	5.0	3.2	5.0	2.6	8.9	5.2	5.7	5.3	6.5	5.4	7.4	5.2	9.9	2.9	7.4	5.9	7.2	4.3	9.1	5.0	7.9	3.7	10.7	3.5	13.2	3.4
1	2.8	2.6	2.6	1.7	2.6	1.4	6.3	3.7	2.9	2.7	3.3	2.8	4.0	2.8	5.5	1.7	3.9	3.6	3.8	2.3	4.9	2.7	4.3	2.0	6.0	2.3	7.7	2.4
0.75	1.5	1.4	1.3	0.9	1.3	0.7	5.0	2.9	1.5	1.4	1.7	1.5	2.1	1.5	2.8	0.9	2.1	2.4	2.0	1.2	2.6	1.4	2.2	1.0	3.1	1.6	4.0	1.7
0.5	0.0	0.0	0.0	0.0	0.0	0.0	0.0	0.0	0.0	0.0	0.0	0.0	0.0	0.0	0.0	0.0	0.0	1.0	0.0	0.0	0.0	0.0	0.0	0.0	0.0	0.8	0.0	1.0

PSDs for the 106 µm aperture

Size (um)	106 um, 60 %								106 um, 50 %						106 um, 40 %						106 um, 30 %			
	35 t/h		30 t/h		19 t/h		13 t/h		25 t/h		19 t/h		13 t/h		19 t/h		13 t/h		9 t/h		13 t/h		9 t/h	
	U/S	O/S	U/S	O/S	U/S	O/S	U/S	O/S	U/S	O/S	U/S	O/S	U/S	O/S	U/S	O/S	U/S	O/S	U/S	O/S	U/S	O/S	U/S	O/S
8000	100.0	100.0	100.0	100.0	100.0	100.0	100.0	100.0	100.0	100.0	100.0	100.0	100.0	100.0	100.0	100.0	100.0	100.0	100.0	100.0	100.0	100.0	100.0	100.0
5600	100.0	100.0	100.0	100.0	100.0	100.0	100.0	100.0	100.0	100.0	100.0	100.0	100.0	100.0	100.0	100.0	100.0	100.0	100.0	100.0	100.0	100.0	100.0	100.0
4000	100.0	100.0	100.0	100.0	100.0	100.0	100.0	100.0	100.0	100.0	100.0	100.0	100.0	100.0	100.0	100.0	100.0	100.0	100.0	100.0	100.0	100.0	100.0	100.0
2800	100.0	100.0	100.0	100.0	100.0	100.0	100.0	100.0	100.0	100.0	100.0	100.0	100.0	100.0	100.0	100.0	100.0	100.0	100.0	100.0	100.0	100.0	100.0	100.0
2000	100.0	100.0	100.0	100.0	100.0	100.0	100.0	100.0	100.0	100.0	100.0	100.0	100.0	100.0	100.0	100.0	100.0	100.0	100.0	100.0	100.0	100.0	100.0	100.0
1400	100.0	100.0	100.0	100.0	100.0	100.0	100.0	100.0	100.0	100.0	100.0	100.0	100.0	100.0	100.0	100.0	100.0	100.0	100.0	100.0	100.0	100.0	100.0	100.0
1000	100.0	100.0	100.0	100.0	100.0	100.0	100.0	100.0	100.0	100.0	100.0	100.0	100.0	100.0	100.0	99.8	100.0	100.0	100.0	100.0	100.0	100.0	100.0	100.0
850	100.0	99.9	100.0	99.8	100.0	100.0	100.0	100.0	100.0	100.0	100.0	100.0	100.0	100.0	100.0	98.2	100.0	100.0	100.0	99.7	100.0	100.0	100.0	99.8
600	100.0	99.5	100.0	98.8	100.0	99.9	100.0	99.8	100.0	100.0	100.0	100.0	100.0	100.0	100.0	97.6	100.0	98.6	100.0	93.6	100.0	97.4	100.0	95.0
425	100.0	98.3	100.0	96.4	100.0	99.7	100.0	99.3	100.0	99.8	100.0	100.0	100.0	99.8	100.0	91.6	100.0	91.6	100.0	76.7	100.0	87.8	100.0	80.3
300	99.9	94.0	100.0	93.1	100.0	99.5	99.7	97.0	100.0	98.9	100.0	100.0	100.0	98.9	100.0	76.9	100.0	76.9	100.0	51.5	100.0	71.6	100.0	56.5
212	99.3	62.4	99.5	75.8	100.0	98.0	97.8	85.4	100.0	97.6	99.3	100.0	100.0	97.6	99.9	56.6	100.0	57.5	99.6	28.1	100.0	54.3	100.0	32.2
150	95.7	50.9	97.5	69.1	99.9	94.6	93.7	66.5	100.0	68.8	97.3	99.3	99.3	73.5	96.5	39.0	96.2	27.5	97.0	13.4	97.7	41.8	100.0	15.6
106	89.5	44.2	92.0	62.0	99.0	83.4	87.1	46.6	96.7	56.1	92.7	97.3	94.9	55.0	89.9	27.4	89.4	18.0	91.2	7.6	90.1	35.1	98.4	8.4
75	81.2	39.4	83.8	55.5	91.7	67.1	78.6	35.9	89.5	46.4	85.3	92.7	87.6	43.9	80.6	21.7	80.2	13.7	83.0	5.7	82.0	31.6	93.9	6.8
53	71.7	35.9	74.3	50.0	80.9	56.0	69.1	31.9	80.5	40.4	75.4	85.3	76.3	37.1	70.5	19.2	70.4	12.2	74.6	5.3	73.2	28.8	86.1	6.4
38	62.4	32.4	64.8	45.0	68.3	48.0	59.8	28.5	68.7	35.6	64.5	75.4	66.1	32.7	61.3	17.2	61.1	11.1	61.7	4.7	64.5	25.9	75.3	5.7
25	51.2	27.9	53.5	38.5	49.9	37.8	48.4	24.1	56.5	31.2	50.7	64.5	53.0	27.7	49.1	14.5	50.1	9.6	47.1	4.0	54.8	22.2	63.2	4.7
20	45.6	25.4	47.8	34.7	44.3	34.6	42.8	22.0	49.4	28.7	43.9	50.7	46.6	25.3	43.0	13.2	44.5	8.8	41.9	3.7	49.3	20.4	56.7	4.3
15	39.2	22.1	41.1	30.1	37.4	30.3	36.1	19.2	41.3	25.5	36.4	43.9	39.1	22.3	36.2	11.5	37.8	7.8	35.7	3.3	43.0	18.2	49.3	3.9
10	31.2	17.8	33.0	24.0	28.3	24.1	28.0	15.4	32.4	21.6	27.8	36.4	30.6	18.7	28.1	9.3	30.0	6.4	27.5	2.7	35.0	15.0	39.9	3.3
7	25.2	14.3	26.9	19.1	21.9	19.2	21.9	12.4	25.5	18.3	21.7	27.8	24.2	15.7	21.7	7.5	23.8	5.3	21.0	2.2	27.9	12.1	31.7	2.7
5	20.1	11.1	21.8	14.9	16.6	14.9	17.0	9.7	19.6	15.1	16.8	21.7	18.8	12.9	16.4	5.9	18.6	4.2	15.8	1.8	21.5	9.6	24.5	2.2
3	13.5	6.7	15.2	9.3	10.1	9.3	10.8	6.2	13.1	10.8	10.7	16.8	11.6	8.7	10.0	3.8	11.7	2.8	9.3	1.2	13.6	6.2	15.7	1.4
2	9.3	3.7	11.0	5.7	6.3	5.9	7.1	3.9	8.4	7.4	7.0	10.7	7.3	5.8	6.2	2.4	7.5	1.9	5.4	0.7	8.1	4.1	9.7	0.9
1.5	7.0	2.1	8.6	3.7	4.3	4.0	5.1	2.7	5.7	5.2	5.1	7.0	4.9	4.1	4.1	1.7	5.1	1.3	3.3	0.5	4.8	3.0	6.1	0.6
1	4.6	0.4	6.2	1.6	2.2	2.1	3.1	1.4	3.0	2.9	3.2	5.1	2.6	2.2	2.1	0.9	2.7	0.7	1.1	0.2	1.6	1.8	2.6	0.3
0.75	2.4	0.1	3.5	0.8	1.2	1.1	2.1	0.7	1.5	1.5	2.1	3.2	1.3	1.2	1.0	0.4	1.4	0.4	0.0	0.0	0.0	1.1	0.6	0.1
0.5	0.0	0.0	0.0	0.0	0.0	0.0	0.9	0.0	0.0	0.0	1.0	2.1	0.0	0.0	0.0	0.0	0.0	0.0	0.0	0.0	0.0	0.4	0.0	0.0

PSDs for the 106 µm aperture

Size (um)	150 um, 60 %										150 um, 50 %						150 um, 40 %				150 um, 30 %	
	35 t/h		30 t/h		25 t/h		19 t/h		13 t/h		25 t/h		19 t/h		13 t/h		19 t/h		13 t/h		19 t/h	
	U/S	O/S	U/S	O/S	U/S	O/S	U/S	O/S	U/S	O/S	U/S	O/S	U/S	O/S	U/S	O/S	U/S	O/S	U/S	O/S	U/S	O/S
8000	100.0	100.0	100.0	100.0	100.0	100.0	100.0	100.0	100.0	100.0	100.0	100.0	100.0	100.0	100.0	100.0	100.0	100.0	100.0	100.0	100.0	100.0
5600	100.0	100.0	100.0	100.0	100.0	100.0	100.0	100.0	100.0	100.0	100.0	100.0	100.0	100.0	100.0	100.0	100.0	100.0	100.0	100.0	100.0	100.0
4000	100.0	100.0	100.0	100.0	100.0	100.0	100.0	100.0	100.0	100.0	100.0	100.0	100.0	100.0	100.0	100.0	100.0	100.0	100.0	100.0	100.0	100.0
2800	100.0	100.0	100.0	100.0	100.0	100.0	100.0	100.0	100.0	100.0	100.0	100.0	100.0	100.0	100.0	100.0	100.0	100.0	100.0	100.0	100.0	100.0
2000	100.0	100.0	100.0	100.0	100.0	100.0	100.0	100.0	100.0	100.0	100.0	100.0	100.0	100.0	100.0	100.0	100.0	100.0	100.0	100.0	100.0	100.0
1400	100.0	100.0	100.0	100.0	100.0	100.0	100.0	100.0	100.0	100.0	100.0	100.0	100.0	100.0	100.0	100.0	100.0	100.0	100.0	100.0	100.0	100.0
1000	100.0	100.0	100.0	100.0	100.0	100.0	100.0	100.0	100.0	100.0	100.0	100.0	100.0	100.0	100.0	100.0	100.0	100.0	100.0	100.0	100.0	100.0
850	100.0	100.0	100.0	100.0	100.0	100.0	100.0	100.0	100.0	100.0	100.0	100.0	100.0	100.0	100.0	100.0	100.0	100.0	100.0	99.9	100.0	100.0
600	100.0	99.9	100.0	100.0	100.0	99.7	100.0	99.8	100.0	100.0	100.0	100.0	100.0	99.9	100.0	100.0	100.0	99.7	100.0	99.7	100.0	96.7
425	100.0	99.9	100.0	100.0	100.0	99.7	100.0	99.7	100.0	99.8	100.0	99.9	100.0	99.6	100.0	99.9	100.0	99.4	100.0	99.4	100.0	84.1
300	100.0	99.9	100.0	100.0	100.0	99.6	100.0	99.3	100.0	98.9	100.0	98.2	100.0	98.9	100.0	99.0	100.0	94.6	100.0	94.1	99.9	61.8
212	100.0	98.4	100.0	99.5	100.0	61.0	99.9	96.5	99.9	96.1	99.9	89.8	99.9	96.3	99.9	94.2	99.7	72.2	99.7	66.5	99.2	37.3
150	99.8	96.7	100.0	99.2	99.1	55.8	97.6	83.5	98.0	80.7	98.3	73.6	98.7	78.4	99.0	74.5	97.8	50.5	97.8	38.1	96.6	19.5
106	99.1	93.4	100.0	98.2	96.5	47.7	93.9	69.4	94.1	64.4	94.2	55.2	95.0	61.8	95.7	61.5	93.2	38.4	93.2	24.5	91.6	11.2
75	97.2	88.4	99.7	95.9	90.7	38.9	87.1	55.4	90.2	56.4	88.1	43.5	89.2	51.9	90.3	52.7	85.7	31.5	85.7	19.3	83.8	9.2
53	92.1	81.9	96.3	82.4	80.7	33.5	80.8	50.1	82.0	51.5	79.9	36.6	81.4	45.7	82.7	46.2	76.1	28.2	76.1	17.6	73.7	8.8
38	82.8	73.7	92.2	77.8	69.3	29.5	70.9	45.4	73.0	47.1	70.1	32.4	71.6	41.2	73.0	41.6	64.2	24.8	64.2	15.8	62.4	8.2
25	51.8	50.3	79.8	67.5	54.1	24.7	57.7	40.6	63.0	42.5	51.1	28.2	50.9	34.2	50.8	32.2	49.2	20.3	49.2	13.7	48.2	7.2
20	44.5	44.8	68.8	60.0	47.1	22.4	48.9	36.5	53.4	38.0	45.9	25.8	45.5	32.0	45.1	29.5	42.0	18.1	42.0	12.4	41.6	6.7
15	36.2	38.1	54.3	50.8	39.2	19.6	39.7	32.0	43.6	33.0	40.2	22.9	39.5	29.3	38.8	26.4	34.6	15.6	34.6	11.0	34.3	6.2
10	27.2	29.7	46.4	44.9	30.3	16.0	30.7	26.6	34.1	27.4	33.9	19.3	33.0	25.8	32.1	22.7	27.2	13.0	27.2	9.1	26.4	5.4
7	21.1	23.4	25.5	27.3	24.1	13.0	23.2	21.1	26.0	21.6	29.1	16.2	28.0	22.7	26.9	19.6	20.9	10.7	20.9	7.5	20.7	4.6
5	16.2	18.2	18.9	20.6	18.8	10.2	16.4	15.7	19.0	16.2	24.1	13.1	23.0	19.4	21.9	16.3	16.4	8.9	16.4	6.0	16.2	3.8
3	9.8	11.2	14.5	15.9	11.9	6.6	10.6	10.7	12.5	11.0	18.6	9.0	17.3	15.3	16.0	12.4	10.1	6.0	10.1	4.1	10.4	2.6
2	6.1	7.1	10.3	11.2	7.6	4.2	6.9	7.2	8.6	7.7	13.1	6.0	12.1	11.2	11.0	8.8	6.4	4.2	6.5	2.9	7.0	1.7
1.5	4.2	4.9	7.5	7.9	5.2	2.9	4.5	4.8	5.7	5.1	9.2	4.2	8.4	8.0	7.7	6.3	4.5	3.0	4.5	2.1	5.2	1.3
1	2.2	2.6	4.7	4.5	2.8	1.6	2.4	2.6	3.1	2.8	5.7	2.4	5.2	5.0	4.7	3.9	2.4	1.7	2.4	1.3	3.2	0.7
0.75	1.1	1.4	2.8	2.2	1.5	0.8	0.9	1.0	1.1	1.0	2.6	1.3	2.4	2.4	2.2	1.9	1.3	0.9	1.3	0.9	2.2	0.4
0.5	0.0	0.0	1.0	0.0	0.0	0.0	0.0	0.0	0.0	0.0	0.0	0.0	0.0	0.0	0.0	0.0	0.0	0.0	0.0	0.0	1.0	0.1

Actual Partition Curves

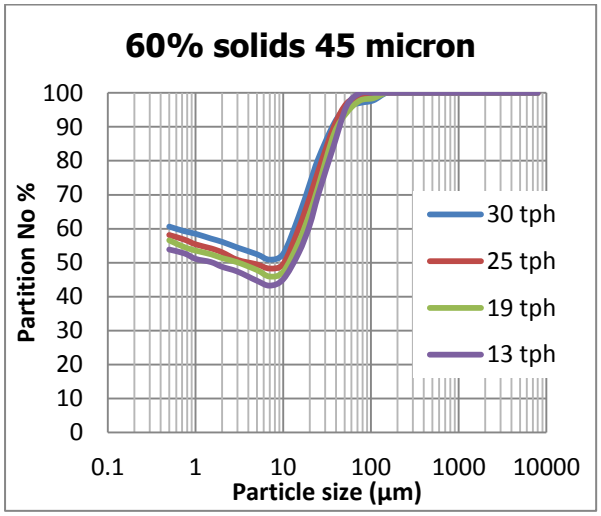

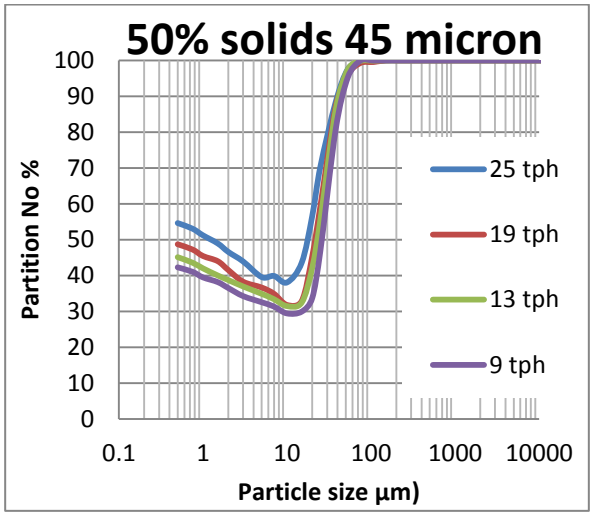

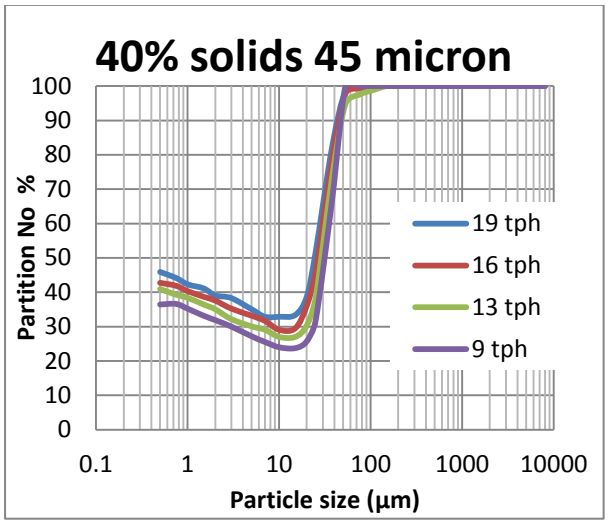

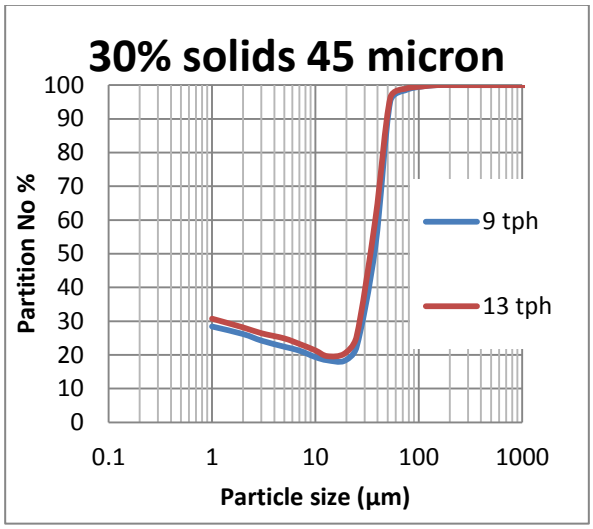

A 3: Partition curves obtained at 45 µm aperture

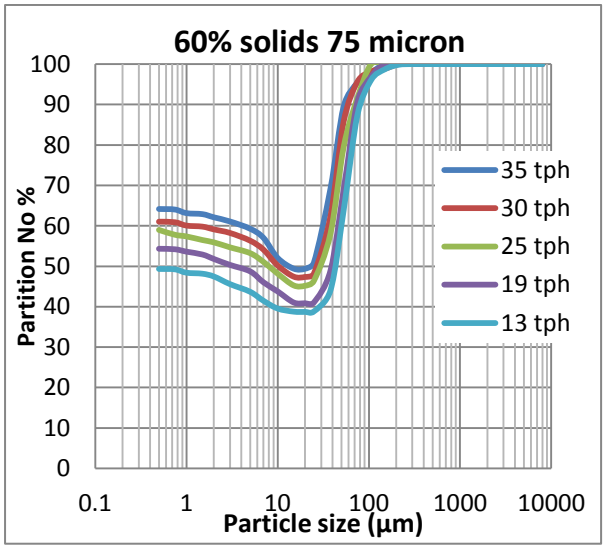

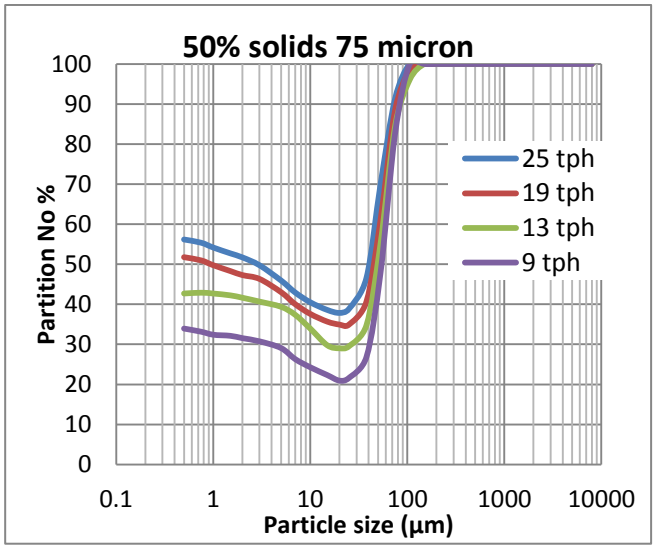

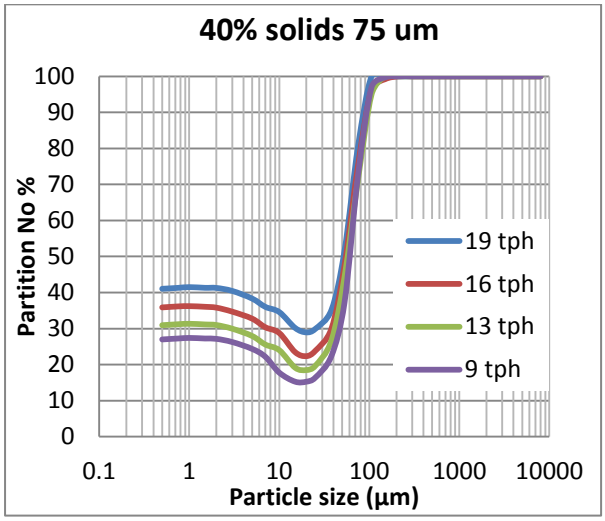

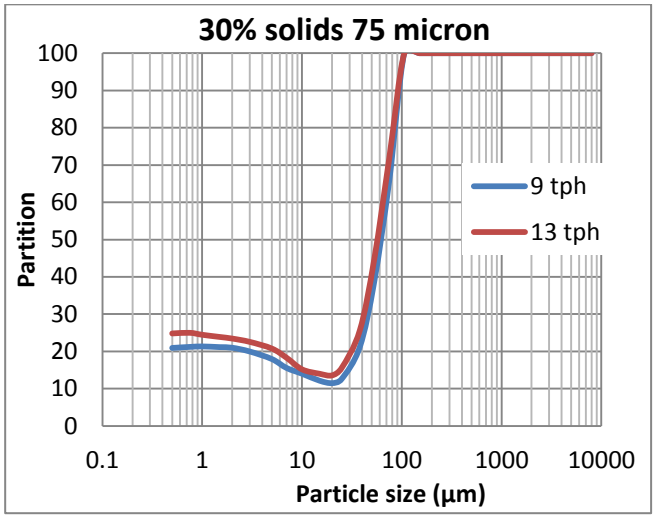

A 4: Partition curves obtained at 75 µm aperture

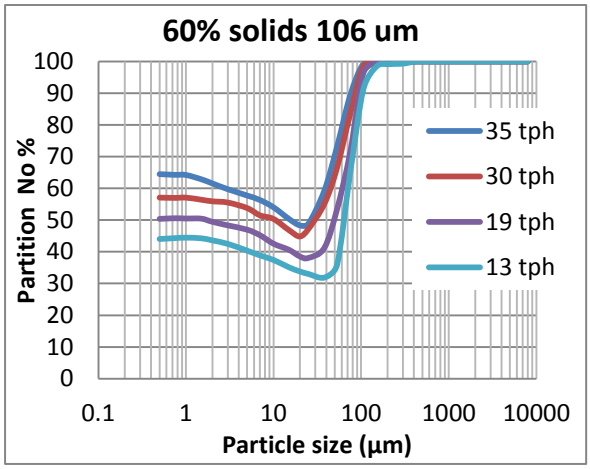

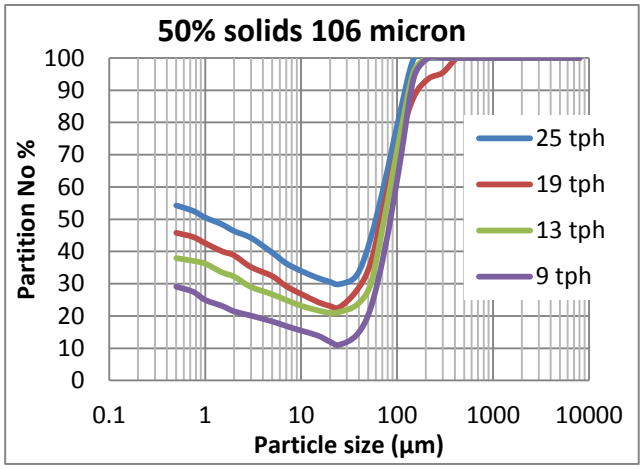

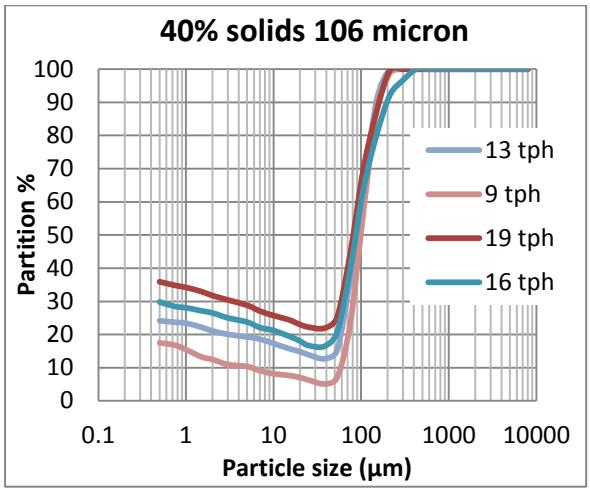

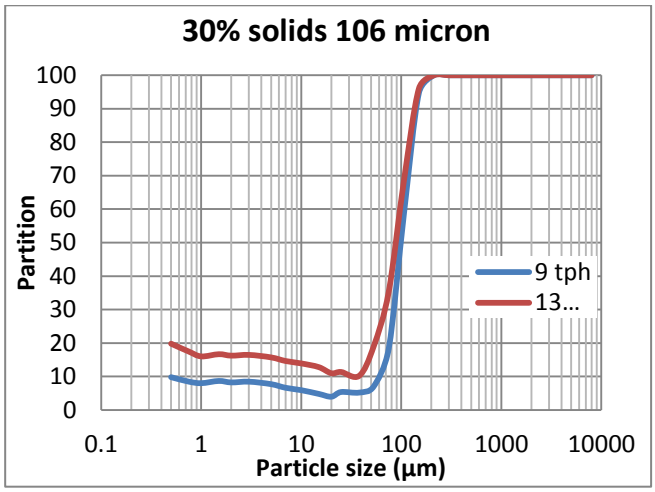

A 5 : Partition curves obtained at 106 µm aperture

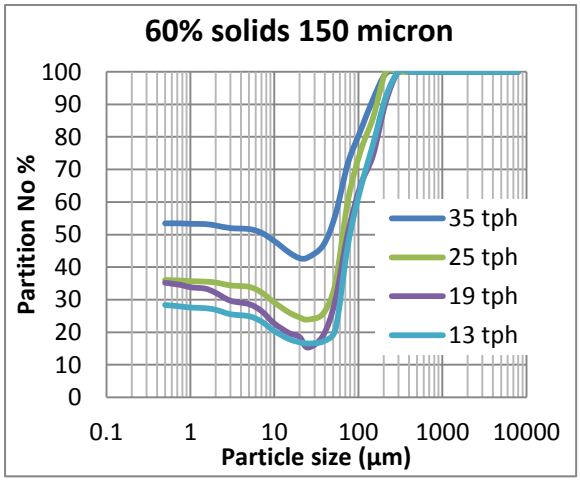

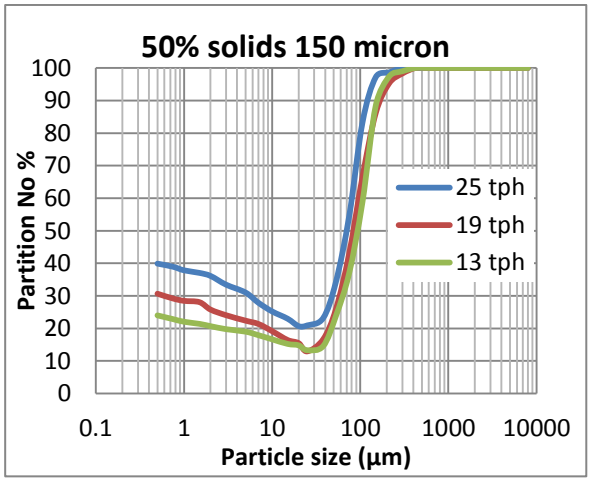

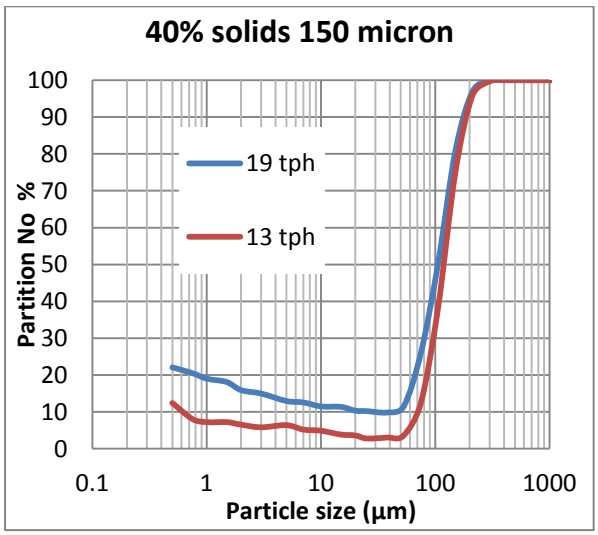

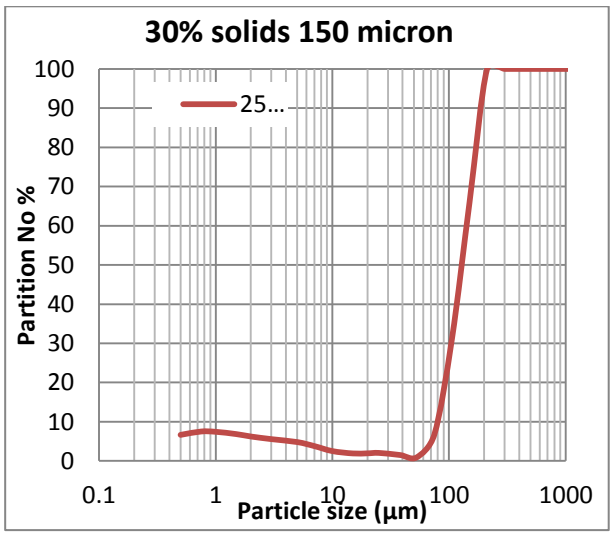

A 6: Partition curves obtained at 106 µm aperture

Calculation of the oversize efficiencies using the modified model

A 7: A comparison of the actual and modified model efficiencies using EXCEL SOLVER – 45 µm aperture

x_a (µm)	45																															
A_o (m^2)	0.43																															
A_o/x_a^2	2.12E+08																															
f_o (%)	**28.00**																															
f_U (%)	**60.00**																															
fs (%)	**60**								**50**								**40**								**30**							
µ (kg/m.s)	0.0066								0.0042								0.0028								0.0014							
ρ_p (kg/m^3)	1743.95								1551.57								1397.42								1271.12							
$\mu/(\rho_s g^{1/2} xa^{3/2})$	0.0002								0.0001								0.0001								0.0001							
N	0.04			0.03			0.03			0.03			0.06			0.05			0.04			0.04			0.07			0.06			0.05	
σ	1.11			1.29			1.43			1.53			0.85			0.97			1.13			1.25			0.76			0.87			0.94	
$\mu x_a/m_f$	8.E-08			6.E-08			4.E-08			4.E-08			8.E-08			5.E-08			4.E-08			3.E-08			5.E-08			4.E-08			3.E-08	
$m_u/(\rho_p g^{0.5} xa^{2.5})$	3.E+07			4.E+07			6.E+07			7.E+07			2.E+07			3.E+07			5.E+07			6.E+07			3.E+07			4.E+07			4.E+07	
m_u (TPH)	7.8			11.4			15.0			18.0			5.4			7.8			11.4			15.0			5.4			7.8			9.6	
m_f (TPH)	**13**			**19**			**25**			**30**			**9**			**13**			**19**			**25**			**9**			**13**			**16**	
Size (µm)	Actual	Model	SSE	Actual	Model	SSE	Actual	Model	SSE	Actual	Model	SSE	Actual	Model	SSE	Actual	Model	SSE	Actual	Model	SSE	Actual	Model	SSE	Actual	Model	SSE	Actual	Model	SSE	Actual	Model	SSE
8000	1.00	1.00	0.00	1.00	1.00	0.00	1.00	1.00	0.00	1.000	1.00	0.00	1.00	1.00	0.00	1.00	1.00	0.00	1.00	1.00	0.00	1.00	1.00	0.00	1.00	1.00	0.00	1.00	1.00	0.00	1.00	1.00	0.00
5600	1.00	1.00	0.00	1.00	1.00	0.00	1.00	1.00	0.00	1.000	1.00	0.00	1.00	1.00	0.00	1.00	1.00	0.00	1.00	1.00	0.00	1.00	1.00	0.00	1.00	1.00	0.00	1.00	1.00	0.00	1.00	1.00	0.00
4000	1.00	1.00	0.00	1.00	1.00	0.00	1.00	1.00	0.00	1.000	1.00	0.00	1.00	1.00	0.00	1.00	1.00	0.00	1.00	1.00	0.00	1.00	1.00	0.00	1.00	1.00	0.00	1.00	1.00	0.00	1.00	1.00	0.00
2800	1.00	1.00	0.00	1.00	1.00	0.00	1.00	1.00	0.00	1.000	1.00	0.00	1.00	1.00	0.00	1.00	1.00	0.00	1.00	1.00	0.00	1.00	1.00	0.00	1.00	1.00	0.00	1.00	1.00	0.00	1.00	1.00	0.00
2000	1.00	1.00	0.00	1.00	1.00	0.00	1.00	1.00	0.00	1.000	1.00	0.00	1.00	1.00	0.00	1.00	1.00	0.00	1.00	1.00	0.00	1.00	1.00	0.00	1.00	1.00	0.00	1.00	1.00	0.00	1.00	1.00	0.00
1400	1.00	1.00	0.00	1.00	1.00	0.00	1.00	1.00	0.00	1.000	1.00	0.00	1.00	1.00	0.00	1.00	1.00	0.00	1.00	1.00	0.00	1.00	1.00	0.00	1.00	1.00	0.00	1.00	1.00	0.00	1.00	1.00	0.00
1000	1.00	1.00	0.00	1.00	1.00	0.00	1.00	1.00	0.00	1.000	1.00	0.00	1.00	1.00	0.00	1.00	1.00	0.00	1.00	1.00	0.00	1.00	1.00	0.00	1.00	1.00	0.00	1.00	1.00	0.00	1.00	1.00	0.00
850	1.00	1.00	0.00	1.00	1.00	0.00	1.00	1.00	0.00	1.000	1.00	0.00	1.00	1.00	0.00	1.00	1.00	0.00	1.00	1.00	0.00	1.00	1.00	0.00	1.00	1.00	0.00	1.00	1.00	0.00	1.00	1.00	0.00
600	1.00	1.00	0.00	1.00	1.00	0.00	1.00	1.00	0.00	1.000	1.00	0.00	1.00	1.00	0.00	1.00	1.00	0.00	1.00	1.00	0.00	1.00	1.00	0.00	1.00	1.00	0.00	1.00	1.00	0.00	1.00	1.00	0.00
425	1.00	1.00	0.00	1.00	1.00	0.00	1.00	1.00	0.00	1.000	1.00	0.00	1.00	1.00	0.00	1.00	1.00	0.00	1.00	1.00	0.00	1.00	1.00	0.00	1.00	1.00	0.00	1.00	1.00	0.00	1.00	1.00	0.00
300	1.00	1.00	0.00	1.00	1.00	0.00	1.00	1.00	0.00	1.000	1.00	0.00	1.00	1.00	0.00	1.00	1.00	0.00	1.00	1.00	0.00	1.00	1.00	0.00	1.00	1.00	0.00	1.00	1.00	0.00	1.00	1.00	0.00
212	1.00	1.00	0.00	1.00	1.00	0.00	1.00	1.00	0.00	1.000	1.00	0.00	1.00	1.00	0.00	1.00	1.00	0.00	1.00	1.00	0.00	1.00	1.00	0.00	1.00	1.00	0.00	1.00	1.00	0.00	1.00	1.00	0.00
150	1.00	1.00	0.00	1.00	1.00	0.00	1.00	1.00	0.00	1.000	1.00	0.00	1.00	1.00	0.00	1.00	1.00	0.00	1.00	1.00	0.00	1.00	1.00	0.00	1.00	1.00	0.00	1.00	1.00	0.00	1.00	1.00	0.00
106	1.00	1.00	0.00	0.98	1.00	0.00	0.99	1.00	0.00	0.978	1.00	0.00	1.00	1.00	0.00	1.00	1.00	0.00	1.00	1.00	0.00	1.00	1.00	0.00	1.00	1.00	0.00	0.99	1.00	0.00	1.00	1.00	0.00
75	1.00	1.00	0.00	0.98	1.00	0.00	0.99	1.00	0.00	0.970	1.00	0.00	1.00	1.00	0.00	1.00	1.00	0.00	0.99	1.00	0.00	1.00	1.00	0.00	1.00	1.00	0.00	0.98	1.00	0.00	0.99	1.00	0.00
53	0.96	1.00	0.00	0.94	1.00	0.00	0.97	1.00	0.00	0.958	1.00	0.00	0.95	1.00	0.00	0.98	1.00	0.00	0.96	1.00	0.00	0.98	1.00	0.00	1.00	1.00	0.00	0.95	1.00	0.00	0.98	1.00	0.00
38	0.85	0.87	0.00	0.88	0.92	0.00	0.90	0.94	0.00	0.910	0.96	0.00	0.81	0.71	0.01	0.86	0.80	0.00	0.87	0.87	0.00	0.88	0.91	0.00	0.67	0.62	0.00	0.74	0.72	0.00	0.79	0.77	0.00
25	0.70	0.63	0.00	0.72	0.72	0.00	0.77	0.77	0.00	0.805	0.80	0.00	0.47	0.44	0.00	0.56	0.54	0.00	0.59	0.63	0.00	0.70	0.69	0.00	0.32	0.35	0.00	0.38	0.45	0.00	0.46	0.50	0.00
20	0.61	0.56	0.00	0.65	0.64	0.00	0.69	0.70	0.00	0.732	0.74	0.00	0.34	0.37	0.00	0.42	0.46	0.00	0.45	0.55	0.01	0.57	0.62	0.00	0.26	0.29	0.00	0.30	0.38	0.01	0.36	0.43	0.00
15	0.53	0.49	0.00	0.56	0.57	0.00	0.60	0.63	0.00	0.637	0.67	0.00	0.30	0.31	0.00	0.33	0.40	0.00	0.33	0.48	0.02	0.44	0.54	0.01	0.24	0.24	0.00	0.27	0.32	0.00	0.30	0.36	0.00
10	0.45	0.43	0.00	0.47	0.51	0.00	0.50	0.57	0.00	0.527	0.60	0.01	0.29	0.27	0.00	0.31	0.34	0.00	0.32	0.42	0.01	0.38	0.48	0.01	0.24	0.20	0.00	0.27	0.27	0.00	0.29	0.31	0.00
7	0.43	0.41	0.00	0.46	0.49	0.00	0.48	0.54	0.00	0.509	0.58	0.00	0.31	0.26	0.00	0.33	0.33	0.00	0.35	0.40	0.00	0.40	0.46	0.00	0.26	0.19	0.00	0.29	0.26	0.00	0.32	0.30	0.00
5	0.45	0.41	0.00	0.48	0.49	0.00	0.50	0.54	0.00	0.525	0.58	0.00	0.33	0.26	0.00	0.35	0.33	0.00	0.37	0.40	0.00	0.40	0.46	0.00	0.27	0.20	0.01	0.30	0.26	0.00	0.33	0.30	0.00
3	0.47	0.43	0.00	0.50	0.51	0.00	0.51	0.57	0.00	0.545	0.61	0.00	0.34	0.28	0.00	0.37	0.35	0.00	0.38	0.43	0.00	0.44	0.50	0.00	0.30	0.22	0.01	0.32	0.29	0.00	0.35	0.33	0.00
2	0.49	0.45	0.00	0.51	0.54	0.00	0.53	0.60	0.01	0.562	0.65	0.01	0.37	0.29	0.01	0.39	0.37	0.00	0.42	0.46	0.00	0.47	0.53	0.00	0.32	0.24	0.01	0.35	0.31	0.00	0.38	0.36	0.00
1.5	0.50	0.45	0.00	0.52	0.55	0.00	0.54	0.62	0.01	0.571	0.67	0.01	0.38	0.30	0.01	0.40	0.38	0.00	0.44	0.48	0.00	0.49	0.55	0.00	0.33	0.25	0.01	0.36	0.33	0.00	0.39	0.38	0.00
1	0.51	0.46	0.00	0.54	0.56	0.00	0.55	0.63	0.01	0.585	0.68	0.01	0.40	0.31	0.01	0.42	0.40	0.00	0.45	0.49	0.00	0.51	0.57	0.00	0.35	0.26	0.01	0.38	0.34	0.00	0.40	0.39	0.00
0.75	0.53	0.47	0.00	0.55	0.57	0.00	0.57	0.64	0.01	0.593	0.69	0.01	0.41	0.32	0.01	0.44	0.40	0.00	0.47	0.50	0.00	0.53	0.58	0.00	0.37	0.27	0.01	0.39	0.35	0.00	0.42	0.40	0.00
0.5	0.54	0.47	0.00	0.57	0.57	0.00	0.58	0.65	0.00	0.606	0.70	0.01	0.42	0.32	0.01	0.45	0.41	0.00	0.49	0.51	0.00	0.55	0.59	0.00	0.36	0.27	0.01	0.41	0.36	0.00	0.43	0.41	0.00
Sum			**0.03**			**0.01**			**0.05**			**0.07**			**0.06**			**0.02**			**0.06**			**0.05**			**0.06**			**0.03**			**0.02**

x_a (µm)	45																															
A_o (m^2)	0.43																															
A_o/x_a^2	2.12E+08																															
f_o (%)	**28.00**																															
f_U (%)	**60.00**																															
fs (%)	**60**								**50**								**40**								**30**							
µ (kg/m.s)	0.0066								0.0042								0.0028								0.0014							
ρ_p (kg/m^3)	1743.95								1551.57								1397.42								1271.12							
$\mu/(\rho_s g^{1/2} xa^{3/2})$	0.0002								0.0001								0.0001								0.0001							
N	0.04			0.03			0.03			0.03			0.06			0.05			0.04			0.04			0.07			0.06			0.05	
σ	1.11			1.29			1.43			1.53			0.85			0.97			1.13			1.25			0.76			0.87			0.94	
$\mu x_a/m_f$	8.E-08			6.E-08			4.E-08			4.E-08			8.E-08			5.E-08			4.E-08			3.E-08			5.E-08			4.E-08			3.E-08	
$m_u/(\rho_p g^{0.5} xa^{2.5})$	3.E+07			4.E+07			6.E+07			7.E+07			2.E+07			3.E+07			5.E+07			6.E+07			3.E+07			4.E+07			4.E+07	
m_u (TPH)	7.8			11.4			15.0			18.0			5.4			7.8			11.4			15.0			5.4			7.8			9.6	
m_f (TPH)	**13**			**19**			**25**			**30**			**9**			**13**			**19**			**25**			**9**			**13**			**16**	
Size (µm)	Actual	Model	SSE	Actual	Model	SSE	Actual	Model	SSE	Actual	Model	SSE	Actual	Model	SSE	Actual	Model	SSE	Actual	Model	SSE	Actual	Model	SSE	Actual	Model	SSE	Actual	Model	SSE	Actual	Model	SSE
8000	1.00	1.00	0.00	1.00	1.00	0.00	1.00	1.00	0.00	1.000	1.00	0.00	1.00	1.00	0.00	1.00	1.00	0.00	1.00	1.00	0.00	1.00	1.00	0.00	1.00	1.00	0.00	1.00	1.00	0.00	1.00	1.00	0.00
5600	1.00	1.00	0.00	1.00	1.00	0.00	1.00	1.00	0.00	1.000	1.00	0.00	1.00	1.00	0.00	1.00	1.00	0.00	1.00	1.00	0.00	1.00	1.00	0.00	1.00	1.00	0.00	1.00	1.00	0.00	1.00	1.00	0.00
4000	1.00	1.00	0.00	1.00	1.00	0.00	1.00	1.00	0.00	1.000	1.00	0.00	1.00	1.00	0.00	1.00	1.00	0.00	1.00	1.00	0.00	1.00	1.00	0.00	1.00	1.00	0.00	1.00	1.00	0.00	1.00	1.00	0.00
2800	1.00	1.00	0.00	1.00	1.00	0.00	1.00	1.00	0.00	1.000	1.00	0.00	1.00	1.00	0.00	1.00	1.00	0.00	1.00	1.00	0.00	1.00	1.00	0.00	1.00	1.00	0.00	1.00	1.00	0.00	1.00	1.00	0.00
2000	1.00	1.00	0.00	1.00	1.00	0.00	1.00	1.00	0.00	1.000	1.00	0.00	1.00	1.00	0.00	1.00	1.00	0.00	1.00	1.00	0.00	1.00	1.00	0.00	1.00	1.00	0.00	1.00	1.00	0.00	1.00	1.00	0.00
1400	1.00	1.00	0.00	1.00	1.00	0.00	1.00	1.00	0.00	1.000	1.00	0.00	1.00	1.00	0.00	1.00	1.00	0.00	1.00	1.00	0.00	1.00	1.00	0.00	1.00	1.00	0.00	1.00	1.00	0.00	1.00	1.00	0.00
1000	1.00	1.00	0.00	1.00	1.00	0.00	1.00	1.00	0.00	1.000	1.00	0.00	1.00	1.00	0.00	1.00	1.00	0.00	1.00	1.00	0.00	1.00	1.00	0.00	1.00	1.00	0.00	1.00	1.00	0.00	1.00	1.00	0.00
850	1.00	1.00	0.00	1.00	1.00	0.00	1.00	1.00	0.00	1.000	1.00	0.00	1.00	1.00	0.00	1.00	1.00	0.00	1.00	1.00	0.00	1.00	1.00	0.00	1.00	1.00	0.00	1.00	1.00	0.00	1.00	1.00	0.00
600	1.00	1.00	0.00	1.00	1.00	0.00	1.00	1.00	0.00	1.000	1.00	0.00	1.00	1.00	0.00	1.00	1.00	0.00	1.00	1.00	0.00	1.00	1.00	0.00	1.00	1.00	0.00	1.00	1.00	0.00	1.00	1.00	0.00
425	1.00	1.00	0.00	1.00	1.00	0.00	1.00	1.00	0.00	1.000	1.00	0.00	1.00	1.00	0.00	1.00	1.00	0.00	1.00	1.00	0.00	1.00	1.00	0.00	1.00	1.00	0.00	1.00	1.00	0.00	1.00	1.00	0.00
300	1.00	1.00	0.00	1.00	1.00	0.00	1.00	1.00	0.00	1.000	1.00	0.00	1.00	1.00	0.00	1.00	1.00	0.00	1.00	1.00	0.00	1.00	1.00	0.00	1.00	1.00	0.00	1.00	1.00	0.00	1.00	1.00	0.00
212	1.00	1.00	0.00	1.00	1.00	0.00	1.00	1.00	0.00	1.000	1.00	0.00	1.00	1.00	0.00	1.00	1.00	0.00	1.00	1.00	0.00	1.00	1.00	0.00	1.00	1.00	0.00	1.00	1.00	0.00	1.00	1.00	0.00
150	1.00	1.00	0.00	1.00	1.00	0.00	1.00	1.00	0.00	1.000	1.00	0.00	1.00	1.00	0.00	1.00	1.00	0.00	1.00	1.00	0.00	1.00	1.00	0.00	1.00	1.00	0.00	1.00	1.00	0.00	1.00	1.00	0.00
106	1.00	1.00	0.00	0.98	1.00	0.00	0.99	1.00	0.00	0.978	1.00	0.00	1.00	1.00	0.00	1.00	1.00	0.00	1.00	1.00	0.00	1.00	1.00	0.00	1.00	1.00	0.00	1.00	1.00	0.00	1.00	1.00	0.00
75	1.00	1.00	0.00	0.98	1.00	0.00	0.99	1.00	0.00	0.970	1.00	0.00	1.00	1.00	0.00	1.00	1.00	0.00	0.99	1.00	0.00	1.00	1.00	0.00	1.00	1.00	0.00	0.98	1.00	0.00	0.99	1.00	0.00
53	0.96	1.00	0.00	0.94	1.00	0.00	0.97	1.00	0.00	0.958	1.00	0.00	0.95	1.00	0.00	0.98	1.00	0.00	0.96	1.00	0.00	0.98	1.00	0.00	1.00	1.00	0.00	0.95	1.00	0.00	0.98	1.00	0.00
38	0.85	0.87	0.00	0.88	0.92	0.00	0.90	0.94	0.00	0.910	0.96	0.00	0.81	0.71	0.01	0.86	0.80	0.00	0.87	0.87	0.00	0.88	0.91	0.00	0.67	0.62	0.00	0.74	0.72	0.00	0.79	0.77	0.00
25	0.70	0.63	0.00	0.72	0.72	0.00	0.77	0.77	0.00	0.805	0.80	0.00	0.47	0.44	0.00	0.56	0.54	0.00	0.59	0.63	0.00	0.70	0.69	0.00	0.32	0.35	0.00	0.38	0.45	0.00	0.46	0.50	0.00
20	0.61	0.56	0.00	0.65	0.64	0.00	0.69	0.70	0.00	0.732	0.74	0.00	0.34	0.37	0.00	0.42	0.46	0.00	0.45	0.55	0.01	0.57	0.62	0.00	0.26	0.29	0.00	0.30	0.38	0.01	0.36	0.43	0.00
15	0.53	0.49	0.00	0.56	0.57	0.00	0.60	0.63	0.00	0.637	0.67	0.00	0.30	0.31	0.00	0.33	0.40	0.00	0.33	0.48	0.02	0.44	0.54	0.01	0.24	0.24	0.00	0.27	0.32	0.00	0.30	0.36	0.00
10	0.45	0.43	0.00	0.47	0.51	0.00	0.50	0.57	0.00	0.527	0.60	0.01	0.29	0.27	0.00	0.31	0.34	0.00	0.32	0.42	0.01	0.38	0.48	0.01	0.24	0.20	0.00	0.27	0.27	0.00	0.29	0.31	0.00
7	0.43	0.41	0.00	0.46	0.49	0.00	0.48	0.54	0.00	0.509	0.58	0.00	0.31	0.26	0.00	0.33	0.33	0.00	0.35	0.40	0.00	0.40	0.46	0.00	0.26	0.19	0.00	0.29	0.26	0.00	0.32	0.30	0.00
5	0.45	0.41	0.00	0.48	0.49	0.00	0.50	0.54	0.00	0.525	0.58	0.00	0.33	0.26	0.00	0.35	0.33	0.00	0.37	0.40	0.00	0.40	0.46	0.00	0.27	0.20	0.01	0.30	0.26	0.00	0.33	0.30	0.00
3	0.47	0.43	0.00	0.50	0.51	0.00	0.51	0.57	0.00	0.545	0.61	0.00	0.34	0.28	0.00	0.37	0.35	0.00	0.38	0.43	0.00	0.44	0.50	0.00	0.30	0.22	0.01	0.32	0.29	0.00	0.35	0.33	0.00
2	0.49	0.45	0.00	0.51	0.54	0.00	0.53	0.60	0.01	0.562	0.65	0.01	0.37	0.29	0.01	0.39	0.37	0.00	0.42	0.46	0.00	0.47	0.53	0.00	0.32	0.24	0.01	0.35	0.31	0.00	0.38	0.36	0.00
1.5	0.50	0.45	0.00	0.52	0.55	0.00	0.54	0.62	0.01	0.571	0.67	0.01	0.38	0.30	0.01	0.40	0.38	0.00	0.44	0.48	0.00	0.49	0.55	0.00	0.33	0.25	0.01	0.36	0.33	0.00	0.39	0.38	0.00
1	0.51	0.46	0.00	0.54	0.56	0.00	0.55	0.63	0.01	0.585	0.68	0.01	0.40	0.31	0.01	0.42	0.40	0.00	0.45	0.49	0.00	0.51	0.57	0.00	0.35	0.26	0.01	0.38	0.34	0.00	0.40	0.39	0.00
0.75	0.53	0.47	0.00	0.55	0.57	0.00	0.57	0.64	0.01	0.593	0.69	0.01	0.41	0.32	0.01	0.44	0.40	0.00	0.47	0.50	0.00	0.53	0.58	0.00	0.37	0.27	0.01	0.39	0.35	0.00	0.42	0.40	0.00
0.5	0.54	0.47	0.00	0.57	0.57	0.00	0.58	0.65	0.00	0.606	0.70	0.01	0.42	0.32	0.01	0.45	0.41	0.00	0.49	0.51	0.00	0.55	0.59	0.00	0.36	0.27	0.01	0.41	0.36	0.00	0.43	0.41	0.00
Sum			**0.03**			**0.01**			**0.05**			**0.07**			**0.06**			**0.02**			**0.06**			**0.05**			**0.06**			**0.03**			**0.02**

A 8: A comparison of the actual and modified model efficiencies using EXCEL SOLVER – 75 µm aperture

x_a (µm)	75
A_o (m^2)	0.47
A_o/x_a^2	8.41E+07
f_o (%)	30.80
f_U (%)	70.00

fs (%)	60														
µ (kg/m.s)	0.006592														
ρ_p (kg/m^3)	1743.951613														
N	3.9E-02			3.2E-02			2.8E-02			2.6E-02			2.4E-02		
σ	6.9E-01			8.0E-01			8.9E-01			9.5E-01			1.0E+00		
$\mu x_a/m_f$	1.37E-07			9.37E-08			7.12E-08			5.93E-08			5.09E-08		
$m_u/(\rho_p g^{0.5} x_a^{2.5})$	9499851			13884398			18268944			21922733			25576522		
m_u (TPH)	9.1			13.3			17.5			21			24.5		
m_f (TPH)	13			19			25			30			35		
Size (µm)	Actual	Model	SSE	Actual	Model	SSE	Actual	Model	SSE	Actual	Model	SSE	Actual	Model	SSE
8000	1.00	1.00	0.00	1.00	1.00	0.00	1.00	1.00	0.00	1.000	1.00	0.00	1.00	1.00	0.00
5600	1.00	1.00	0.00	1.00	1.00	0.00	1.00	1.00	0.00	1.000	1.00	0.00	1.00	1.00	0.00
4000	1.00	1.00	0.00	1.00	1.00	0.00	1.00	1.00	0.00	1.000	1.00	0.00	1.00	1.00	0.00
2800	1.00	1.00	0.00	1.00	1.00	0.00	1.00	1.00	0.00	1.000	1.00	0.00	1.00	1.00	0.00
2000	1.00	1.00	0.00	1.00	1.00	0.00	1.00	1.00	0.00	1.000	1.00	0.00	1.00	1.00	0.00
1400	1.00	1.00	0.00	1.00	1.00	0.00	1.00	1.00	0.00	1.000	1.00	0.00	1.00	1.00	0.00
1000	1.00	1.00	0.00	1.00	1.00	0.00	1.00	1.00	0.00	1.000	1.00	0.00	1.00	1.00	0.00
850	1.00	1.00	0.00	1.00	1.00	0.00	1.00	1.00	0.00	1.000	1.00	0.00	1.00	1.00	0.00
600	1.00	1.00	0.00	1.00	1.00	0.00	1.00	1.00	0.00	1.000	1.00	0.00	1.00	1.00	0.00
425	1.00	1.00	0.00	1.00	1.00	0.00	1.00	1.00	0.00	1.000	1.00	0.00	1.00	1.00	0.00
300	1.00	1.00	0.00	1.00	1.00	0.00	1.00	1.00	0.00	1.000	1.00	0.00	1.00	1.00	0.00
212	1.00	1.00	0.00	1.00	1.00	0.00	1.00	1.00	0.00	1.000	1.00	0.00	1.00	1.00	0.00
150	0.99	1.00	0.00	1.00	1.00	0.00	1.00	1.00	0.00	0.989	1.00	0.00	1.00	1.00	0.00
106	0.96	1.00	0.00	0.97	1.00	0.00	1.00	1.00	0.00	0.982	1.00	0.00	0.98	1.00	0.00
75	0.87	1.00	0.02	0.91	1.00	0.01	0.92	1.00	0.01	0.956	1.00	0.00	0.95	1.00	0.00
53	0.64	0.60	0.00	0.69	0.69	0.00	0.80	0.75	0.00	0.858	0.78	0.01	0.90	0.81	0.01
38	0.44	0.48	0.00	0.49	0.57	0.01	0.58	0.63	0.00	0.624	0.67	0.00	0.69	0.70	0.00
25	0.39	0.41	0.00	0.41	0.49	0.01	0.46	0.55	0.01	0.482	0.58	0.01	0.51	0.61	0.01
20	0.39	0.39	0.00	0.41	0.46	0.00	0.45	0.52	0.00	0.474	0.55	0.01	0.49	0.58	0.01
15	0.39	0.37	0.00	0.41	0.44	0.00	0.45	0.50	0.00	0.474	0.53	0.00	0.49	0.56	0.00
10	0.40	0.37	0.00	0.44	0.44	0.00	0.48	0.50	0.00	0.502	0.53	0.00	0.52	0.56	0.00
7	0.41	0.38	0.00	0.46	0.46	0.00	0.51	0.52	0.00	0.541	0.55	0.00	0.57	0.59	0.00
5	0.44	0.40	0.00	0.49	0.48	0.00	0.53	0.54	0.00	0.563	0.58	0.00	0.59	0.62	0.00
3	0.46	0.42	0.00	0.50	0.51	0.00	0.55	0.58	0.00	0.582	0.62	0.00	0.61	0.66	0.00
2	0.47	0.43	0.00	0.52	0.52	0.00	0.56	0.59	0.00	0.591	0.64	0.00	0.62	0.69	0.00
1.5	0.48	0.44	0.00	0.53	0.53	0.00	0.56	0.60	0.00	0.598	0.65	0.00	0.63	0.70	0.00
1	0.48	0.44	0.00	0.54	0.54	0.00	0.57	0.61	0.00	0.601	0.66	0.00	0.63	0.71	0.01
0.75	0.49	0.44	0.00	0.54	0.54	0.00	0.58	0.62	0.00	0.609	0.67	0.00	0.64	0.71	0.01
0.5	0.49	0.44	0.00	0.54	0.54	0.00	0.59	0.62	0.00	0.610	0.67	0.00	0.64	0.72	0.01
Sum			0.04			0.03			0.03			0.05			0.06

fs (%)	50											
µ (kg/m.s)	0.004196											
ρ_p (kg/m^3)	1551.569507											
N	5.6E-02			4.7E-02			3.9E-02			3.5E-02		
σ	5.3E-01			6.0E-01			7.0E-01			7.8E-01		
$\mu x_a/m_f$	1.26E-07			8.71E-08			5.96E-08			4.53E-08		
$m_u/(\rho_p g^{0.5} x_a^{2.5})$	7392293			10677756			15605951			20534146		
m_u (TPH)	6.3			9.1			13.3			17.5		
m_f (TPH)	9			13			19			25		
Size (µm)	Actual	Model	SSE	Actual	Model	SSE	Actual	Model	SSE	Actual	Model	SSE
8000	1.00	1.00	0.00	1.00	1.00	0.00	1.00	1.00	0.00	1.00	1.00	0.00
5600	1.00	1.00	0.00	1.00	1.00	0.00	1.00	1.00	0.00	1.00	1.00	0.00
4000	1.00	1.00	0.00	1.00	1.00	0.00	1.00	1.00	0.00	1.00	1.00	0.00
2800	1.00	1.00	0.00	1.00	1.00	0.00	1.00	1.00	0.00	1.00	1.00	0.00
2000	1.00	1.00	0.00	1.00	1.00	0.00	1.00	1.00	0.00	1.00	1.00	0.00
1400	1.00	1.00	0.00	1.00	1.00	0.00	1.00	1.00	0.00	1.00	1.00	0.00
1000	1.00	1.00	0.00	1.00	1.00	0.00	1.00	1.00	0.00	1.00	1.00	0.00
850	1.00	1.00	0.00	1.00	1.00	0.00	1.00	1.00	0.00	1.00	1.00	0.00
600	1.00	1.00	0.00	1.00	1.00	0.00	1.00	1.00	0.00	1.00	1.00	0.00
425	1.00	1.00	0.00	1.00	1.00	0.00	1.00	1.00	0.00	1.00	1.00	0.00
300	1.00	1.00	0.00	1.00	1.00	0.00	1.00	1.00	0.00	1.00	1.00	0.00
212	1.00	1.00	0.00	1.00	1.00	0.00	1.00	1.00	0.00	1.00	1.00	0.00
150	1.00	1.00	0.00	1.00	1.00	0.00	1.00	1.00	0.00	1.00	1.00	0.00
106	1.00	1.00	0.00	0.96	1.00	0.00	0.99	1.00	0.00	1.00	1.00	0.00
75	0.83	1.00	0.03	0.85	1.00	0.02	0.88	1.00	0.01	0.91	1.00	0.01
53	0.48	0.40	0.01	0.55	0.50	0.00	0.61	0.60	0.00	0.70	0.66	0.00
38	0.27	0.30	0.00	0.35	0.39	0.00	0.41	0.48	0.00	0.47	0.54	0.01
25	0.22	0.25	0.00	0.29	0.32	0.00	0.35	0.40	0.00	0.39	0.46	0.01
20	0.21	0.23	0.00	0.29	0.30	0.00	0.35	0.38	0.00	0.38	0.43	0.00
15	0.22	0.22	0.00	0.30	0.29	0.00	0.36	0.36	0.00	0.39	0.41	0.00
10	0.24	0.22	0.00	0.34	0.29	0.00	0.38	0.36	0.00	0.41	0.41	0.00
7	0.26	0.24	0.00	0.37	0.30	0.00	0.40	0.38	0.00	0.43	0.44	0.00
5	0.29	0.25	0.00	0.39	0.32	0.00	0.43	0.40	0.00	0.46	0.46	0.00
3	0.31	0.27	0.00	0.41	0.35	0.00	0.46	0.44	0.00	0.50	0.50	0.00
2	0.32	0.28	0.00	0.42	0.36	0.00	0.47	0.45	0.00	0.52	0.53	0.00
1.5	0.32	0.29	0.00	0.42	0.37	0.00	0.48	0.46	0.00	0.53	0.54	0.00
1	0.32	0.29	0.00	0.43	0.38	0.00	0.50	0.47	0.00	0.54	0.55	0.00
0.75	0.33	0.29	0.00	0.43	0.38	0.00	0.51	0.48	0.00	0.55	0.55	0.00
0.5	0.34	0.30	0.00	0.43	0.38	0.00	0.52	0.48	0.00	0.56	0.56	0.00
Sum			0.05			0.06			0.03			0.02

fs (%)	40											
µ (kg/m.s)	0.002842											
ρ_p (kg/m^3)	1397.415186											
N	6.7E-02			5.6E-02			5.1E-02			4.7E-02		
σ	4.7E-01			5.4E-01			5.9E-01			6.2E-01		
$\mu x_a/m_f$	8.53E-08			5.9E-08			4.8E-08			4.04E-08		
$m_u/(\rho_p g^{0.5} x_a^{2.5})$	8207765			11855661			14591583			17327504		
m_u (TPH)	6.3			9.1			11.2			13.3		
m_f (TPH)	9			13			16			19		
Size (µm)	Actual	Model	SSE	Actual	Model	SSE	Actual	Model	SSE	Actual	Model	SSE
8000	1.00	1.00	0.00	1.00	1.00	0.00	1.00	1.00	0.00	1.00	1.00	0.00
5600	1.00	1.00	0.00	1.00	1.00	0.00	1.00	1.00	0.00	1.00	1.00	0.00
4000	1.00	1.00	0.00	1.00	1.00	0.00	1.00	1.00	0.00	1.00	1.00	0.00
2800	1.00	1.00	0.00	1.00	1.00	0.00	1.00	1.00	0.00	1.00	1.00	0.00
2000	1.00	1.00	0.00	1.00	1.00	0.00	1.00	1.00	0.00	1.00	1.00	0.00
1400	1.00	1.00	0.00	1.00	1.00	0.00	1.00	1.00	0.00	1.00	1.00	0.00
1000	1.00	1.00	0.00	1.00	1.00	0.00	1.00	1.00	0.00	1.00	1.00	0.00
850	1.00	1.00	0.00	1.00	1.00	0.00	1.00	1.00	0.00	1.00	1.00	0.00
600	1.00	1.00	0.00	1.00	1.00	0.00	1.00	1.00	0.00	1.00	1.00	0.00
425	1.00	1.00	0.00	1.00	1.00	0.00	1.00	1.00	0.00	1.00	1.00	0.00
300	1.00	1.00	0.00	1.00	1.00	0.00	1.00	1.00	0.00	1.00	1.00	0.00
212	1.00	1.00	0.00	1.00	1.00	0.00	1.00	1.00	0.00	1.00	1.00	0.00
150	1.00	1.00	0.00	1.00	1.00	0.00	0.99	1.00	0.00	1.00	1.00	0.00
106	0.97	1.00	0.00	0.95	1.00	0.00	0.96	1.00	0.00	1.00	1.00	0.00
75	0.73	0.88	0.02	0.71	0.75	0.00	0.75	1.00	0.06	0.81	1.00	0.04
53	0.37	0.31	0.00	0.44	0.41	0.00	0.47	0.47	0.00	0.52	0.51	0.00
38	0.22	0.23	0.00	0.27	0.31	0.00	0.30	0.35	0.00	0.35	0.40	0.00
25	0.16	0.18	0.00	0.20	0.25	0.00	0.24	0.29	0.00	0.30	0.33	0.00
20	0.15	0.17	0.00	0.18	0.23	0.00	0.22	0.27	0.00	0.29	0.31	0.00
15	0.15	0.16	0.00	0.19	0.22	0.00	0.23	0.26	0.00	0.30	0.29	0.00
10	0.18	0.17	0.00	0.24	0.23	0.00	0.29	0.26	0.00	0.35	0.29	0.00
7	0.22	0.18	0.00	0.26	0.24	0.00	0.30	0.28	0.00	0.36	0.31	0.00
5	0.24	0.20	0.00	0.28	0.27	0.00	0.33	0.31	0.00	0.38	0.34	0.00
3	0.26	0.23	0.00	0.30	0.30	0.00	0.35	0.34	0.00	0.40	0.38	0.00
2	0.27	0.24	0.00	0.31	0.31	0.00	0.36	0.36	0.00	0.41	0.40	0.00
1.5	0.27	0.24	0.00	0.31	0.32	0.00	0.36	0.37	0.00	0.41	0.41	0.00
1	0.27	0.25	0.00	0.31	0.33	0.00	0.36	0.38	0.00	0.42	0.42	0.00
0.75	0.27	0.25	0.00	0.31	0.33	0.00	0.36	0.38	0.00	0.41	0.42	0.00
0.5	0.27	0.25	0.00	0.31	0.33	0.00	0.36	0.38	0.00	0.41	0.43	0.00
Sum			0.04			0.01			0.07			0.05

fs (%)	30					
µ (kg/m.s)	0.001398					
ρ_p (kg/m^3)	1271.124173					
N	1.0E-01			8.6E-02		
σ	3.5E-01			4.0E-01		
$\mu x_a/m_f$	4.19E-08			2.9E-08		
$m_u/(\rho_p g^{0.5} x_a^{2.5})$	9023238			13033566		
m_u (TPH)	6.3			9.1		
m_f (TPH)	9			13		
Size (µm)	Actual	Model	SSE	Actual	Model	SSE
8000	1.00	1.00	0.00	1.00	1.00	0.00
5600	1.00	1.00	0.00	1.00	1.00	0.00
4000	1.00	1.00	0.00	1.00	1.00	0.00
2800	1.00	1.00	0.00	1.00	1.00	0.00
2000	1.00	1.00	0.00	1.00	1.00	0.00
1400	1.00	1.00	0.00	1.00	1.00	0.00
1000	1.00	1.00	0.00	1.00	1.00	0.00
850	1.00	1.00	0.00	1.00	1.00	0.00
600	1.00	1.00	0.00	1.00	1.00	0.00
425	1.00	1.00	0.00	1.00	1.00	0.00
300	1.00	1.00	0.00	1.00	1.00	0.00
212	1.00	1.00	0.00	1.00	1.00	0.00
150	1.00	1.00	0.00	1.00	1.00	0.00
106	1.00	1.00	0.00	1.00	1.00	0.00
75	1.00	1.00	0.00	0.72	0.75	0.00
53	0.39	0.25	0.02	0.45	0.42	0.00
38	0.21	0.21	0.00	0.26	0.14	0.01
25	0.13	0.10	0.00	0.16	0.10	0.00
20	0.11	0.10	0.00	0.14	0.10	0.00
15	0.12	0.11	0.00	0.14	0.09	0.00
10	0.14	0.07	0.01	0.15	0.10	0.00
7	0.16	0.09	0.00	0.18	0.12	0.00
5	0.18	0.11	0.01	0.21	0.15	0.00
3	0.20	0.14	0.00	0.23	0.18	0.00
2	0.21	0.15	0.00	0.23	0.20	0.00
1.5	0.21	0.16	0.00	0.24	0.21	0.00
1	0.21	0.17	0.00	0.00	0.22	0.05
0.75	0.21	0.17	0.00	0.25	0.23	0.00
0.5	0.21	0.17	0.00	0.25	0.23	0.00
Sum			0.05			0.04

A 9: A comparison of the actual and modified model efficiencies using EXCEL SOLVER – 106 µm aperture

x_a (m)	106																																			
A_o (m^2)	0.55																																			
A_o/x_a^2	4.89E+07																																			
f_o (%)	35.80																																			
f_U (%)	80.00																																			
fs (%)	60									50									40									30								
µ (kg/m.s)	0.006592									0.004196									0.002842									0.001398								
ρ_p (kg/m^3)	1743.951613									1551.569507									1397.415186									1271.124173								
N	0.04			0.04			0.03			0.03			0.06			0.05			0.04			0.04			0.07			0.06			0.06			0.05		
σ	0.83			0.96			1.14			1.21			0.63			0.73			0.84			0.93			0.57			0.65			0.71			0.75		
$\mu x_a/m_f$	1.94E-07			1.3E-07			8.4E-08			7.2E-08			1.8E-07			1.2E-07			8.4E-08			6.4E-08			1.2E-07			8.3E-08			6.8E-08			5.7E-08		
$m_u/(\rho_p g^{1/2} x a^{5/2})$	4.57E+06			6.7E+06			1.1E+07			1.2E+07			3.6E+06			5.1E+06			7.5E+06			9.9E+06			4.0E+06			5.7E+06			7.0E+06			8.3E+06		
m_u (TPH)	10.4			15.2			24			28			7.2			10.4			15.2			20			7.2			10.4			12.8			15.2		
m_f (TPH)	13			19			30			35			9			13			19			25			9			13			16			19		
Size (µm)	Actual	Model	SSE	Actual	Model	SSE	Actual	Model	SSE	Actual	Model	SSE	Actual	Model	SSE	Actual	Model	SSE	Actual	Model	SSE	Actual	Model	SSE	Actual	Model	SSE	Actual	Model	SSE	Actual	Model	SSE	Actual	Model	SSE
8000	1.00	1.00	0.00	1.00	1.00	0.00	1.000	1.00	0.00	1.00	1.00	0.00	1.00	1.00	0.00	1.00	1.00	0.00	1.00	1.00	0.00	1.00	1.00	0.00	1.00	1.00	0.00	1.00	1.00	0.00	1.00	1.00	0.00	1.00	1.00	0.00
5600	1.00	1.00	0.00	1.00	1.00	0.00	1.000	1.00	0.00	1.00	1.00	0.00	1.00	1.00	0.00	1.00	1.00	0.00	1.00	1.00	0.00	1.00	1.00	0.00	1.00	1.00	0.00	1.00	1.00	0.00	1.00	1.00	0.00	1.00	1.00	0.00
4000	1.00	1.00	0.00	1.00	1.00	0.00	1.000	1.00	0.00	1.00	1.00	0.00	1.00	1.00	0.00	1.00	1.00	0.00	1.00	1.00	0.00	1.00	1.00	0.00	1.00	1.00	0.00	1.00	1.00	0.00	1.00	1.00	0.00	1.00	1.00	0.00
2800	1.00	1.00	0.00	1.00	1.00	0.00	1.000	1.00	0.00	1.00	1.00	0.00	1.00	1.00	0.00	1.00	1.00	0.00	1.00	1.00	0.00	1.00	1.00	0.00	1.00	1.00	0.00	1.00	1.00	0.00	1.00	1.00	0.00	1.00	1.00	0.00
2000	1.00	1.00	0.00	1.00	1.00	0.00	1.000	1.00	0.00	1.00	1.00	0.00	1.00	1.00	0.00	1.00	1.00	0.00	1.00	1.00	0.00	1.00	1.00	0.00	1.00	1.00	0.00	1.00	1.00	0.00	1.00	1.00	0.00	1.00	1.00	0.00
1400	1.00	1.00	0.00	1.00	1.00	0.00	1.000	1.00	0.00	1.00	1.00	0.00	1.00	1.00	0.00	1.00	1.00	0.00	1.00	1.00	0.00	1.00	1.00	0.00	1.00	1.00	0.00	1.00	1.00	0.00	1.00	1.00	0.00	1.00	1.00	0.00
1000	1.00	1.00	0.00	1.00	1.00	0.00	1.000	1.00	0.00	1.00	1.00	0.00	1.00	1.00	0.00	1.00	1.00	0.00	1.00	1.00	0.00	1.00	1.00	0.00	1.00	1.00	0.00	1.00	1.00	0.00	1.00	1.00	0.00	1.00	1.00	0.00
850	1.00	1.00	0.00	1.00	1.00	0.00	1.000	1.00	0.00	1.00	1.00	0.00	1.00	1.00	0.00	1.00	1.00	0.00	1.00	1.00	0.00	1.00	1.00	0.00	1.00	1.00	0.00	1.00	1.00	0.00	1.00	1.00	0.00	1.00	1.00	0.00
600	1.00	1.00	0.00	1.00	1.00	0.00	1.000	1.00	0.00	1.00	1.00	0.00	1.00	1.00	0.00	1.00	1.00	0.00	1.00	1.00	0.00	1.00	1.00	0.00	1.00	1.00	0.00	1.00	1.00	0.00	1.00	1.00	0.00	1.00	1.00	0.00
425	1.00	1.00	0.00	1.00	1.00	0.00	1.000	1.00	0.00	1.00	1.00	0.00	1.00	1.00	0.00	1.00	1.00	0.00	1.00	1.00	0.00	1.00	1.00	0.00	1.00	1.00	0.00	1.00	1.00	0.00	1.00	1.00	0.00	1.00	1.00	0.00
300	0.99	1.00	0.00	1.00	1.00	0.00	0.998	1.00	0.00	1.00	1.00	0.00	1.00	1.00	0.00	1.00	1.00	0.00	1.00	1.00	0.00	1.00	1.00	0.00	1.00	1.00	0.00	1.00	1.00	0.00	1.00	1.00	0.00	1.00	1.00	0.00
212	0.99	1.00	0.00	0.99	1.00	0.00	0.996	1.00	0.00	1.00	1.00	0.00	1.00	1.00	0.00	1.00	1.00	0.00	1.00	1.00	0.00	1.00	1.00	0.00	1.00	1.00	0.00	0.99	1.00	0.00	1.00	1.00	0.00	1.00	1.00	0.00
150	0.98	1.00	0.00	1.00	1.00	0.00	0.994	1.00	0.00	0.99	1.00	0.00	0.94	1.00	0.00	0.96	1.00	0.00	0.95	1.00	0.00	1.00	1.00	0.00	0.88	1.00	0.01	0.91	1.00	0.01	0.97	0.99	0.00	0.97	1.00	0.00
106	0.91	1.00	0.01	0.96	1.00	0.00	0.984	1.00	0.00	0.99	1.00	0.00	0.66	0.75	0.01	0.75	0.78	0.00	0.74	0.88	0.02	0.82	1.00	0.03	0.57	0.55	0.00	0.63	0.75	0.01	0.64	0.78	0.02	0.70	0.84	0.02
75	0.65	0.65	0.00	0.71	0.67	0.00	0.835	0.78	0.00	0.89	0.81	0.01	0.41	0.35	0.00	0.51	0.46	0.00	0.56	0.57	0.00	0.62	0.64	0.00	0.23	0.26	0.00	0.37	0.36	0.00	0.39	0.42	0.00	0.44	0.48	0.00
53	0.36	0.42	0.00	0.53	0.52	0.00	0.664	0.63	0.00	0.73	0.66	0.00	0.22	0.23	0.00	0.30	0.32	0.00	0.36	0.41	0.00	0.44	0.48	0.00	0.07	0.06	0.00	0.15	0.24	0.01	0.21	0.29	0.01	0.25	0.33	0.01
38	0.32	0.34	0.00	0.41	0.43	0.00	0.551	0.54	0.00	0.59	0.57	0.00	0.14	0.18	0.00	0.23	0.25	0.00	0.28	0.34	0.00	0.33	0.40	0.01	0.05	0.12	0.01	0.13	0.19	0.00	0.16	0.23	0.00	0.22	0.26	0.00
25	0.33	0.30	0.00	0.38	0.37	0.00	0.472	0.47	0.00	0.49	0.50	0.00	0.11	0.15	0.00	0.21	0.21	0.00	0.23	0.29	0.00	0.30	0.34	0.00	0.06	0.10	0.00	0.14	0.15	0.00	0.17	0.19	0.00	0.22	0.22	0.00
20	0.34	0.29	0.00	0.39	0.36	0.00	0.448	0.46	0.00	0.48	0.49	0.00	0.12	0.15	0.00	0.21	0.21	0.00	0.23	0.28	0.00	0.31	0.33	0.00	0.07	0.10	0.00	0.15	0.15	0.00	0.18	0.18	0.00	0.23	0.21	0.00
15	0.35	0.29	0.00	0.41	0.36	0.00	0.468	0.45	0.00	0.50	0.49	0.00	0.14	0.15	0.00	0.22	0.21	0.00	0.24	0.28	0.00	0.32	0.33	0.00	0.08	0.11	0.00	0.16	0.16	0.00	0.19	0.19	0.00	0.24	0.21	0.00
10	0.37	0.30	0.01	0.43	0.38	0.00	0.503	0.48	0.00	0.54	0.51	0.00	0.15	0.17	0.00	0.23	0.23	0.00	0.27	0.30	0.00	0.34	0.36	0.00	0.08	0.13	0.00	0.17	0.18	0.00	0.21	0.21	0.00	0.26	0.24	0.00
7	0.39	0.32	0.00	0.45	0.40	0.00	0.515	0.51	0.00	0.56	0.55	0.00	0.17	0.19	0.00	0.25	0.25	0.00	0.29	0.33	0.00	0.36	0.39	0.00	0.09	0.15	0.00	0.19	0.20	0.00	0.22	0.24	0.00	0.27	0.27	0.00
5	0.40	0.33	0.00	0.47	0.42	0.00	0.538	0.53	0.00	0.58	0.58	0.00	0.18	0.20	0.00	0.27	0.27	0.00	0.32	0.35	0.00	0.40	0.42	0.00	0.10	0.17	0.00	0.19	0.23	0.00	0.24	0.26	0.00	0.29	0.30	0.00
3	0.42	0.35	0.01	0.48	0.44	0.00	0.555	0.56	0.00	0.60	0.61	0.00	0.20	0.22	0.00	0.29	0.29	0.00	0.35	0.38	0.00	0.44	0.45	0.00	0.11	0.19	0.01	0.20	0.25	0.00	0.25	0.29	0.00	0.30	0.33	0.00
2	0.44	0.36	0.01	0.49	0.45	0.00	0.559	0.58	0.00	0.62	0.63	0.00	0.21	0.23	0.00	0.32	0.30	0.00	0.39	0.39	0.00	0.46	0.46	0.00	0.13	0.20	0.01	0.21	0.26	0.00	0.27	0.31	0.00	0.32	0.35	0.00
1.5	0.44	0.36	0.01	0.50	0.46	0.00	0.564	0.59	0.00	0.63	0.63	0.00	0.23	0.23	0.00	0.34	0.30	0.00	0.40	0.40	0.00	0.48	0.47	0.00	0.13	0.20	0.00	0.22	0.27	0.00	0.27	0.31	0.00	0.33	0.35	0.00
1	0.44	0.36	0.01	0.50	0.46	0.00	0.571	0.59	0.00	0.64	0.64	0.00	0.25	0.23	0.00	0.36	0.31	0.00	0.43	0.40	0.00	0.51	0.48	0.00	0.15	0.20	0.00	0.23	0.27	0.00	0.28	0.32	0.00	0.34	0.36	0.00
0.75	0.44	0.36	0.01	0.51	0.46	0.00	0.570	0.59	0.00	0.64	0.64	0.00	0.25	0.23	0.00	0.36	0.31	0.00	0.44	0.40	0.00	0.53	0.48	0.00	0.17	0.21	0.00	0.24	0.27	0.00	0.28	0.32	0.00	0.35	0.36	0.00
0.5	0.44	0.36	0.01	0.50	0.46	0.00	0.571	0.60	0.00	0.64	0.65	0.00	0.25	0.24	0.00	0.36	0.31	0.00	0.44	0.41	0.00	0.53	0.48	0.00	0.18	0.21	0.00	0.24	0.28	0.00	0.28	0.32	0.00	0.35	0.36	0.00
Sum			**0.07**			**0.03**			**0.01**			**0.02**			**0.02**			**0.02**			**0.04**			**0.05**			**0.06**			**0.05**			**0.04**			**0.03**		

A 10: A comparison of the actual and modified model efficiencies using EXCEL SOLVER –150 µm aperture

x_a (m)	150																													
A_o (m^2)	0.53																													
A_o/x_a^2	2.35E+07																													
f_o (%)	34.50																													
f_U (%)	85.00																													
fs (%)	60												50									40						30		
µ (kg/m.s)	0.006592												0.004196									0.002842						0.001398		
ρ_p (kg/m^3)	1743.951613												1551.569507									1397.415186						1271.124173		
$\mu/(\rho_s g^{1/2} xa^{3/2})$	6.21832E-09												3.95814E-09									2.6809E-09						1.31875E-09		
N	6.60E-02			5.5E-02			4.4E-02			4.1E-02			8.1E-02			6.8E-02			5.9E-02			9.6E-02			8.0E-02			1.2E-01		
σ	1.41E+00			1.6E+00			1.9E+00			2.1E+00			1.2E+00			1.4E+00			1.6E+00			1.1E+00			1.3E+00			9.5E-01		
$\mu x_a/m_f$	2.738E-07			1.9E-07			1.2E-07			1.0E-07			1.7E-07			1.2E-07			9.1E-08			1.2E-07			8.1E-08			4.0E-08		
$m_u/(\rho_p g^{1/2} xa^{5/2})$	2039213.5			3.0E+06			4.7E+06			5.5E+06			2.3E+06			3.3E+06			4.4E+06			2.5E+06			3.7E+06			4.1E+06		
m_u (TPH)	11.1			16.2			25.5			29.8			11.1			16.2			21.3			11.1			16.2			16.2		
m_f (TPH)	13			19			30			35			13			19			25			13			19			19		
Size (µm)	Actual	Model	SSE	Actual	Model	SSE	Actual	Model	SSE	Actual	Model	SSE	Actual	Model	SSE	Actual	Model	SSE	Actual	Model	SSE	Actual	Model	SSE	Actual	Model	SSE	Actual	Model	SSE
8000	1.00	1.00	0.00	1.00	1.00	0.00	1.00	1.00	0.00	1.00	1.00	0.00	1.00	1.00	0.00	1.00	1.00	0.00	1.00	1.00	0.00	1.00	1.00	0.00	1.00	1.00	0.00	1.00	1.00	0.00
5600	1.00	1.00	0.00	1.00	1.00	0.00	1.00	1.00	0.00	1.00	1.00	0.00	1.00	1.00	0.00	1.00	1.00	0.00	1.00	1.00	0.00	1.00	1.00	0.00	1.00	1.00	0.00	1.00	1.00	0.00
4000	1.00	1.00	0.00	1.00	1.00	0.00	1.00	1.00	0.00	1.00	1.00	0.00	1.00	1.00	0.00	1.00	1.00	0.00	1.00	1.00	0.00	1.00	1.00	0.00	1.00	1.00	0.00	1.00	1.00	0.00
2800	1.00	1.00	0.00	1.00	1.00	0.00	1.00	1.00	0.00	1.00	1.00	0.00	1.00	1.00	0.00	1.00	1.00	0.00	1.00	1.00	0.00	1.00	1.00	0.00	1.00	1.00	0.00	1.00	1.00	0.00
2000	1.00	1.00	0.00	1.00	1.00	0.00	1.00	1.00	0.00	1.00	1.00	0.00	1.00	1.00	0.00	1.00	1.00	0.00	1.00	1.00	0.00	1.00	1.00	0.00	1.00	1.00	0.00	1.00	1.00	0.00
1400	1.00	1.00	0.00	1.00	1.00	0.00	1.00	1.00	0.00	1.00	1.00	0.00	1.00	1.00	0.00	1.00	1.00	0.00	1.00	1.00	0.00	1.00	1.00	0.00	1.00	1.00	0.00	1.00	1.00	0.00
1000	1.00	1.00	0.00	1.00	1.00	0.00	1.00	1.00	0.00	1.00	1.00	0.00	1.00	1.00	0.00	1.00	1.00	0.00	1.00	1.00	0.00	1.00	1.00	0.00	1.00	1.00	0.00	1.00	1.00	0.00
850	1.00	1.00	0.00	1.00	1.00	0.00	1.00	1.00	0.00	1.00	1.00	0.00	1.00	1.00	0.00	1.00	1.00	0.00	1.00	1.00	0.00	1.00	1.00	0.00	1.00	1.00	0.00	1.00	1.00	0.00
600	1.00	1.00	0.00	1.00	1.00	0.00	1.00	1.00	0.00	1.00	1.00	0.00	1.00	1.00	0.00	1.00	1.00	0.00	1.00	1.00	0.00	1.00	1.00	0.00	1.00	1.00	0.00	1.00	1.00	0.00
425	1.00	1.00	0.00	1.00	1.00	0.00	1.00	1.00	0.00	1.00	1.00	0.00	1.00	1.00	0.00	1.00	1.00	0.00	1.00	1.00	0.00	1.00	1.00	0.00	1.00	1.00	0.00	1.00	1.00	0.00
300	1.00	1.00	0.00	1.00	1.00	0.00	1.00	1.00	0.00	1.00	1.00	0.00	0.99	1.00	0.00	0.98	1.00	0.00	1.00	1.00	0.00	1.00	1.00	0.00	1.00	1.00	0.00	1.00	1.00	0.00
212	0.92	1.00	0.01	0.91	0.95	0.00	1.00	1.00	0.00	0.99	1.00	0.00	0.97	1.00	0.00	0.95	1.00	0.00	0.99	1.00	0.00	0.96	0.95	0.00	0.97	1.00	0.00	1.00	1.00	0.00
150	0.78	0.78	0.00	0.74	0.74	0.00	1.00	1.00	0.00	0.92	1.00	0.01	0.88	1.00	0.01	0.86	1.00	0.02	0.97	1.00	0.00	0.75	0.78	0.00	0.81	1.00	0.04	0.66	0.68	0.00
106	0.64	0.67	0.00	0.65	0.67	0.00	1.00	0.87	0.02	0.82	0.89	0.01	0.59	0.54	0.00	0.67	0.67	0.00	0.83	0.75	0.01	0.38	0.42	0.00	0.50	0.56	0.00	0.31	0.27	0.00
75	0.47	0.42	0.00	0.50	0.54	0.00	0.97	0.67	0.09	0.72	0.71	0.00	0.37	0.30	0.00	0.43	0.42	0.00	0.55	0.51	0.00	0.12	0.21	0.01	0.26	0.32	0.00	0.07	0.11	0.00
53	0.21	0.29	0.01	0.30	0.39	0.01	0.88	0.52	0.13	0.56	0.56	0.00	0.24	0.20	0.00	0.26	0.29	0.00	0.34	0.36	0.00	0.04	0.13	0.01	0.11	0.20	0.01	0.01	0.06	0.00
38	0.17	0.23	0.00	0.19	0.31	0.01	0.75	0.42	0.11	0.47	0.46	0.00	0.15	0.15	0.00	0.17	0.22	0.00	0.23	0.28	0.00	0.03	0.09	0.00	0.10	0.15	0.00	0.02	0.04	0.00
25	0.17	0.19	0.00	0.15	0.26	0.01	0.46	0.36	0.01	0.43	0.40	0.00	0.13	0.12	0.00	0.13	0.18	0.00	0.21	0.23	0.00	0.03	0.08	0.00	0.10	0.13	0.00	0.02	0.04	0.00
20	0.17	0.19	0.00	0.19	0.26	0.01	0.39	0.35	0.00	0.43	0.39	0.00	0.15	0.13	0.00	0.15	0.18	0.00	0.21	0.23	0.00	0.04	0.09	0.00	0.10	0.13	0.00	0.02	0.05	0.00
15	0.18	0.19	0.00	0.20	0.26	0.00	0.35	0.36	0.00	0.44	0.39	0.00	0.15	0.13	0.00	0.16	0.19	0.00	0.23	0.24	0.00	0.04	0.10	0.00	0.11	0.14	0.00	0.02	0.07	0.00
10	0.20	0.20	0.00	0.23	0.27	0.00	0.33	0.37	0.00	0.48	0.41	0.01	0.17	0.15	0.00	0.19	0.21	0.00	0.25	0.26	0.00	0.05	0.12	0.01	0.11	0.17	0.00	0.03	0.10	0.01
7	0.23	0.21	0.00	0.27	0.28	0.00	0.37	0.39	0.00	0.51	0.43	0.01	0.18	0.17	0.00	0.21	0.23	0.00	0.28	0.28	0.00	0.05	0.14	0.01	0.13	0.19	0.00	0.04	0.13	0.01
5	0.25	0.22	0.00	0.29	0.29	0.00	0.39	0.40	0.00	0.52	0.44	0.01	0.19	0.18	0.00	0.22	0.24	0.00	0.31	0.30	0.00	0.06	0.15	0.01	0.13	0.21	0.01	0.05	0.15	0.01
3	0.26	0.22	0.00	0.30	0.30	0.00	0.44	0.41	0.00	0.52	0.45	0.00	0.20	0.19	0.00	0.24	0.25	0.00	0.33	0.31	0.00	0.06	0.17	0.01	0.15	0.22	0.01	0.06	0.18	0.01
2	0.27	0.23	0.00	0.32	0.30	0.00	0.46	0.42	0.00	0.53	0.46	0.00	0.21	0.19	0.00	0.26	0.26	0.00	0.36	0.32	0.00	0.07	0.17	0.01	0.16	0.23	0.01	0.06	0.19	0.02
1.5	0.27	0.23	0.00	0.33	0.31	0.00	0.46	0.42	0.00	0.53	0.46	0.01	0.21	0.19	0.00	0.28	0.26	0.00	0.37	0.32	0.00	0.07	0.18	0.01	0.18	0.23	0.00	0.07	0.19	0.02
1	0.28	0.23	0.00	0.34	0.31	0.00	0.47	0.42	0.00	0.53	0.46	0.00	0.22	0.20	0.00	0.28	0.26	0.00	0.38	0.32	0.00	0.07	0.18	0.01	0.19	0.24	0.00	0.07	0.20	0.01
0.75	0.28	0.23	0.00	0.35	0.31	0.00	0.48	0.42	0.00	0.53	0.46	0.01	0.23	0.20	0.00	0.29	0.26	0.00	0.39	0.32	0.00	0.08	0.18	0.01	0.21	0.24	0.00	0.08	0.20	0.02
0.5	0.28	0.23	0.00	0.35	0.31	0.00	0.48	0.42	0.00	0.53	0.46	0.00	0.24	0.20	0.00	0.31	0.26	0.00	0.40	0.32	0.01	0.12	0.18	0.00	0.22	0.24	0.00	0.07	0.20	0.02
Sum			**0.03**			**0.06**			**0.37**			**0.07**			**0.03**			**0.03**			**0.03**			**0.11**			**0.09**			**0.08**

EBE Faculty: Assessment of Ethics in Research Projects

Any person planning to undertake research in the Faculty of Engineering and the Built Environment at the University of Cape Town is required to complete this form before collecting or analysing data. When completed it should be submitted to the supervisor (where applicable) and from there to the Head of Department. If any of the questions below have been answered YES, and the applicant is NOT a fourth year student, the Head should forward this form for approval by the Faculty EIR committee: submit to Ms Zakiya Chikte (Zakiya.chikte@uct.ac.za); New EBE Building, Ph 021 650 5739). Students must include a copy of the completed form with the dissertation/thesis when it is submitted for examination.

Name of Principal Researcher/Student: Seipati Mabote Department: Chemical Engineering

If a Student: Degree: MSc Supervisor: Prof. Aubrey Mainza

If a Research Contract indicate source of funding/sponsorship: Centre for Minerals Research

Research Project Title: An Investigation of the effect of operating and design parameters on screening performance in fine wet screening

Overview of ethics issues in your research project:

Question 1: Is there a possibility that your research could cause harm to a third party (i.e. a person not involved in your project)?	YES	NO ✓
Question 2: Is your research making use of human subjects as sources of data? If your answer is YES, please complete Addendum 2.	YES	NO ✓
Question 3: Does your research involve the participation of or provision of services to communities? If your answer is YES, please complete Addendum 3.	YES	NO ✓
Question 4: If your research is sponsored, is there any potential for conflicts of interest? If your answer is YES, please complete Addendum 4.	YES	NO ✓

If you have answered YES to any of the above questions, please append a copy of your research proposal, as well as any interview schedules or questionnaires (Addendum 1) and please complete further addenda as appropriate.

I hereby undertake to carry out my research in such a way that

- there is no apparent legal objection to the nature or the method of research; and
- the research will not compromise staff or students or the other responsibilities of the University;
- the stated objective will be achieved, and the findings will have a high degree of validity;
- limitations and alternative interpretations will be considered;
- the findings could be subject to peer review and publicly available; and
- I will comply with the conventions of copyright and avoid any practice that would constitute plagiarism.

Signed by:

	Full name and signature	Date
Principal Researcher/Student:	Seipati Mabote	12/02/2016

This application is approved by:

Supervisor (if applicable):	Aubrey Mainza	12/02/2016
HOD (or delegated nominee): Final authority for all assessments with NO to all questions and for all undergraduate research.		12/02/16
Chair : Faculty EIR Committee For applicants other than undergraduate students who have answered YES to any of the above questions.		

ADDENDUM 1:
Please append a copy of the research proposal here, as well as any interview schedules or questionnaires:

ADDENDUM 2: To be completed if you answered YES to Question 2:

It is assumed that you have read the UCT Code for Research involving Human Subjects (available at http://web.uct.ac.za/depts/educate/download/uctcodeforresearchinvolvinghumansubjects.pdf) in order to be able to answer the questions in this addendum.

2.1 Does the research discriminate against participation by individuals, or differentiate between participants, on the grounds of gender, race or ethnic group, age range, religion, income, handicap, illness or any similar classification?	YES	NO
2.2 Does the research require the participation of socially or physically vulnerable people (children, aged, disabled, etc) or legally restricted groups?	YES	NO
2.3 Will you not be able to secure the informed consent of all participants in the research? (In the case of children, will you not be able to obtain the consent of their guardians or parents?)	YES	NO
2.4 Will any confidential data be collected or will identifiable records of individuals be kept?	YES	NO
2.5 In reporting on this research is there any possibility that you will not be able to keep the identities of the individuals involved anonymous?	YES	NO
2.6 Are there any foreseeable risks of physical, psychological or social harm to participants that might occur in the course of the research?	YES	NO
2.7 Does the research include making payments or giving gifts to any participants?	YES	NO

If you have answered YES to any of these questions, please describe how you plan to address these issues (append to form):

ADDENDUM 3: To be completed if you answered YES to Question 3:

3.1 Is the community expected to make decisions for, during or based on the research?	YES	NO
3.2 At the end of the research will any economic or social process be terminated or left unsupported, or equipment or facilities used in the research be recovered from the participants or community?	YES	NO
3.3 Will any service be provided at a level below the generally accepted standards?	YES	NO

If you have answered YES to any of these questions, please describe how you plan to address these issues (append to form)

ADDENDUM 4: To be completed if you answered YES to Question 4

4.1 Is there any existing or potential conflict of interest between a research sponsor, academic supervisor, other researchers or participants?	YES	NO
4.2 Will information that reveals the identity of participants be supplied to a research sponsor, other than with the permission of the individuals?	YES	NO
4.3 Does the proposed research potentially conflict with the research of any other individual or group within the University?	YES	NO

If you have answered YES to any of these questions, please describe how you plan to address these issues(append to form)